

UNIVERSITY OF CALIFORNIA

Los Angeles

Competitive Adsorption of Cyclotrimethylenetrinitramine (RDX) and
Cyclotetramethylenetetranitramine (HMX)

A thesis submitted in partial satisfaction of the
requirements for the degree Master of Science
in Civil Engineering

by

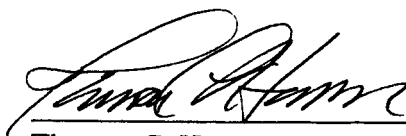
Carmen Kar Men Lee

1996

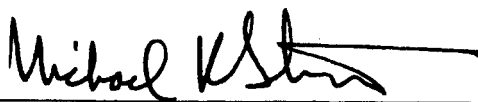
The thesis of Carmen Kar Men Lee is approved.



Menachem Elimelech



Thomas C. Harmon



Michael K. Stenstrom, Committee Chair

University of California, Los Angeles

1996

TABLE OF CONTENTS

TABLE OF CONTENTS.....	iii
LIST OF FIGURES.....	vii
LIST OF TABLES.....	x
ABSTRACT.....	xi
1. INTRODUCTION.....	1
2. LITERATURE REVIEW.....	5
2.1 Properties and Toxicity of RDX.....	5
2.2 Properties and Toxicity of HMX.....	7
2.3 Principal Treatment Technologies for RDX and HMX.....	10
2.3.1 Alkaline Hydrolysis.....	10
2.3.2 Ultraviolet Radiation/Photolysis.....	10
2.3.3 Polymer Adsorption.....	11
2.3.4 Biological Treatment.....	12
2.3.5 Activated Carbon Adsorption.....	14
2.4 Adsorption Isotherm Models.....	14
2.4.1 Monocomponent Isotherm Models.....	15
2.4.1.1 Langmuir Monocomponent Isotherm.....	15
2.4.1.2 Brunauer, Emmett, Teller (BET) Isotherm.....	17
2.4.1.3 Freundlich Monocomponent Isotherm.....	17
2.4.2 Multicomponent Isotherm Models.....	19

2.4.2.1	Langmuir Multicomponent Isotherm.....	19
2.4.2.2	Langmuir Extension- First Approximation Model.....	20
2.4.2.3	Langmuir Partially Competitive Multicomponent Isotherm.....	21
2.4.2.4	Freundlich Multicomponent Isotherm.....	22
2.4.2.5	Empirical Bisolute Extension of the Freundlich Isotherm.....	24
2.4.2.6	Crittenden et al.'s IAS-Freundlich Isotherm.....	24
2.4.2.7	Fritz & Schlunder's IAS-Freundlich Model.....	26
2.4.2.8	Simplified Ideal Adsorbed Solution (SIAS) Isotherm.....	27
2.4.2.9	Improved Simplified Ideal Adsorbed Solution (ISIAS) Isotherm.....	28
2.4.2.10	Ideal Adsorbed Solution (IAS) Model.....	30
2.4.2.11	Polanyi Adsorption Potential Theory.....	32
2.5	Previous Work on Activated Carbon Adsorption of RDX and HMX.....	40
3.	EXPERIMENTAL METHODS.....	57
3.1	Analytical Techniques.....	57
3.1.1	High Performance Liquid Chromatography (HPLC).....	57
3.1.2	Solid Phase Extraction (SPE).....	58

3.1.2.1 Previous Work on SPE and Other Extraction	
Methods.....	59
3.1.2.2 SPE Method Development.....	61
3.1.2.3 The SPE Method.....	63
3.2 Experimental Design and Methods.....	66
3.2.1 Isotherm Experimental Design.....	66
3.2.1.1 Program's Results & Usage.....	66
3.2.1.2 Experimental Conditions.....	71
3.2.1.3 Isotherm Experiments: Materials & Method.....	71
3.2.2 Solubility Tests: Materials & Methods.....	72
3.3 Error Analysis.....	73
4. RESULTS AND DISCUSSIONS.....	84
4.1 RDX and HMX Adsorption.....	84
4.2 Multicomponent Adsorption Isotherms.....	94
4.2.1 Langmuir Multicomponent Isotherm.....	96
4.2.2 Langmuir Partially Competitive Isotherm.....	102
4.2.3 Freundlich Multicomponent Isotherm.....	105
4.2.4 Simplified Ideal Adsorbed Solution (SIAS) Isotherm.....	110
4.2.5 Improved Simplified Ideal Adsorbed Solution (ISIAS)	
Isotherm.....	113
4.3 RDX and HMX Aqueous Solubility Limits.....	119

5. CONCLUSION.....	121
APPENDIX A CALIBRATION CURVES.....	124
APPENDIX B SPE RECOVERY STUDIES	129
APPENDIX C PASCAL PROGRAM.....	131
APPENDIX D COMPETITIVE ISOTHERM EXPERIMENTAL DATA.....	142
REFERENCES.....	146

LIST OF FIGURES

Figure 1 Structural Formula of RDX and HMX.....	6
Figure 2 Solid Phase Extraction Setup.....	64
Figure 3 Flowchart for the Pascal Program.....	67
Figure 4 Computer Program Prediction for RDX.....	68
Figure 5 Computer Program Prediction for HMX.....	69
Figure 6a Estimated Error for RDX Sorbed Concentration Subject to 0.00025g Error in Measuring Carbon Dosages.....	75
Figure 6b Estimated Error for HMX Sorbed Concentration Subject to 0.00025g Error in Measuring Carbon Dosages.....	75
Figure 7a Estimated Error for RDX Sorbed Concentration Subject to 0.005L Error in Measuring Volume.....	76
Figure 7b Estimated Error for HMX Sorbed Concentration Subject to 0.005L Error in Measuring Volume.....	77
Figure 8a Estimated Error for RDX Sorbed Concentration Subject to 0.000339mg/L Error in Measuring Concentration.....	79
Figure 8b Estimated Error for HMX Sorbed Concentration Subject to 0.0255mg/L Error in Measuring Concentration.....	79
Figure 9a Estimated Error for RDX Sorbed Concentration Subject to 1% Error in Freundlich Parameter K.....	81
Figure 9b Estimated Error for HMX Sorbed Concentration Subject to	

1% Error in Freundlich Parameter K.....	81
Figure 10a Estimated Error for RDX Sorbed Concentration Subject to	
1% Error in Freundlich Parameter n.....	82
Figure 10b Estimated Error for HMX Sorbed Concentration Subject to	
1% Error in Freundlich Parameter n.....	82
Figure 11 Linearized Langmuir, BET, Freundlich Isotherms for RDX.....	85
Figure 12 Linearized Langmuir, BET, Freundlich Isotherms for HMX.....	86
Figure 13 Freundlich Monocomponent Isotherm for RDX and HMX.....	88
Figure 14 Freundlich Linearized Single-Solute Isotherm for Independent and	
Competitive RDX and HMX.....	90
Figure 15 Langmuir Multicomponent Isotherm Contour for RDX.....	97
Figure 16 Langmuir Multicomponent Isotherm Contour for HMX.....	98
Figure 17 Experimental Results for RDX.....	99
Figure 18 Experimental Results for HMX.....	100
Figure 19 Langmuir Partially Competitive Isotherm Contour for RDX.....	103
Figure 20 Langmuir Partially Competitive Isotherm Contour for HMX.....	104
Figure 21 Freundlich Linearized Bisolute Isotherm for RDX.....	106
Figure 22 Freundlich Linearized Bisolute Isotherm for HMX.....	106
Figure 23 Freundlich Multicomponent Isotherm Contour for RDX.....	107
Figure 24 Freundlich Multicomponent Isotherm Contour for HMX.....	108
Figure 25 SIAS Isotherm Contour for RDX.....	111

Figure 26 SIAS Isotherm Contour for HMX.....	112
Figure 27 Sum of Least Squares as Functions of η_2	114
Figure 28 ISIAS Isotherm Contour for RDX.....	115
Figure 29 ISIAS Isotherm Contour for HMX.....	116
Figure 30 RDX and HMX Aqueous Solubility Tests.....	120

LIST OF TABLES

Table 1	Properties and Toxicity of RDX and HMX.....	9
Table 2	Multicomponent Adsorption Isotherms/Models.....	34
Table 3a	Batch Isotherm Parameters for Independent Adsorption of Explosives.....	50
Table 3b	Batch Isotherm Parameters for Competitive Adsorption of Explosives.....	51
Table 4	Solid Phase Extraction Procedures.....	65
Table 5	Root Mean Squares Error for Various Multicomponent Isotherms.....	119

ABSTRACT OF THE THESIS

Competitive Adsorption of Cyclotrimethylenetrinitramine (RDX) and Cyclotetramethylenetetranitramine (HMX)

by

Carmen Kar Men Lee

Master of Science in Civil Engineering

University of California, Los Angeles, 1996

Professor Michael K. Stenstrom, Chair

Military wastes have always been a problem due to their threat to humans and the environment. Since the end of the Cold War, removal of such wastes has become a more important issue due to various countries' demilitarizing effort. Two common constituents of military wastes are the high explosives RDX and HMX. Wastewaters which contain these explosives must be treated for their toxicity.

Carbon adsorption is a common treatment for explosives-contaminated wastewaters. In order to optimize the adsorption process, developing a multicomponent isotherm for the competitive adsorption of RDX and HMX is essential. Although researchers have studied adsorption of explosives, no one has developed a multicomponent isotherm to represent the process. The purpose of this thesis is to develop a multicomponent adsorption isotherm which describes this bisolute system.

The RDX-HMX adsorption process is a partially competitive process; the adsorption of both species is inhibited by the presence of each other. HMX is preferentially adsorbed because it has lower aqueous solubility and an additional nitro group which contributes to stronger sorbate-sorbent complex. The RDX-HMX adsorption data were used for fitting five isotherms: the Langmuir Multicomponent Isotherm, the Langmuir Partially Competitive Isotherm, the Freundlich Multicomponent Isotherm, the SIAS Isotherm, and the ISIAS Isotherm. The equilibrium concentration examined ranged from 0.0018 mg/L to 36.6 mg/L RDX, and 0.00086 mg/L to 4.4 mg/L HMX. The ISIAS Isotherm, which incorporates the IAS Theory and the Freundlich Isotherm, best represented the RDX-HMX bisolute system. This isotherm may be applicable to competitive adsorption of other explosives mixtures.

1. INTRODUCTION

Explosives have been manufactured in the United States for many decades. Among all the high explosives (HEs) that are manufactured, RDX (Hexahydro-1,3,5-trinitro-1,3,5-triazine), HMX (Octahydro-1,3,5,7-tetranitro-1,3,5,7-tetrazocine), and TNT (2,4,6-trinitrotoluene) are among the most common. RDX and HMX are more energetic than TNT and they are used in both conventional and nuclear weapons (Patterson et al., 1976b). In the U.S., TNT has been primarily used in conventional weapons but had occasionally been used in nuclear weapons.

HEs have been produced continuously in the U.S. since the World War I, but the rates of production varied and peaked during war times; for example, the U.S. was producing about 15×10^6 kg of RDX per month by the end of the World War II (W.W.II) (Urbanski, 1964). Towards the end of the Vietnam War, between 1969 and 1971, the U.S. was producing 7.2×10^6 kg of RDX and 0.9×10^6 kg of HMX monthly (Patterson et al., 1976a). Worldwide production also peaked during the W.W.II, with Germany's production reaching 7×10^6 kg per month (Urbanski, 1964).

The end of the Cold War has caused a worldwide surplus of munitions. Both the U.S. and the countries composing the former Soviet Union have nuclear weapons to dismantle. Many countries, such as the former German Democratic Republic (GDR, East Germany), have excess inventories of conventional weapons. The U.S. Department of Defense (DOD) has an inventory of 358,763,000 kg of ordnance items (Ansell, 1993). More specifically, there are 48 million kilograms of energetic materials, which included

explosives and propellants, in the U.S. DOD's inventory, and the number is increasing at a rate of 2.7 million kilograms per year. The destruction of excess nuclear weapons in the next ten years will produce about 1.7×10^5 kg of explosives, which include TNT, RDX, and HMX, for disposal (Pruneda et al., 1993).

Weapons manufacturing plants as well as load, assemble, and pack (LAP) facilities have produced a variety of problems with HE wastes. Many of these facilities are operated in times of national emergency, and proper waste disposal is a secondary priority. During the production of the HEs, wastewaters are produced from dewatering operation and house-keeping operations, such as floor and equipment washing. LAP facilities also produce contaminated wastewaters from explosive-melting, washdown and steam cleaning of reject warheads. These waters are sometimes called pink waters if they contain TNT and breakdown products. Wastewaters that contain only RDX or HMX do not have the pink coloration; however, pink waters may contain RDX or HMX if they are used in conjunction with TNT.

In the past, unlined lagoons or pits were used for holding wastewaters contaminated with HEs. These pits and uncontrolled spills from wastewater-holding facilities have caused soil and groundwater contamination. Explosives-contaminated wastewaters may have high concentrations of explosives, including explosives in colloidal or particulate form. Groundwaters usually have lower concentrations and they do not have explosives particulates.

Treatment of pink water and contaminated groundwater has become a more pressing issue due to worldwide demilitarization effort and widespread contamination from previous explosives manufacturing and processing plants. Although open burning/open detonation (OB/OD) has been used for disposing energetic material for a long time, it may soon be prohibited because OB/OD leads to soil and air contamination. Since these explosives are not easily biodegraded, one must use physiochemical means to treat the wastewater. Activated carbon (AC) adsorption is a common method for treating pink water, and studies have shown that it can also be used to treat explosives-contaminated groundwater.

Since most explosives and all propellants are blends of ingredients instead of a single substance, the wastewater is likely to contain various explosives and other compounds. Treating the wastewater with AC will involve adsorption of more than one kind of explosive. Carbon adsorption in this case is competitive because some compounds will adsorb strongly while others will adsorb weakly; some compounds might displace others in order to compete for adsorption sites. As a result, multicomponent isotherm models are needed to develop more efficient and reliable AC adsorption treatment systems. Although previous researchers have investigated adsorption of wastewaters containing explosives mixture, such as RDX, HMX, and TNT, no one has developed a multicomponent isotherm or a model which describes the chemical and physical interaction among the components. These researchers used the linearized Freundlich monocomponent isotherm to fit multicomponent data, but the suitability of the

fit is limited. Furthermore, the equilibrium concentration of the explosives over which the Freundlich parameters were derived was restricted to a narrow range. (Vlahakis, 1974; Burrows, 1982; Haberman, 1983; Hinshaw et al., 1987; Dennis et al., 1990).

The objective of this thesis is to describe the bisolute adsorption behavior of RDX and HMX over a wide equilibrium concentration range and to find a multicomponent isotherm model that will describe the experimental data. RDX and HMX are chosen for this study because the two compounds are usually found together as environmental contaminants. Industrial grade and military grade RDX usually contain HMX as impurity, and HMX can be produced in such a way that RDX becomes an impurity. (Patterson et al., 1976b; Yinon, 1990; Major et al., 1992). Although the isotherm is developed from the RDX-HMX adsorption system, it may be applicable for competitive adsorption of other kinds of explosives or other combination of explosives, such as TNT-RDX and TNT-RDX-HMX.

This thesis is arranged into five chapters. Chapter 1 is an introduction, and Chapter 2 is a literature review of RDX and HMX properties, and the existing multicomponent adsorption isotherms and models. Chapter 3 presents the analytical techniques and describes the experimental methods used for obtaining competitive RDX and HMX adsorption data. Various isotherm models were used to fit the data. Comparisons of various fits and all the experimental results are discussed in Chapter 4. Chapter 5 contains the conclusions and highlights the important results found from competitive adsorption of RDX and HMX.

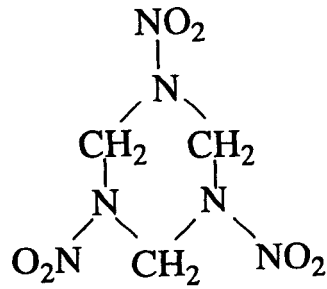
2. LITERATURE REVIEW

2.1 *Properties and Toxicity of RDX*

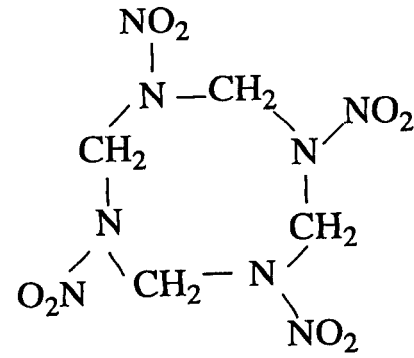
RDX (CAS Registry No. 121-82-4) is one of the most important military HEs in the U.S. The name RDX is a British code name for *Research Department or Royal Demolition Explosive* (McLellan et al., 1988a). During the W.W.II, RDX became an important high-power explosive, and it was used in detonators, primers, and boosters. More recently it has been used as a plastic explosive or combined with other explosives such as TNT (Yinon, 1990). Military grade RDX contains 8-12% HMX by weight, which is unintentionally manufactured with the RDX.

RDX is a heterocyclic compound with 3 nitro groups, and it appears as a white orthorhombic crystal (Layton et al., 1987; Yinon, 1990); its structure is shown in Figure 1a. Although RDX's chemical stability is similar to TNT, it is a more powerful explosive than TNT, and it is a nitramine instead of a nitroaromatic (Layton et al., 1987; Yinon, 1990). RDX is sparingly soluble in water at room temperature, but its solubility is greatly enhanced in warm water or in the presence of polar organic solvents.

RDX is a Class C Carcinogen, and it is toxic at 0.25 mg/L (Patterson, 1976; McLellan et al., 1988a). Acute human exposure to RDX, such as workers inhaling RDX dust particles in munition plants, can lead to hyperirritability, nausea, hepatic effects or liver injury, muscle twitching, seizures, prolonged confusion, unconsciousness, convulsions, amnesia, and vertigo (Layton et al., 1987; McLellan, 1988a; Yinon, 1990; Rosenblatt, et al., 1991). Several studies have been done on RDX's toxicity in rats and



(a) RDX



(b) HMX

Figure 1 Structural Formula of RDX and HMX

miniature swine. Researchers have found that RDX can be metabolized by the liver through gastrointestinal absorption. Although RDX is not carcinogenic for rats, it can cause convulsions, anemia, increased liver weight, and decreased fertility. Lifetime feeding of RDX to rats and mice will have adverse effects on their central nervous system, and it can lead to weight loss, renal toxicity, and increase in mortality. The U.S. EPA has set a Lifetime Health Advisory for exposure to RDX at 0.002 mg/L for a 70 kg adult, and the American Conference of Government Industrial Hygienist and OSHA recommends the threshold limit value for RDX to be 0.0015 mg/L or 1.5 mg/m³ (McLellan et al., 1988a). A list of most RDX's important characteristics are shown in Table 1.

2.2 Properties and Toxicity of HMX

HMX (CAS Registry No. 2691-41-0) stands for *High Melting Explosive* (Rosenblatt et al., 1991). While HMX is the most energetic conventional explosive known, it is predominantly used as a propellant and in maximum-performance explosives (Rosenblatt et al., 1991; Maleki, 1994). Other applications of HMX include burster charges for artillery shells, components for solid-fuel rocket propellants, and imploding fissionable material in nuclear devices in order to achieve critical mass (McLellan et al., 1988b; Yinon, 1990). HMX's higher density also allows it to replace RDX in explosive applications when energy and volume are important (Gibbs et al., 1980). It has replaced RDX in importance in the U.S. due to its greater energetic yield and its resistance to unwanted detonation (Heilmann, 1994).

HMX is a colorless, polycrystalline material, and it exists in four polymorphic forms: alpha orthorhombic, beta monoclinic, gamma monoclinic, and delta hexagonal. Among the four, the beta form is the most stable and is the one suitable for military applications (McLellan et al., 1988b; Yinon, 1990). As shown in Table 1, HMX has higher density and melting point than RDX, but it is less soluble than RDX. Like RDX, HMX can be extremely soluble in warm water or organic solvents (Patterson et al., 1976c; Yinon, 1990). HMX is an impurity in production grade RDX, which is generally acceptable. The Bachmann process usually yields 80-85% RDX with 10% HMX as impurity. By modifying this process, one can obtain 55-60% HMX, with RDX being an impurity (Yinon, 1990; Rosenblatt et al., 1991).

HMX is a Class D Carcinogen. This means that its chemical nature suggests that it might be carcinogenic, but no toxicity or carcinogenicity studies have been performed to show that it is not a carcinogen. Nevertheless its primary toxic effect is cardiovascular depression, and it has adverse effects on mammals' central nervous system when taken at a significantly higher dosage than RDX (McLellan et al., 1988b). HMX is poorly absorbed when administered orally to mice or rats, and it has adverse hepatic and renal effects on the animals. Although there have not been any adverse effects found among workers exposed to HMX in munition plants, patch testing with solid HMX can cause skin irritation among humans (Ryon et al., 1984; McLellan et al., 1988b). The Lifetime Health Advisory for exposure to HMX for a 70 kg adult is 0.40 mg/L, but the threshold limit value for HMX has not been designated (McLellan et al., 1988b). Gibbs et al.

Table 1 Properties and Toxicity of RDX and HMX^a

	RDX	HMX
Chemical Formula	C ₃ H ₆ N ₆ O ₆	C ₄ H ₈ N ₈ O ₈
CAS Registry Number	121-82-4	2691-41-0
Synonyms	Cyclonite, T4, hexogen, cyclotrimethylenetrinitramine, hexahydro-1,3,5-trinitro-1,3,5-triazine, 1,3,5-triaza-1,3,5-trinitrocyclohexane, 1,3,5-trinitro-1,3,5-triazacyclohexane, sym-Trimethylenetrinitramine, 1,3,5-Trinitrohexahydro-s-triazine	Octogen, cyclotetramethylenetetranitramine, octahydro-1,3,5,7-tetranitro-1,3,5,7-tetrazocine, 1,3,5,7-tetranitro-1,3,5,7-tetrazacyclooctane, RRI, Octahydro-1,3,5,7-tetranitroazocine
Molecular Weight	222.26 amu	296.16 amu
Melting Point	202°C, 204.1°C, 205°C	246°C, 286°C
Density	1.83 g/cm ³	1.96 g/cm ³ (beta form)
Aqueous Solubility @ 25°C	40-60 mg/L	4-5 mg/L
@ 20°C	50-70 mg/L 7.6-42.3 mg/L	
Vapor Pressure @ 25°C	4.03 x 10 ⁻⁹ torr	3.33 x 10 ⁻¹⁴ torr
U.S. EPA Carcinogenic Classification	Class C ^b	Class D ^c
Toxicity	Adverse Effects on Mammals' Central Nervous System	Adverse Effects on Mammals' Central Nervous System at a Significantly Higher Dosage than RDX
Lifetime Health Advisory	0.002 mg/L	0.40 mg/L
Threshold Limit Value	1.5 mg/m ³	Has not been designated

^aData collected from McLellan et. al., 1988a & b; Rosenblatt et. al., 1991; Schneider et. al., 1976; Wilkie, 1994; Yinon, 1990;

^bClass C: possible human carcinogen; limited evidence of carcinogenicity in animals and insufficient data in humans

^cClass D: not classified as carcinogen; no evidence from animal studies

(1980) suggested a maximum concentration of 1.5mg/m^3 HMX of air.

2.3 Principal Treatment Technologies for RDX and HMX

Among all the treatment technologies for removing RDX and HMX, the more common methods include direct chemical hydrolysis, ultraviolet radiation, polymeric adsorption, biological degradation, and AC adsorption. This section briefly discusses all the methods listed above, but AC adsorption will be examined further in the later part of this thesis.

2.3.1 Alkaline Hydrolysis

Alkaline hydrolysis of RDX gives byproducts which include nitrite, nitrate, nitrous oxide, ammonia, formate, formaldehyde, formic acid, nitrogen, and hydrogen (Hoffsommer et al., 1977; Yinon, 1990). HMX tends to be more resistant to alkaline hydrolysis than RDX, but the byproducts are similar to that of RDX (Yinon, 1990; Heilmann et al., 1995). Direct chemical hydrolysis is not very practical because the treated effluent needs to be neutralized, and it is only cost-effective for bulk quantities. It is not cost-effective for the concentrations normally found in munitions processing wastewaters. Furthermore, some of the hydrolysates may be hazardous.

2.3.2 Ultraviolet Radiation/Photolysis

UV radiation or photolysis is the dominant fate process for HMX in aquatic environment, and it can degrade RDX rapidly (McLellan et al., 1988a & 1988b). Nevertheless explosives production wastewaters usually contain high concentration of other strong UV absorbents, and exposure of an RDX solution to UV light results in

formation of other pollutants, such as formaldehyde, nitrous oxide, carbon monoxide, and N-nitroso-methylenediamine. (McCormick et al., 1981; McCormick et al., 1984; Yinon, 1990). The treatment cost of generating UV light for large volumes of wastewater is very high, which makes UV uneconomical for high concentrations. Research has been performed using UV and ozone to treat the RDX-laden wastewaters. The method is cost-competitive with GAC adsorption for small systems that treat wastewaters containing 1 to 20 mg/L RDX; however, this treatment method yields cyanic acid, formic acid, formaldehyde, and other byproducts (McCormick et al., 1981; Burrows et al., 1984; Yinon, 1990).

2.3.3 Polymer Adsorption

Using polymeric adsorption for treating explosives-contaminated wastewater is a relatively new idea. Szachta (1978) compared carbon and resin adsorption for treating pink water. His research showed that AC and Amberlite XAD-4 were capable of removing TNT and other nitrocompounds, such as RDX and HMX, from munition wastewaters to target level of less than 1 mg/L total nitrocompounds. Furthermore, Amberlite XAD was found to have greater capacity for TNT than AC. AC had higher capacity for RDX and HMX, and better color-removal than Amberlite XAD. While the cost of carbon and polymeric resin adsorption varied from plant to plant, Szachta concluded that AC with regeneration capacity was consistently more cost-effective than resin adsorption.

2.3.4 Biological Treatment

Biological treatment can be grouped into two main categories: aerobic and anaerobic processes. Aerobic transformation of RDX and HMX is not possible, but anaerobic and anoxic (with nitrate as the electron acceptor) transformation is possible. (Spanggord et al., 1980; McCormick et al., 1981; Hesselmann et al., 1992). Sublette et al. (1992) found that aerobic white-rot fungus *Phanerochaete Chrysosporium*, when put under specialized conditions, could treat pink water efficiently by using a rotating biological contractor.

More research work has been performed on anaerobic biotransformation of explosives. Spanggord et al. (1980) found that RDX transformation was a cometabolic process in which RDX and a cosubstrate, such as yeast extract, must be present at the same time to ensure RDX transformation. Anaerobic transformation of RDX was known to yield byproducts such as hydrazine, formaldehyde, and methanol, but no hydrazine was detected from McCormick et al.'s continuous cultures even though a trace amount of hydrazine was found in their batch studies (McCormick et al., 1981; McCormick et al., 1984). As RDX was being transformed, various reduced forms of RDX were produced. Some of these products were found to be carcinogenic (McCormick et al., 1981). Some researchers have considered using aerobic biological systems to further degrade these hazardous intermediates.

Hesselmann (1992) found that anoxic transformation of RDX was fortuitous cometabolism. Furthermore, he found that RDX transformed under fermentative, sulfate-

reducing, and nitrate-reducing conditions. Wilkie employed Hesselmann's idea and tried to degrade RDX in two steps: first, adsorbing RDX onto AC with subsequent solvent desorption; second, the regeneration fluid was treated using mixed culture of denitrifying bacteria. The continuous-flow anoxic biotransformation was effective. Both Hesselmann and Wilkie found that ethanol was the best cosubstrate among various organic solvents, such as acetone and methanol, because the alcohol gave the highest growth rate and highest transformation rate of RDX. Wilkie's experimental data also showed that RDX transformation could be enhanced by increasing temperature.

HMX tends to be more resistant to biological treatment. In Hesselmann's study, considerable disappearance of HMX occurred only under nitrate-reducing conditions. McLellan et al. (1988b) found that 100% removal of HMX was possible under anaerobic fermentative conditions with carbon sources as supplements.

McCormick et al. (1984) tried the concurrent removal of RDX, HMX, and their N-acetylated derivatives using microbiological denitrifying systems. RDX transformed faster than HMX. While HMX showed resistance to biotransformation, there was complete disappearance of RDX when molasses, acid hydrolyzed sludge, alkaline hydrolyzed sludge, or nutrient broth was used as a medium. Due to lower transformation rate of HMX, longer retention time and increased amount of supplemental nutrients are required for satisfactory HMX transformation. Addition of phosphate, basal salts, and rich organic sediments was also able to stimulate RDX and HMX disappearance, and low oxidation reduction potential was linked to successful denitrification.

2.3.5 Activated Carbon Adsorption

AC adsorption is the current industrial method for treating pink water, and it is being considered as a treatment technology for contaminated groundwater. Considerable research has been performed on carbon adsorption of explosives, and a discussion of this research is in the last section of this chapter.

Although AC adsorption is a very popular method for treating explosives, there has been concern regarding the danger of explosives-laden carbon. If the carbon can be regenerated, and if the regeneration fluid, which contains the explosives' byproducts, can be further treated using some satisfactory means, then the problem can be solved. Research on a combined chemical and biological treatment process for explosives is currently underway at UCLA. Under the treatment process, explosives are adsorbed onto AC which will be regenerated using alkaline hydrolysis. The hydrolysates, some of which are hazardous, will then be transformed using anoxic biotreatment. If this combined treatment is successful in transforming RDX and HMX to nonhazardous material, then AC adsorption will play a very important role in removing explosives from wastewater or groundwater in the future. Since the carbon can be recycled, the overall treatment cost will be reduced immensely.

2.4 Adsorption Isotherm Models

Generally speaking, adsorption isotherm models are used for describing how sorbate concentration is related to sorbent concentration during adsorption at constant temperature. Usually the sorbent and sorbate concentration are proportional to each

other, but they are not necessarily related to each other by a single constant. Different isotherm models have different assumptions in order to simplify the isotherm expressions while trying to maintain the accuracy of the predictions. Isotherms have wide applications in the environmental field because they can be used for predicting the amount of sorbent, such as carbon or resin, required to achieve the desired sorbate or contaminant concentration.

Among all the existing isotherms, the classical ones are the Langmuir, the Freundlich, and the BET isotherms. Isotherms can also be divided into monocomponent and multicomponent models. This section first discusses the classical monocomponent isotherms and their corresponding multicomponent forms. Other multicomponent isotherms are reviewed next. They include Crittenden et al.'s Ideal Adsorbed Solution (IAS)-Freundlich Isotherm (1985), Fritz et al.'s IAS-Freundlich Model (1981), the Simplified Ideal Adsorbed Solution (SIAS) Isotherm, the Improved Simplified Ideal Adsorbed Solution (ISIAS) Isotherm, and the Ideal Adsorbed Solution (IAS) Model. Although various isotherms are derived from the IAS Model, the IAS Model is discussed last due to its complexity. A summary of the multicomponent isotherms is presented in Table 2.

2.4.1 Monocomponent Isotherm Models

2.4.1.1 Langmuir Monocomponent Isotherm

The Langmuir adsorption model is only valid for single-layer adsorption, and it assumes that the maximum adsorption corresponds to a saturated monolayer of solutes on

the adsorbent surface. According to the Langmuir model, there are a fixed number of sites available on the adsorbent surface, and all sites have the same adsorption energy. Furthermore, each molecule adsorbed is affixed to a specific site, and there is no transmigration of adsorbate in the plane of surface (Keinath, 1971; Weber, 1972).

The Langmuir isotherm has the following form:

$$q_e = \frac{Q^o b C}{(1 + b C)} \quad (2.1)$$

where q_e = mass of solute or sorbate per unit mass of adsorbent;

C = equilibrium concentration of the solutes;

Q^o = maximum adsorption capacity, i.e. maximum mass of solute per unit mass of adsorbent, and

b = Langmuir constant which corresponds to adsorption energy.

Linearizing the isotherm gives

$$\frac{1}{q_e} = \frac{1}{Q^o} + \left(\frac{1}{bQ^o}\right)\left(\frac{1}{C}\right) \quad (2.2)$$

with $1/q_e$ as a function of $1/C$. Although the Langmuir assumptions seem too ideal for actual adsorption systems, the isotherm has been found useful in data interpretation; for example, while Q^o may not be the monolayer's maximum capacity, it can represent the overall maximum adsorption capacity for certain sorbate-sorbent system which exhibits multilayer adsorption behavior (Weber, 1972). When one decides to use the Langmuir isotherm to interpret the data, one should be aware that this isotherm does not provide adequate fit for many single-solute systems. Overall the Langmuir isotherm is useful in

comparing adsorption behavior for various adsorbate-adsorbent systems and for the same system under different experimental conditions.

2.4.1.2 Brunauer, Emmett, Teller (BET) Isotherm

The BET model assumes multilayer adsorption, and multiple, incomplete layers are possible. Both the Langmuir and the BET isotherm share the assumption that the adsorption system is homogeneous; therefore, there is uniform energy of adsorption on the surface. Furthermore, the Langmuir isotherm applies to each layer defined by the BET model. (Keinath, 1971; Weber, 1972).

From the above assumptions, the BET isotherm for adsorption from solution becomes

$$q_e = \frac{BCQ^o}{(C_s - C)[1 + (B - 1)(C/C_s)]} \quad (2.3)$$

where C_s = saturation concentration of the solute, and

B = BET constant pertaining to energy of interaction with the surface.

The other variables are defined as before. It is easier to interpret the data using the linearized BET equation, as follows:

$$\frac{C}{(C_s - C)q_e} = \frac{1}{BQ^o} + \left(\frac{B-1}{BQ^o}\right)\left(\frac{C}{C_s}\right), \quad (2.4)$$

and plot $C/(C_s - C)q_e$ versus C/C_s (Weber, 1972).

2.4.1.3 Freundlich Monocomponent Isotherm

The Freundlich isotherm is also referred as the van Bemmelen isotherm (Weber,

1972). Unlike the Langmuir and the BET models, the Freundlich model assumes heterogeneous surface energies for adsorption, and adsorption energies are distributed exponentially. The surface coverage for each energy level can be represented by the Langmuir equation (Weber, 1972; Sheindorf et al., 1981). Although this isotherm is purely empirical, the Freundlich isotherm agrees quite well with the Langmuir isotherm and experimental data over moderate range of concentrations. The Freundlich isotherm is also widely used, especially for water or wastewater treatment processes that use AC because its surfaces are heterogeneous (Weber, 1972).

The Freundlich isotherm is

$$q_e = KC^{1/n} \quad (2.5)$$

where K = Freundlich parameter that corresponds to total adsorption capacity, and

$1/n$ = Freundlich parameter that indicates adsorption intensity.

The Freundlich isotherm can be linearized and written as

$$\ln q_e = \ln K + \frac{1}{n} \ln C \quad (2.6)$$

The parameters K and n can be identified by plotting $\ln|q_e|$ versus $\ln|C|$. The slope of the line is $1/n$, and the intercept is $\ln|K|$. A higher slope (small n) represents lower adsorption energy, and a lower slope (large n) corresponds to higher adsorption energy (Weber, 1972). Some researchers write the Freundlich isotherm as

$$q_e = KC^n \quad (2.7)$$

In this case, the interpretation of n will need to be adjusted accordingly.

2.4.2 Multicomponent Isotherm Models

2.4.2.1 Langmuir Multicomponent Isotherm

The Langmuir Multicomponent model was first developed by Butler and Ockrent (McKay et al., 1989). For n components in one adsorption system, the isotherm expression is

$$q_{e,i} = \frac{Q_i^0 b_i C_i}{1 + \sum_{j=1}^n b_j C_j} \quad (2.8)$$

This model is only applicable when each adsorbate in the multicomponent system obeys the Langmuir monocomponent adsorption behavior. For a bisolute system, the linear form of the isotherm becomes

$$\frac{C_1}{C_2 q_{e,1}} = \frac{b_2}{b_1 Q_1^0} + \frac{C_1}{C_2 Q_1^0} \quad (2.9a)$$

$$\frac{C_2}{C_1 q_{e,2}} = \frac{b_1}{b_2 Q_2^0} + \frac{C_2}{C_1 Q_2^0} \quad (2.9b)$$

where $1,2$ = subscripts representing the two species in the bisolute system.

The primary assumptions of this model are the same as that for the Langmuir single-component model: homogeneous surface energies of adsorption; no interaction between adsorbed species; single-layer adsorption; equal availability of adsorption sites to all species; reversible adsorption, and maximum adsorption equivalent to saturated monolayer adsorption of solutes (Keinath, 1971; Weber, 1972; McKay et al., 1989; Tchobanoglous et al., 1991). One major criticism of this model is that it violates the

Gibbs adsorption equation and it is thermodynamically inconsistent (Radke et al., 1972b). The fact that the Langmuir isotherm does not usually fit single-solute isotherm data very well may discourage one from using its multicomponent form; however, this isotherm is probably the most commonly known, and hence, it is good as a basis for comparing various models.

2.4.2.2 Langmuir Extension- First Approximation Model

Since the Langmuir Multicomponent Isotherm is very general and does not always fit data very well, some researchers modified it to predict adsorption of two competitive isomers (Lin et al., 1989). In order to extend the Langmuir isotherm to account for this competition, one additional assumption is made: the rate of adsorption and desorption of each compound are linear functions of both compounds' concentrations in the stationary and the mobile phases respectively. This means that there are molecular interactions in both the solution and the sorbed monolayer.

As a first approximation, the influence of species i 's concentration on species j 's rate of desorption is neglected, and the modified isotherm for the binary system becomes:

$$q_1 = \frac{A_1 C_1 + A_{12} C_1 C_2}{1 + B_1 C_1 + B_2 C_2 + B_{12} C_1 C_2} \quad (2.10a)$$

$$q_2 = \frac{A_2 C_2 + A_{21} C_1 C_2}{1 + B_1 C_1 + B_2 C_2 + B_{12} C_1 C_2} \quad (2.10b)$$

There is no linearized form for this isotherm. Apart from the Langmuir single-solute parameters A_i and B_i which correspond to Q^0 and b in the Langmuir Monocomponent Isotherm for species i , the cross terms A_{ij} and B_{ij} are used to account for the interactions

between the two components in the mixture. These cross terms depend on the rate constant of adsorption and desorption of the two components, and their molecular interaction (Lin et al., 1989). One can use least squares fitting to determine these cross terms, but the process is rather time-consuming. The researchers who derived this isotherm restricted its application to competitive isomers; however, its application for other compounds have not been explored. For the adsorption experiment of the competitive isomers, the experimental data and the calculated values from the isotherm was better for high concentration than for low concentration.

2.4.2.3 Langmuir Partially Competitive Multicomponent Isotherm

Since the Langmuir Multicomponent Isotherm assumes complete competition, Jain and Snoeyink (1973) modified the isotherm so that it would allow partial competition during adsorption of two species. The isotherm is as follows:

$$q_1 = \frac{(Q_1^0 - Q_2^0)b_1C_1}{1 + b_1C_1} + \frac{Q_2^0b_1C_1}{1 + b_1C_1 + b_2C_2} \quad (2.11a)$$

$$q_2 = \frac{Q_2^0b_2C_2}{1 + b_1C_1 + b_2C_2} \quad (2.11b)$$

where $Q_1^0 > Q_2^0$, and

Q_i^0 = the maximum loading of species i.

The hypotheses for this isotherm are (i) adsorption without competition occurs when Q_1^0 does not equal to Q_2^0 , and (ii) the number of sites for which there is no competition is equal to $(Q_1^0 - Q_2^0)$, where $Q_1^0 > Q_2^0$. When $Q_1^0 = Q_2^0$ there is absolute competition and hence, this isotherm will reduce to the original Langmuir Multicomponent Isotherm.

The first term of the q_i accounts for the mass of species 1 adsorbed without competition on surface area which is proportional to $(Q_1^0 - Q_2^0)$. The second term, which is based on the original Langmuir Multicomponent Isotherm, refers to the mass of species 1 adsorbed on surface area that is proportional to Q_2^0 under competition with species 2. The q_2 expression is the mass of species 2 adsorbed on surface area that is proportional to Q_2^0 under competition with species 1. This isotherm is only applicable to bisolute systems which involve solutes with large differences in molecular size or chemical properties (Jain et al., 1973; McKay et al., 1989).

2.4.2.4 Freundlich Multicomponent Isotherm

Sheindorf et al. (1981) derived the Freundlich Multicomponent Isotherm from the Freundlich Monocomponent Isotherm $q_e = KC^n$. As mentioned earlier, the Freundlich single-solute isotherm can be expressed in two different ways; nevertheless, the basic concept is generally the same. The main criterion for using this model is that each component individually obeys the Freundlich Monocomponent Isotherm. It is assumed that for each component, there is an exponential distribution of adsorption energy which is equivalent to the distribution function in the monocomponent system. While the multicomponent isotherm takes the form

$$q_i = K_i C_i \left(\sum_{j=1}^k a_{ij} C_j \right)^{n_i - 1}, \quad (2.12)$$

the isotherm for a bisolute system is as follows:

$$\frac{C_1}{C_2} = \frac{1}{C_2} \beta_1 - a_{12} \quad (2.13a)$$

$$\frac{C_2}{C_1} = \frac{1}{C_1} \beta_2 - a_{21} \quad (2.13b)$$

To put equations (2.13a) and (2.13b) in a simple linearized form, they become

$$C_1 = \beta_1 - a_{12}C_2 \quad (2.14a)$$

$$C_2 = \beta_2 - a_{21}C_1 \quad (2.14b)$$

where $\beta_i = \left(\frac{K_i C_i}{q_i}\right)^{\frac{1}{1-n_i}}$;

a_{ij} = the competition coefficient for the system, and

$a_{ij} = 1/a_{ji}$.

There are two different ways to determine a_{ij} , and the method of determination depends on the adsorption process. If one component's concentration is kept constant throughout the adsorption process, one can plot C_i versus β_i . The slope of the line will be 1, and the intercept will be $-a_{ij}C_j$. If both components vary in concentration during adsorption, then one should plot C_i/C_j versus β_i/C_j (for $i \neq j$). The slope of the line remains 1, but the intercept will be $-a_{ij}$. If one set of single-solute Freundlich parameters (K_i, n_i) represents a restricted range of equilibrium concentrations, then various sets of adsorption coefficients are necessary to describe other ranges of concentrations.

LeVan et al. (1981) criticized the Freundlich isotherm because it failed to satisfy the Gibbs adsorption isotherm. Since the Freundlich isotherm fits many single-solute systems very well, there is incentive to use its multicomponent form. Sheintuch et al. (1988) reported that this model has been successful in fitting bisolute and trisolute systems.

2.4.2.5 Empirical Bisolute Extension of the Freundlich Isotherm

The bisolute isotherm was proposed by Fritz et al. (1981) and was defined as follows:

$$Y_1 = \frac{a_1 X_1^{b_1+b_{11}}}{X_1^{b_{11}} + a_{12} X_2^{b_{12}}} \quad (\lim_{c_2 \rightarrow 0} Y_1 = a_1 X_1^{b_1}) \quad (2.15a)$$

$$Y_2 = \frac{a_2 X_2^{b_2+b_{22}}}{X_2^{b_{22}} + a_{21} X_1^{b_{21}}} \quad (\lim_{c_1 \rightarrow 0} Y_2 = a_2 X_2^{b_2}) \quad (2.15b)$$

It is also based on $Y_1 = a_1 X_1^{b_1}$ or $q_e = KC^n$. This isotherm has rarely been used, but it has been shown to fit some bisolute data better than Crittenden et al.'s (1985) IAS-Freundlich Isotherm, which is explained next (Sheintuch et al., 1988). The parameters a_1 , a_2 , b_1 , and b_2 are from the single-solute Freundlich isotherm (K_1 , K_2 , n_1 , n_2), and the six parameters, such as a_{ij} and b_{ij} , need to be derived from experimental data.

2.4.2.6 Crittenden et al.'s IAS-Freundlich Isotherm

This isotherm is one of the many that tries to simplify the IAS Model, and it uses only one set of Freundlich parameters for the spreading pressure equation. The explicit

nature of this isotherm also makes calculations easier (Crittenden et al., 1985). For n components the IAS-Freundlich equation is:

$$c_i = \frac{q_i}{\sum_{j=1}^N q_j} \left(\frac{\sum_{j=1}^N n_j q_j}{n_i K_i} \right)^{n_i} \quad (2.16)$$

where i, j = sorbates in the multicomponent system.

For a two-component system, the above equation becomes

$$c_1 = \frac{q_1}{q_1 + q_2} \left(\frac{n_1 q_1 + n_2 q_2}{n_1 K_1} \right)^{n_1} \quad (2.17a)$$

$$c_2 = \frac{q_2}{q_1 + q_2} \left(\frac{n_1 q_1 + n_2 q_2}{n_2 K_2} \right)^{n_2} \quad (2.17b)$$

Crittenden et al.'s IAS-Freundlich Isotherm is based on the Freundlich equation $q_e = KC^{1/n}$, and it requires only one set of Freundlich parameters for each component because no curvature is observed in their single-solute isotherms. Consequently, any system that utilizes this isotherm must have all its adsorbates assume linear behavior in the Freundlich single-solute log-log plots. If there is significant error in calculating the spreading pressure due to extrapolation of the Freundlich isotherm to high and zero surface coverages, this isotherm cannot be used. This isotherm was successful in representing competitive adsorption of similar volatile organic compounds in a bisolute, trisolute, and six-solute system. The propriety of using this isotherm to account for adsorption of

dissimilar solutes was unknown to the researchers, and Sheintuch et al. (1988) suggested that the isotherm's predictions were not always satisfactory.

2.4.2.7 Fritz & Schlunder's IAS-Freundlich Model

This model is another simplification of the IAS Model, but it is very different from Crittenden et al.'s IAS-Freundlich Isotherm. Fritz and Schlunder's model (1981) is based on $Y_i = a_{i,k} X_i^{b_{i,k}}$ (which is equivalent to $q_{e,i} = K_{i,k} C_i^{n_{i,k}}$) and is written as follows:

$$\frac{Y_1^o}{b_{1,k}} - C_{1,k} = \frac{Y_2^o}{b_{2,k}} - C_{2,k} \quad (2.18)$$

$$X_1 = X_1^o Z_1 \quad (2.19)$$

$$X_2 = X_2^o (1 - Z_1) \quad (2.20)$$

$$\frac{Y_1}{Y_1^o} + \frac{Y_2}{Y_2^o} = 1 \quad (2.21)$$

Equation (2.18) is a relation derived from the integral of the IAS Model's spreading pressure theory. Spreading pressure is defined as the difference between interfacial tension of the pure solvent-solid interface and that of the solution-solid interface at the same temperature (Radke et al., 1972b). Equation (2.19) to (2.21) are taken directly from the IAS Model. The variables in the above four equations are defined as follows:

k = numerical index indicating concentration range in which the constant $a_{i,k}$ and

$b_{i,k}$ are valid;

C = integration constant from the integral for spreading pressure (mmol/g);

X = fluid-phase concentration (mmol/L);

Y = carbon loading (mmol/g);

z = mole fraction in adsorbed phase, and

o = as superscripts, refers to single-solute data.

As one can see, this model does not have an explicit equation that relates the equilibrium liquid concentration to the sorbed concentration. The model can use as many sets of Freundlich parameters as necessary in order to adequately represent different concentration ranges (Fritz et al., 1981). The conclusion is that it will require a lot of computational work, and it is not recommended (Yen et al., 1984).

2.4.2.8 Simplified Ideal Adsorbed Solution (SIAS) Isotherm

The SIAS model is simple and is based on the same concepts as the IAS Model.

As shown from the isotherm below

$$q_i = K' \left(\frac{n'-1}{n'} \right) \left[K_i C_i^{n_i} \right]^{\frac{1}{n'}} \left[\sum_N \left(\frac{K_i}{K'} C_i^{n_i} \right)^{\frac{1}{n'}} \right]^{(n'-1)}, \quad (2.22)$$

the number of equations required is the same as the number of components in the adsorption system, and these equations do not need to be solved simultaneously. n_i and K_i are the Freundlich single-solute parameters for species i , and the Freundlich isotherm is defined as $q_e = KC^n$. n' and K' are the average values of n_i and K_i respectively.

DiGiano et al. (1978) studied this isotherm to describe the adsorption of phenolic compounds, and their data showed that the IAS Model and the SIAS Isotherm agreed with each other within the equilibrium concentration range of 0.01 to 0.1mmol/L. For higher concentration ranges, the two models differed. The SIAS Isotherm is capable of

producing identical results with the IAS Model if the components are isomers with identical single-solute isotherms. For compounds with different isotherms and compounds which need only one Freundlich isotherm to describe the entire concentration range, the SIAS Isotherm will also give identical results as the IAS's Model if the values of n for all species are the same. If the n and K values for all species are not the same, and when several sets of parameters are required to cover various concentration ranges, the SIAS Isotherm can only approximate the IAS Model. Furthermore, the ability of the SIAS Isotherm to predict the IAS Model's results declines with increasing differences between the n values which associate with the concentration range of interest. The reason is the differences between n values make n' in the SIAS Isotherm less representative.

2.4.2.9 Improved Simplified Ideal Adsorbed Solution (ISIAS) Isotherm

The ISIAS Isotherm was derived to account for adsorption behavior which both the IAS Model and the SIAS Isotherm failed to predict. It is similar to the SIAS Isotherm in terms of the equation. The main difference is the inclusion of the competition coefficient (η_i) which correlates with a solubility factor. By adding a competition factor, the ISIAS Isotherm can be used to account for nonideal competition during adsorption. The ISIAS Isotherm is written as follows:

$$q_i = K' \left(\frac{n'-1}{n'} \right) \left[\frac{K_i}{\eta_i} C_i^{n_i} \right]^{\frac{1}{n'}} \left[\sum_N \left(\frac{K_i / \eta_i}{K'} C_i^{n_i} \right)^{\frac{1}{n'}} \right]^{(n'-1)} \quad (2.23)$$

$$K' = \frac{\sum K_i / \eta_i}{N}$$

where

Yonge et al. (1986) used Statistical Analysis Systems (Barr, 1976) to determine an η_i that gave the lowest residual sum of squares of the competitive adsorption data. For a bisolute system, species 2 is the less competitive of the two species and it has higher solubility. The competition factor η_2 associates with species 2 and it is a function of the solubility factor

$$(\delta_2 - \delta_1) / \delta_2$$

where δ_i = sorbate i 's solubility, and

$$\delta_2 > \delta_1.$$

Since η_1 does not seem to improve data interpretation as much as η_2 , the researchers suggest setting η_1 to 1.

There is no known application of this isotherm except the one presented by the authors of the isotherm. Yonge et al. studied various bisolute adsorption systems composed of phenol, o-cresol, o-methoxyphenol, 4-isopropylphenol, and 2-ethyl phenol. They found that the ISIAS Isotherm described the systems better than the Langmuir Multicomponent Isotherm, the Langmuir Partially Competitive Isotherm, the IAS Model, and the SIAS Isotherm. Although the authors did not specify the ideal conditions for this

isotherm, they implied that the ISIAS Isotherm was a good alternative for data description when nonideal competition was being considered.

2.4.2.10 Ideal Adsorbed Solution (IAS) Model

Among all the multicomponent isotherms, the most complex one is the IAS Model. Perhaps the complexity of this model is justified when one considers its accuracy in predicting adsorption systems involving dilute solutions. The IAS Model can predict multicomponent adsorption behavior from single-solute adsorption from dilute solution. The IAS Model is based on the thermodynamics of adsorption from dilute solution, and it assumes the adsorbent has identical specific surface area for all adsorbates. When solutes adsorb simultaneously from dilute solution at constant temperature and spreading pressure, the adsorbed phase forms an ideal solution, hence the name Ideal Adsorbed Solution Model (Radke et al., 1972b).

In order to understand the IAS Model, the role of spreading pressure (π) in the model must not be underestimated. The spreading pressure of species i (π_i) is related to the equilibrium concentration of species i (c_i^o) in the following way:

$$\pi_i = \frac{RT}{A} \int_0^{c_i^o} \frac{q_{e,i}(c_i^o)}{c_i^o} dc_i^o \quad (2.24)$$

where R = ideal gas constant ;

T = absolute temperature;

A = surface area of the adsorbent;

o = as superscripts, refers to single-solute data;

$q_{e,i}^o$ = the solid phase concentration loading, and

$q_{e,i}^o(c_i^o)$ = any single-solute isotherm equation used for describing species i and it

is usually a function of species i's equilibrium concentration (c_i^o).

For a bisolute system, there will be two spreading pressure functions:

$$\pi_i = f_1(c_i^o) \quad (2.25a)$$

$$\pi_j = f_2(c_j^o) \quad (2.25b)$$

There are other important relations for a bisolute IAS Model. These relations are

$$c_i = c_T x_i = c_i^o z_i \quad (2.26a)$$

$$c_T x_j = c_j^o (1 - z_j) \quad (2.26b)$$

$$\sum_{i=1}^N z_i = z_i + z_j = 1 \quad (2.27)$$

$$q_{e,i} = q_{e,T}^* z_i \quad (2.28)$$

$$\frac{1}{q_{e,T}} = \sum_{i=1}^N \frac{z_i}{q_{e,i}^o} = \sum_{i=1}^2 \frac{z_i}{q_{e,i}^o} \quad (2.29)$$

where z_i = the mole fraction of i in the adsorbed phase;

x_i = the liquid phase solvent-free mole fraction of i, and

c_T = the total concentration of all solutes in liquid phase.

Since single-solute concentrations are defined at the same spreading pressure as that of the mixture, $\pi_i = \pi_j = \pi_{\text{mix}}$. In order to solve for c_i and c_j in the bisolute adsorption system,

one must first define the adsorbent mass and the initial liquid concentration for i and j .

From solving equation (2.25) to (2.29) together with the mass balance equation

$$q_{e,i} = \frac{(c_{i,0} - c_i)V}{M} \quad (2.30)$$

all the variables can be found for each z_i value assumed. Various z_i values have to be assumed until there is one that satisfies the constraint $\pi_i = \pi_j = \pi_{\text{mix}}$.

Although the above equations are only applicable for a 2-component system, the method and the equations can be extended to n components. As n increases, the number of equations that have to be solved simultaneously increases. Consequently the number of computations increases proportionally with the number of adsorbates (Radke et al., 1972b; Singer et al., 1980).

The IAS Model is good for predicting volatile organic solutes' system at low coverages, but the calculated values and experimental data differ from each other at high sorbed concentration or for more strongly adsorbing solutes. This deviation may attribute to the nonidealities in the adsorbed phase (Radke et al., 1972b). In general, the IAS Model becomes decreasingly reliable as the adsorption loading increases from moderate to high. For high solute loading, the IAS Model's assumptions may need to be modified to account for solute interactions on the sorbent. Singer et al. (1980) found that the IAS Model successfully characterized competitive adsorption among alkyl phenols in bisolute and trisolute systems. Satisfactory predictions of the IAS Model are also reported by Annesini et al. (1987).

2.4.2.11 Polanyi Adsorption Potential Theory

Polanyi's model (Rosene et al., 1976) has three main assumptions:

- (i) adsorption isotherms of a number of individual solids from a given solvent, when expressed in terms of volume adsorbed versus adsorption potential per unit volume, can generate correlation curves that are identical except for an abscissa scale factor;
- (ii) individual solutes are mutually insoluble as solids or as adsorbates;
- (iii) different solids may occupy different regions in adsorption space.

This theory is good for estimating adsorption of a trace component while the other components are at near saturated concentration. Like the IAS Model, the mathematical complexity increases with the number of components. When Aytakin (1991) tried to apply Polanyi's Theory to phenol and its derivatives over wide range of equilibrium concentrations, the theoretical calculations were very different from the experimental values. The application of this isotherm is not useful for this thesis because the theory is valid for adsorption of partially miscible solutes from dilute solution, or for solutes that can undergo separation into a nearly pure solute phase (Radke et al., 1972a). Since RDX and HMX are soluble in water, Polanyi's theory cannot describe the explosives'

Table 2 Multicomponent Adsorption Isotherms/Models

Isotherm Names	Isotherm Equations	Remarks
Langmuir Multicomponent Isotherm (Weber, 1972)	$q_{e,i} = \frac{Q_i^o b_i C_i}{1 + \sum_{j=1}^n b_j C_j}$ <p>or in bisolute linear form</p> $\frac{C_1}{C_2 q_{e,1}} = \frac{b_2}{b_1 Q_1^o} + \frac{C_1}{C_2 Q_1^o}$ $\frac{C_2}{C_1 q_{e,2}} = \frac{b_1}{b_2 Q_2^o} + \frac{C_2}{C_1 Q_2^o}$	<ul style="list-style-type: none"> • Assumptions: i. each component obeys monocomponent Langmuir behavior ii. reversible, single layer, and homogeneous surface adsorption iii. all adsorption sites are equally available to all species • Advantages: i. this model is good to use as a reference when compared with other models ii. parameters are derived from single-solute data • Disadvantages: i. violated Gibbs adsorption equation and thermodynamically inconsistent ii. difficult to find adsorption behavior following Langmuir behavior, too ideal; or Langmuir cannot provide reasonable fit for many single-solute isotherm data • b_j: Langmuir parameters • Q_i^o: maximum sorbed concentration of species i
Langmuir Extension--First Approximation Model (Lin et al., 1989)	$q_1 = \frac{A_1 C_1 + A_{12} C_1 C_2}{1 + B_1 C_1 + B_2 C_2 + B_{12} C_1 C_2}$ $q_2 = \frac{A_2 C_2 + A_{21} C_1 C_2}{1 + B_1 C_1 + B_2 C_2 + B_{12} C_1 C_2}$	<ul style="list-style-type: none"> • Assumptions: i. rates of adsorption and desorption of each compound are linear functions of the concentrations of both compounds in the sorbed phase and in the liquid phase, i.e. molecular interaction in both solution and solid phase ii. one component's concentration has no influence on the other's rate of desorption • Advantage: i. the model is good for competitive isomers at high concentrations • Disadvantage: i. accounts for some experimental data at low concentrations ii. requires multicomponent data and least square fitting of data to derive the cross terms

Table 2 (Continue)

Isotherm Names	Isotherm Equations	Remarks
Langmuir Extension--First Approximation Model		<ul style="list-style-type: none"> • A_i, B_i: Langmuir monocomponent isotherm's parameters for species i (i.e. Q_i°, b_i) • A_{ij}, B_{ij}: cross terms that account for interactions between species i & j; they are functions of adsorption and desorption rate constants
Langmuir Partially Competitive Multicomponent Isotherm (Jain et al., 1973)	$q_1 = \frac{(Q_1^\circ - Q_2^\circ)b_1C_1}{1 + b_1C_1} + \frac{Q_2^\circ b_1C_1}{1 + b_1C_1 + b_2C_2}$ $q_2 = \frac{Q_2^\circ b_2C_2}{1 + b_1C_1 + b_2C_2}$ <p>$Q_1^\circ > Q_2^\circ$</p>	<ul style="list-style-type: none"> • Assumptions: i. partial competition between species during adsorption ii. adsorption without competition occurs when $Q_1^\circ < Q_2^\circ$ iii. number of sites for which there is no competition is: $Q_1^\circ - Q_2^\circ$ • Advantage: i. valid for bisolute systems involving dissimilar solutes ii. account for partial competition instead of complete competition iii. parameters are derived from single-solute data • Disadvantage: i. isotherm is not applicable for more than two species • Q_i°: maximum loading of species i
Freundlich Multicomponent Isotherm (Sheindorf et al., 1981)	$q_i = K_i C_i \left(\sum_{j=1}^k a_{ij} C_j \right)^{n_i - 1}$ <p>or in bisolute linear form</p> $C_1 = \beta_1 - a_{12} C_2$ $C_2 = \beta_2 - a_{21} C_1$ <p>where $\beta_i = \left(\frac{K_i C_i}{q_i} \right)^{\frac{1}{1-n_i}}$</p>	<ul style="list-style-type: none"> • Assumptions: i. each component obeys Freundlich isotherm $q_e = KC^n$ ii. exponential distribution of adsorption energies for each species • Advantages: i. suitable for highly heterogeneous surface ii. the isotherm was found to represent bisolute and trisolute adsorption data well • Disadvantages: i. only an empirical isotherm ii. may need to use various sets of adsorption parameters to describe all ranges of concentration iii. needs multicomponent data to find a_{ij} • a_{ij}: competition coefficient

Table 2 (Continue)

Isotherm Names	Isotherm Equations	Remarks
Empirical Bisolute Extension of Freundlich Isotherm (Fritz et al., 1981)	$Y_1 = \frac{a_1 X_1^{b_1+b_{11}}}{X_1^{b_{11}} + a_{12} X_2^{b_{12}}} \quad (\lim_{c_1 \rightarrow 0} Y_1 = a_1 X_1^{b_1})$ $Y_2 = \frac{a_2 X_2^{b_2+b_{22}}}{X_2^{b_{22}} + a_{21} X_1^{b_{21}}} \quad (\lim_{c_2 \rightarrow 0} Y_2 = a_2 X_2^{b_2})$	<ul style="list-style-type: none"> • Assumptions: i. $Y_i = a_i X_i^{b_i}$ or $q_e = KC^n$ • Advantage: i. was claimed to fit experimental data better than Crittenden et al.'s IAS-Freundlich Model • Disadvantage: i. the six parameters a_{ij}, b_{ij} need to be determined from multicomponent adsorption data; a lot of computational work ii. no much application is known
IAS-Freundlich Isotherm (Crittenden et al., 1985)	$c_i = \frac{q_i}{\sum_{j=1}^N q_j} \left(\frac{\sum_{j=1}^N n_j q_j}{n_i K_i} \right)^{n_i}$ <p>or for bisolute system,</p> $c_1 = \frac{q_1}{q_1 + q_2} \left(\frac{n_1 q_1 + n_2 q_2}{n_1 K_1} \right)^{n_1}$ $c_2 = \frac{q_2}{q_1 + q_2} \left(\frac{n_1 q_1 + n_2 q_2}{n_2 K_2} \right)^{n_2}$	<ul style="list-style-type: none"> • Assumptions: i. based on the IAS Model and the Freundlich isotherm $q_{e,i} = K_i c_i^{1/n_i}$ • Advantages: i. simpler than the IAS Model and Fritz et al.'s IAS-Freundlich Model ii. simpler than other models because one π equation is used iii. based on single-solute data only iv. equations sufficiently represent adsorption behavior of similar volatile organic compounds sufficiently • Disadvantages: i. cannot be used if single-solute isotherm data show curvature on Freundlich log-log plot ii. can be used only if extrapolation of Freundlich isotherm to high and zero surface coverages do not result in significant errors in calculating π iii. is criticized that the isotherm's predictions are not always satisfactory

Table 2 (Continue)

Isotherm Names	Isotherm Equations	Remarks
IAS-Freundlich Model (Fritz et al., 1981)	$\frac{Y_1^o}{b_{1,k}} - C_{1,k} = \frac{Y_2^o}{b_{2,k}} - C_{2,k}$ $X_1 = X_1^o Z_1$ $X_2 = X_2^o (1 - Z_1)$ $\frac{Y_1}{Y_1^o} + \frac{Y_2}{Y_2^o} = 1$	<ul style="list-style-type: none"> • Assumptions: i. based on Freundlich isotherm $Y_i = a_{ik} X_i^{b_{ik}}$ or $q_e = KC^n$ • Advantage: i. simpler than the IAS Model • Disadvantages: i. involves considerable computational work ii. no explicit equation for sorbed or liquid concentration iii. not recommended by other researchers • k: numerical index indicating the concentration range i constants a_{ik} and b_{ik} are valid • C: integration constant from the integral for spreading pressure (mmol/g) • X: fluid-phase concentration (mmol/L) • Y: carbon loading (mmol/g) • Z: mole fraction in adsorbed phase • o: as superscript, means single-solute data
Simplified Ideal Adsorbed Solution (SIAS) Isotherm (DiGiano et al., 1978)	$q_i = K' \left(\frac{n'-1}{n'} \right) \left[K_i C_i^n \right]^{\frac{1}{n'}} \left[\sum_N \left(\frac{K_i}{K'} C_i^n \right)^{\frac{1}{n'}} \right]^{(n'-1)}$	<ul style="list-style-type: none"> • Assumptions: i. the IAS Model's assumptions ii. $q_e = KC^n$ • Advantages: i. the mathematics are simpler than that of the IAS Model, esp. when there are more than two solutes ii. good agreement between the SIAS Isotherm and the IAS Model under limited conditions; fair prediction for other conditions iii. uses single-solute data for predicting multicomponent data • Disadvantages: i. deviation between the SIAS Isotherm and the IAS Model occurs if there are differences between values of n associating with concentration range of interest ii. for ideal competition only • n', K': average value of n_i, K_i • n, K: Freundlich single-solute parameters

Table 2 (Continue)

Isotherm Names	Isotherm Equations	Remarks
Improved Simplified Ideal Adsorbed Solution (ISIAS) Isotherm (Yonge et al., 1986)	$q_i = K' \left(\frac{c_i^{n-1}}{c_i^n} \right) \left[\frac{K_i}{\eta_i} C_i^n \right]^{\frac{1}{n}} \left[\sum_N \left(\frac{K_i}{K} \eta_i C_i^n \right)^{\frac{1}{n}} \right]^{n-1}$ <p>where $K' = \frac{\sum (K_i / \eta_i)}{N}$</p>	<ul style="list-style-type: none"> • Assumptions: i. $q_e = KC^n$ ii. $\eta_1 = 1$ iii. $\delta_1 > \delta_2$ for a bisolute system • Advantages: i. this model accounts for nonideal system, or nonideal competition ii. equations are simple to use • Disadvantages: i. this model requires multisolute data to determine parameter η_i • η_i: competition factor that correlates with solubility of species i
Ideal Adsorbed Solution (IAS) Model (Radke et al., 1972)	<p>(i) $\pi_i = \frac{RT}{A} \int_0^{c_i^o} \frac{q_{e,i}(c_i^o)}{c_i^o} dc_i^o$</p> <p>(ii) $\pi_i = f_i(c_i^o) \quad \pi_j = f_j(c_j^o)$</p> <p>(iii) $c_i = c_T x_i = c_i^o z_i$ $c_T x_j = c_j^o (1 - z_j)$</p> <p>(iv) $\sum_{i=1}^N z_i = z_i + z_j = 1$</p> <p>(v) $q_{e,i} = q_{e,T} z_i$</p> <p>(vi) $\frac{1}{q_{e,T}} = \sum_{i=1}^N \frac{z_i}{q_{e,i}^o} = \sum_{i=1}^2 \frac{z_i}{q_{e,i}^o}$</p> <p>(vii) $q_{e,i} = \frac{(c_{i,o} - c_i)V}{M}$</p> <p>(viii) $\pi_i = \pi_j = \pi_{mix}$</p>	<ul style="list-style-type: none"> • Assumptions: i. adsorbent has specific surface area identical for all adsorbates i.e. ideal competition ii. when solutes adsorb simultaneously from dilute solution at constant temperature and spreading pressure, the adsorbed phase forms an ideal solution • Advantages: i. good for predicting volatile organic solutes' system in bisolute and trisolute systems ii. model uses data from single-solute adsorption from dilute solution for prediction • Disadvantages: i. model's prediction at moderate or high sorbed concentration is not very good because its assumptions do not take sorbates-sorbent interaction into consideration ii. the mathematics is tedious and complicated iii. for ideal competition • π: spreading pressure • $q_{e,i}$: solid phase concentration loading • $q_{e,i}^o(c_i^o)$: any appropriate isotherm equation • A: surface area of adsorbent

Table 2 (Continue)

Isotherm Names	Isotherm Equations	Remarks
Ideal Adsorbed Solution (IAS) Model		<ul style="list-style-type: none">• R: ideal gas constant• T: absolute temperature• x: liquid phase solvent-free mole fraction of species i• z: adsorbed phase mole fraction of species i• $^{\circ}$: single-solute data• c_i: concentration of species i in liquid phase

adsorption phenomenon.

2.5 Previous Work on Activated Carbon Adsorption of RDX and HMX

As indicated in Chapter 1, a lot of research has been done on obtaining data from multicomponent adsorption of explosives, and these data have been treated as if they were collected from single-solute adsorption systems. While this type of interpretation may not be theoretically correct, it can help one understand the competitive adsorption of explosives to a certain extent. This section reviews the important results from previous research on multicomponent adsorption of explosives. As shown in Table 3a and 3b at the end of this section, isotherm data from separate research experiments were all interpreted using the Freundlich Monocomponent Isotherm. Note that the experiments with RDX indicated in the tables may include HMX as an impurity.

Vlahakis (1974) performed one of the earliest experiments on carbon adsorption of HEs when he investigated the plausible treatment methods for decontaminating groundwater that contained RDX. His goal was to treat the groundwater so that it would be safe for drinking. When Vlahakis compared reverse osmosis, ion exchange, hydrolysis, boiling, chlorination, and polymeric adsorption to carbon adsorption, he found that carbon adsorption was consistently effective and simple to use.

Vlahakis's adsorption experiments included both batch isotherm and small-diameter column studies. From his isotherm experiments, he found that Filtrasorb 400's (F400) saturation capacity for RDX to be 0.125 g RDX/g carbon for a feed concentration of 19.5 mg/L RDX. When he added approximately 60 mg/L TNT to the original RDX solution, he found that the adsorption capacity dropped approximately 39%, to 0.076 g RDX/g carbon. Although the adsorption capacity for RDX decreased under the competition of TNT, the adsorption intensity ($1/n$) remained constant. The column studies of RDX and TNT adsorption showed that preferential adsorption of TNT caused an early breakthrough for RDX. The specific Freundlich isotherm parameters for RDX, with or without TNT present, are shown in Tables 3a and 3b at the end of the chapter. Since RDX was Vlahakis's main concern, he provided no Freundlich parameters for TNT in both independent and competitive adsorption experiments.

Haberman et al. (1982) performed isotherm tests on RDX and TNT separately in order to determine if Lindelius' Rule applied to the two compounds. Lindelius' Rule states that less soluble solutes are more strongly adsorbed. Haberman et al. found that TNT, which was more soluble than RDX, had higher adsorption affinity than RDX. The researchers claimed that the three nitro groups on TNT and RDX were electron-

withdrawing groups which allowed the formation of charge transfer complexes. Since RDX was aliphatic and TNT was aromatic, the charge transfer complex was stronger for the TNT-carbon complex than for the RDX-carbon complex. According to Haberman et al., TNT had higher adsorptivity and adsorption energy than RDX for the same reason. Furthermore, they suspected that RDX adsorption, like TNT adsorption, was irreversible because of the progressive decline in carbon capacity for RDX with successive solvent regenerations. Irreversible adsorption suggested that there was a chemical reaction between RDX and the carbon surfaces. This was confirmed when they examined the electron spectra of carbon surfaces with adsorbed RDX and carbon surfaces with the RDX removed by repetitively washing with acetone. While both spectra showed the nitro and amine nitrogen peaks, the spectrum of the desorbed surface showed additional peaks which represented species with reduced oxidative states of nitrogen. One species was nitroso nitrogen, but the Haberman et al. did not specify the name of the species. Nitroso nitrogen could only be formed by a chemical reaction at the surface. Upon studying adsorption-solvent desorption of RDX and TNT separately, Haberman et al. concluded that TNT chemisorbed onto activated carbon surfaces via π - π bonding and $-\text{NO}_2$ transfer, and RDX chemisorbed onto the carbon by $-\text{NO}_2$ transfer alone. The electron transfer or

π - π bonding would form explosives-carbon complexes which built up with adsorption-desorption cycling.

As a continuation of his research, Haberman (1983) studied competitive adsorption between RDX and TNT onto three types of activated carbon: Filtrasorb 300, Filtrasorb 400, and Witco. Results showed that F400 and Witco had higher capacity for RDX than F300, and F400 had higher capacity for TNT than Witco and F300. The isotherm tests' results showed that the total amount adsorbed in a RDX-TNT adsorption system was less than what would have been adsorbed if there were no competition; that is, if there was only one species present. RDX and TNT must have competed at least partially for the same sites. Haberman's data implied that TNT tended to displace RDX from carbon's surfaces at higher concentrations. When one compared the Freundlich linearized isotherm of independent RDX adsorption with one generated from competitive adsorption data, there was a noticeable decrease in the slope for the competitive RDX isotherm despite the intercept remained the same. The difference between the slopes showed that RDX was adsorbed predominantly at higher energy sites (decrease in slope $1/n$ corresponds to higher adsorption energy), and TNT at higher concentration was capable of suppressing RDX adsorption. Haberman's coadsorption of RDX and TNT in a

column confirmed Vlahakis's finding that RDX broke through faster than TNT. He hypothesized that TNT was more competitive and it displaced the RDX which was previously adsorbed onto the carbon. As a result, RDX broke through faster than TNT.

To explain his experimental results, Haberman postulated two kinds of active sites: low concentration of high energy sites, and high concentration of low energy sites. RDX was initially attracted to high energy sites, and when those sites were filled, RDX could not effectively compete for lower energy sites with the TNT molecules. Consequently RDX adsorption was inhibited, but TNT was not greatly affected because there was enough lower energy sites to accommodate all the TNT molecules. Haberman claimed that the postulations were valid because he believed that adsorption at low concentration always took place preferentially at higher energy sites.

Haberman was not the only one who performed research on multicomponent adsorption of explosives. Burrows (1982) used F300 to perform independent and multicomponent adsorption of TNT, RDX, HMX, and byproduct nitramines Hexahydro-1(N)-acetyl-3,5-dinitro-1,3,5-triazine (TAX) and Octahydro-1(N)-acetyl-3,5,7-trinitro-1,3,5,7-tetrazocine (SEX). The main concern was TNT, RDX, and HMX. Observations made from the single-solute Freundlich linear plots indicated that TNT was the most

effectively removed at all measured concentrations, followed by HMX and SEX; RDX and TAX were the least effectively removed. The log-log plots of the Freundlich isotherms for RDX and HMX in mixtures were parallel to the isotherms of the same components examined individually, but the intercepts (which corresponded to adsorption capacity) were reduced by some factor. This implied that competition for adsorption sites was occurring. Burrows also found that the relative adsorption efficiencies among the five compounds were not inversely related to explosives' solubilities in water, and he assumed van der Waals forces to be solely responsible for carbon adsorption of the explosives. The batch study indicated that the competitive adsorption between explosives reduced the overall removal efficiency of explosives although AC was capable of removing each compound individually. The implication of these isotherm results was that in a GAC adsorber, nitramines (RDX, HMX) will be adsorbed in a series of bands at the end of the column and will be gradually displaced by nitroaromatic TNT well before TNT reached breakthrough. Nevertheless continuous-flow column tests are necessary before any conclusion can be reached.

Hinshaw et al. (1987) also conducted a series of competitive isotherm experiments using five ACs: Calgon's F200, F300, F400, Westvaco's Nuchar WV-G, and

Witco's Witcarb 950. The tests included carbon selection, temperature effects, competitive adsorption, adsorption efficiency differences between actual and synthetic pink water, and acetone-spiked effects. For the carbon selection experiment, the above five carbons were tested for their adsorption efficiencies of nitramines and nitroaromatics together. The nitramines were RDX and HMX, and the nitroaromatics were TNT and 2,4-DNT. Witco's Witcarb 950 exhibited the best performance in adsorption of explosives. Witcarb 950 was made from petroleum coke, and the other carbons were made from bituminous coal. All isotherms were nonlinear in regions of minimum or maximum carbon doses; the parameters shown in Table 3b were derived from the experimental data which formed the linear portion of the isotherms.

Since Witcarb 950 was the most efficient among the five carbons, it was selected as the carbon used for the other tests, except for the acetone-spiked test. Adsorption of the four explosives together were studied at 4°C, 22°C, and 49°C. The conclusion was that the adsorption of RDX and HMX was favored by decreasing temperature; as temperature increased, adsorption of TNT and 2, 4-DNT increased. When TNT and 2,4-DNT were eliminated from the adsorption system, RDX and HMX adsorption onto Witcarb 950 was greatly enhanced; however, there was only a small improvement for

TNT and 2,4-DNT removal when RDX and HMX were removed from the solution. The nitroaromatics appeared to be extremely competitive. Since the previous isotherm experiments were done using synthetic pink water, Hinshaw et al. performed another isotherm test using Witcarb 950 and actual pink water from Kansas Army Ammunition. The purpose was to determine if adsorption efficiencies differ between synthetic and actual pink water. The test showed that the general results between synthetic and actual pink water were virtually the same. Finally the researchers used F300 to study acetone effects on various explosives' adsorption behavior. They found that when pink water contained acetone concentration of 2% by volume, it did not have any influence on TNT and 2,4-DNT adsorption, but there was a significant decrease in RDX and HMX adsorption. The reduction factor in RDX and HMX sorbed concentration was about half an order of magnitude. All the Freundlich parameters deduced from Hinshaw's et al. experiments are shown in Table 3b.

From his experiments, Dennis et al. (1990) found that it was feasible to use continuous-flow GAC columns to remove groundwater contaminated with TNT, RDX, HMX, 2,4,6-trinitrophenylmethylnitramine (Tetryl), 2,4-dinitrotoluene (2,4-DNT), 2,6-dinitrotoluene (2,6-DNT), 1,3-dinitrobenzene (1,3-DNB), 1,3,5-trinitrobenzene (1,3,5-

TNB), and nitrobenzene (NB). The batch experiments with five different ACs showed that all explosives, except RDX and TNT, were removed to below detection limits after adsorption. The isotherm parameters derived for RDX and TNT are shown in Table 3b, and they are based on an initial average concentration of 0.486 mg/L RDX and 0.493 mg/L TNT. No parameters were derived for the other explosives because their equilibrium concentrations were below detection limit for all carbon dosages.

Bricka et al. (1992) also investigated the feasibility of using granular activated carbon (GAC) to remove low levels of RDX and HMX from groundwater. With all five GACs, namely Westates's CC-601, Calgon's F200 and F400, American Norit's Norit Row 0.8, and Norit's Hydrodarco 4000, they were able to reduce RDX and HMX concentration to below their detection limits which were 0.617 $\mu\text{g/L}$ and 0.869 $\mu\text{g/L}$ respectively. The concentrations of the groundwater prior to adsorption were 5.5 $\mu\text{g/L}$ RDX and 1.4 $\mu\text{g/L}$ HMX. There were no isotherm parameters or modeling reported in their work.

Most recently Wilkie (1994) also compared the performance of various ACs on adsorption of RDX and HMX. The carbon tested were F400, Darco 20x40, and Norit PK1-3, and F400 showed the best performance. With initial RDX concentration being

approximately 40 mg/L, she was able to get 417 mg RDX/g carbon as the maximum adsorption capacity of F400. She also reported the maximum adsorption capacity for HMX to be 217 mg/g, but the initial HMX concentration was not stated. The Freundlich isotherm parameters for her RDX adsorption experiment are listed in Table 3a.

Heilmann (1995) also conducted RDX and HMX adsorption experiments using F400, and he used the Freundlich isotherm to describe his single-solute data. The parameters are shown in Table 3a. Notice, however, the RDX that he used contained about ten percent HMX; that is, the RDX was not pure. Heilmann's experimental data showed that F400's maximum sorption capacities for RDX and HMX were 309.35mg/g and 300.15mg/g respectively.

Table 3a Batch Isotherm Parameters for Independent Adsorption of Explosives

Reference	Carbon Type	Isotherm	Explosives	Parameters	Remarks
Burrows, 1982	Calgon F300 (PAC)	Freundlich $q_e = KC^{1/n}$	RDX	$K = 0.1118 \text{ (L/mg)}^{1/n}$ $n = 2.938$	$\ln q_e = \ln K + 1/n \cdot \ln C_e$ $C_{o_RDX} = 21 \text{ mg/L}$; C_{e_RDX} range = 1-19.95mg/L
	Calgon F300 (PAC)	Freundlich	HMX	$K = 0.1682 \text{ (L/mg)}^{1/n}$ $n = 2.169$	$C_{o_HMX} = 5.2 \text{ mg/L}$; C_{e_HMX} range = 1-5.01mg/L
Haberman, 1983	Filtrisorb 300 (PAC)	Freundlich	RDX	$K = 127 \text{ } \mu\text{mol/g}$ $n = 2.27$	$C_{o_RDX} = 20 \text{ mg/L}$; C_{e_RDX} range: 0.222-22.21mg/L
	Filtrisorb 300 (PAC)	Freundlich	TNT	$K = 887 \text{ } \mu\text{mol/g}$ $n = 6.993$	$C_{o_TNT} = 100 \text{ mg/L}$; C_{e_TNT} range: 0.227-22.72mg/L
Heilmann, 1994	Filtrisorb 400 (PAC)	Freundlich	RDX (impure)	$K = 0.0970 \text{ (L/mg)}^{1/n}$ $n = 2.822$	$C_{o_RDX} = 36.9 \text{ mg/L}$; C_{e_RDX} range = 0.24-28.18mg/L
			HMX	$K = 0.1901 \text{ (L/mg)}^{1/n}$ $n = 2.707$	$C_{o_HMX} = 3.62 \text{ mg/L}$; C_{e_HMX} range = 0.15-2.95mg/L
Vlahakis, 1974	Filtrisorb 400 (PAC)	Freundlich	RDX	$K = 0.073 \text{ (L/mg)}^{1/n}$ $n = 5.56$	$C_{o_RDX} = 19.5 \text{ mg/L}$; C_{e_RDX} range: 0.5-10mg/L
Wilkie et al., 1994	Filtrisorb 400 (GAC)	Freundlich	RDX	$K = 0.334 \text{ (L/mg)}^{1/n}$ $n = 3.226$	$C_{o_RDX} = 40 \text{ mg/L}$; C_{e_RDX} range: 1-40mg/L
	Darco20x40 (GAC)	Freundlich	RDX	$K = 0.350 \text{ (L/mg)}^{1/n}$ $n = 9.091$	$C_{o_RDX} = 40 \text{ mg/L}$; C_{e_RDX} range: 1-40mg/L
	Norit PK1-3 (GAC)	Freundlich	RDX	$K = 0.344 \text{ (L/mg)}^{1/n}$ $n = 16.667$	$C_{o_RDX} = 40 \text{ mg/L}$; C_{e_RDX} range: 1-40mg/L

Table 3b Batch Isotherm Parameters for Competitive Adsorption of Explosives

Reference	Carbon Type	Isotherm	Explosives	Parameters ^a	Remarks
Burrows, 1982	Calgon F300 (PAC)	Freundlich	TNT	$K = 0.2452 \text{ (L/mg)}^{1/n}$ $n = 7.474$	$C_{o_TNT} = 23.48 \text{ mg/L}$; C_{e_TNT} range: 0.281-25 mg/L Extrapolated from 2 points only
			RDX	$K = 0.06155 \text{ (L/mg)}^{1/n}$ $n = 3.144$	$C_{o_RDX} = 22.6 \text{ mg/L}$; C_{e_RDX} range: 0.264-19.6 mg/L
			HMX	$K = 0.04183 \text{ (L/mg)}^{1/n}$ $n = 2.565$	$C_{o_HMX} = 4.71 \text{ mg/L}$; C_{e_HMX} range: 0.234-4.71 mg/L
			TAX	$K = 0.07357 \text{ (L/mg)}^{1/n}$ $n = -18.587$	$C_{o_TAX} = 26.16 \text{ mg/L}$; C_{e_TAX} range: <0.318 mg/L-26 mg/L
			SEX	$K = 0.02975 \text{ (L/mg)}^{1/n}$ $n = -5.179$	$C_{o_SEX} = 5.85 \text{ mg/L}$; C_{e_SEX} range: <0.377 mg/L-5.06 mg/L
					The above 5 components were in one solution
Dennis et al., 1990 ^b	F200 (PAC)	Freundlich	RDX	$K = 0.052 \text{ (L/mg)}^{1/n}$ $n = 1.87$	Extrapolated from two data points Based on $C_{o_RDX(\text{average})} = 0.486 \text{ mg/L}$ C_{e_RDX} range: 0.001-1.0 mg/L
			TNT	N/A	Equil. Conc. of TNT < D.L.
	F300 (PAC)	Freundlich	RDX	$K = 0.031 \text{ (L/mg)}^{1/n}$ $n = 2.42$	Extrapolated from two data points Based on $C_{o_RDX(\text{average})} = 0.486 \text{ mg/L}$ C_{e_RDX} range: 0.001-1.0 mg/L
			TNT	N/A	Equil. Conc. of TNT < D.L.
	F400 (PAC)	Freundlich	RDX	$K = 0.049 \text{ (L/mg)}^{1/n}$ $n = 1.8$	Extrapolated from two data points Based on $C_{o_RDX(\text{average})} = 0.486 \text{ mg/L}$ C_{e_RDX} range: 0.001-1.0 mg/L
			TNT	N/A	Equil. Conc. of TNT < D.L.
	Hydrodarco 4000 (PAC)	Freundlich	RDX	$K = 0.0012 \text{ (L/mg)}^{1/n}$ $n = 10$	Based on $C_{o_RDX(\text{average})} = 0.486 \text{ mg/L}$ C_{e_RDX} range: 0.001-1.0 mg/L
			TNT	$K = 0.128 \text{ (L/mg)}^{1/n}$	Based on $C_{o_TNT(\text{average})} = 0.493 \text{ mg/L}$

Table 3b (Continue)

Reference	Carbon Type	Isotherm	Explosives	Parameters ^a	Remarks
				n = 1.208	C _{e,TNT} range: 0.001-1.0mg/L
	Atochem Inc. GAC 830 (PAC)	Freundlich	RDX	K = 0.045(L/mg) ^{1/n} n = 1.59	Based on C _{o,RDX} (average) = 0.486mg/L C _{e,RDX} range: 0.001-1.0mg/L
			TNT	K = 0.136 (L/mg) ^{1/n} n = 1.558	Based on C _{o,TNT} (average) = 0.493mg/L C _{e,TNT} range: 0.001-1.0mg/L
Haberman, 1983	Filtrisorb 300 (PAC)	Freundlich	RDX	K = 121 μmol/g n = 12.82	C _{o,RDX} = 20mg/L; C _{e,RDX} range: 0.222-22.21mg/L
			TNT	K = 850 μmol/g n = 8.130	C _{o,TNT} = 100mg/L; C _{e,TNT} range:0.227-22.72mg/L
	Filtrisorb 400 (PAC)	Freundlich	RDX	K = 186 μmol/g n = 47.62	C _{o,RDX} = 20mg/L; C _{e,RDX} range: 0.222-22.21mg/L
			TNT	K = 1276 μmol/g n = 7.874	C _{o,TNT} = 100mg/L; C _{e,TNT} range:0.227-22.72mg/L
	Witco (PAC)	Freundlich	RDX	K = 244μmol/g n = 47.62	C _{o,RDX} = 20mg/L; C _{e,RDX} range: 0.222-22.21mg/L
			TNT	K = 986 μmol/g n = 5.155	C _{o,TNT} = 100mg/L; C _{e,TNT} range:0.227-22.72mg/L
Hinshaw et al. 1987 ^c	Filtrisorb 200 (PAC)	Freundlich	RDX	K = 0.0327 (L/mg) ^{1/n} n = 3.674	R ² = 0.890; linearizing 3 out of 5 data points ^d C _{o,RDX} =27.7mg/L; C _{e,RDX} range:0.004-15.9mg/L
			HMX	K = 0.0198 (L/mg) ^{1/n} n = 4.331	R ² = 0.952; linearizing 3 out of 5 data points C _{o,HMX} =5.71mg/L; C _{e,HMX} range:0.004-4mg/L
			DNT	K = 0.00973 (L/mg) ^{1/n} n = 4.829	R ² = 0.677; linearizing 3 out of 5 data points C _{o,DNT} =0.925mg/L; C _{e,DNT} range: 0.0295-0.855mg/L
			TNT	K = 0.257 (L/mg) ^{1/n} n = 5.678	R ² = 0.998; linearizing 3 out of 5 data points C _{o,TNT} =72.8mg/L; C _{e,TNT} range: 0.000735-46.5mg/L

Table 3b (Continue)

Reference	Carbon Type	Isotherm	Explosives	Parameters ^a	Remarks
	Filtrisorb 300 (PAC)	Freundlich	RDX	$K = 0.0371 \text{ (L/mg)}^{1/n}$ $n = 3.182$	$R^2 = 0.933$; linearizing 3 out of 5 data points $C_{o_RDX}=28\text{mg/L}$; C_{e_RDX} range:0.005-13.5mg/L
HMX			$K = 0.0254 \text{ (L/mg)}^{1/n}$ $n = 3.018$	$R^2 = 0.921$; linearizing 3 out of 5 data points $C_{o_HMX}=5.61\text{mg/L}$; C_{e_HMX} range:0.0002-1mg/L	
DNT			$K = 0.00978 \text{ (L/mg)}^{1/n}$ $n = 5.278$	$R^2 = 1.00$; linearizing 3 out of 5 data points $C_{o_DNT}=0.915\text{mg/L}$; C_{e_DNT} range: 0.017-0.8mg/L	
TNT			$K = 0.327 \text{ (L/mg)}^{1/n}$ $n = 13.268$	$R^2 = 1.00$; linearizing 3 out of 5 data points $C_{o_TNT}=73.7\text{mg/L}$; C_{e_TNT} range: 2.74-68.3mg/L	
	Filtrisorb 400 (PAC)	Freundlich	RDX	$K = 0.0449 \text{ (L/mg)}^{1/n}$ $n = 2.708$	$R^2 = 0.922$; linearizing 3 out of 5 data points $C_{o_RDX}=23.7\text{mg/L}$; C_{e_RDX} range:0.00508-7.29mg/L
HMX			$K = 0.0152 \text{ (L/mg)}^{1/n}$ $n = 5.474$	$R^2 = 0.748$; linearizing 3 out of 5 data points $C_{o_HMX}=4.45\text{mg/L}$; C_{e_HMX} range:0.0027-3.7mg/L	
DNT			$K = 0.0123 \text{ (L/mg)}^{1/n}$ $n = 5.353$	$R^2 = 0.995$; linearizing 3 out of 5 data points $C_{o_DNT}=0.769\text{mg/L}$; C_{e_DNT} range: 0.00178-0.619mg/L	
TNT			$K = 0.272 \text{ (L/mg)}^{1/n}$ $n = 4.751$	$R^2 = 0.976$; linearizing 4 out of 5 data points $C_{o_TNT}=62.7\text{mg/L}$; C_{e_TNT} range: 0.00155-55.3mg/L	
	Nuchar WV-G (PAC)	Freundlich	RDX	$K = 0.0498 \text{ (L/mg)}^{1/n}$ $n = 2.609$	$R^2 = 0.957$; linearizing 3 out of 5 data points $C_{o_RDX}=23.3\text{mg/L}$; C_{e_RDX} range:0.00373-5.91mg/L
HMX			$K = 0.0151 \text{ (L/mg)}^{1/n}$ $n = 5.313$	$R^2 = 0.76$; linearizing 3 out of 5 data points $C_{o_HMX}=4.52\text{mg/L}$; C_{e_HMX} range:0.00317-3.8mg/L	
DNT			$K = 0.0123 \text{ (L/mg)}^{1/n}$ $n = 5.542$	$R^2 = 0.995$; linearizing 3 out of 5 data points $C_{o_DNT}=0.763\text{mg/L}$; C_{e_DNT} range: 0.00144-0.643mg/L	
TNT			$K = 0.298 \text{ (L/mg)}^{1/n}$ $n = 5.098$	$R^2 = 0.986$; linearizing 4 out of 5 data points $C_{o_TNT}=61.6\text{mg/L}$; C_{e_TNT} range: 0.00047-55.5mg/L	
	Witcarb 950 (PAC)	Freundlich	RDX	$K = 0.0657 \text{ (L/mg)}^{1/n}$ $n = 2.402$	$R^2 = 0.934$; linearizing 3 out of 5 data points $C_{o_RDX}=23.3\text{mg/L}$; C_{e_RDX} range:0.00375-3.79mg/L
HMX			$K = 0.0188 \text{ (L/mg)}^{1/n}$ $n = 5.545$	$R^2 = 0.761$; linearizing 4 out of 5 data points $C_{o_HMX}=4.58\text{mg/L}$; C_{e_HMX} range:0.00142-4.26mg/L	

Table 3b (Continue)

Reference	Carbon Type	Isotherm	Explosives	Parameters ^a	Remarks
			DNT	$K = 0.0124 \text{ (L/mg)}^{1/n}$ $n = 5.977$	$R^2 = 1.00$; linearizing 3 out of 5 data points $C_{o_DNT} = 0.779 \text{ mg/L}$; C_{e_DNT} range: 0.00113-0.621 mg/L
			TNT	$K = 0.292 \text{ (L/mg)}^{1/n}$ $n = 5.052$	$R^2 = 0.969$; linearizing 4 out of 5 data points $C_{o_TNT} = 61.8 \text{ mg/L}$; C_{e_TNT} range: 0.000687-54.2 mg/L
	Witcarb 950 (PAC)	Freundlich	RDX	$K = 0.0547 \text{ (L/mg)}^{1/n}$ $n = 3.813$	$R^2 = 0.769$; linearizing 5 out of 5 data points $C_{o_RDX} = 23.1 \text{ mg/L}$; C_{e_RDX} range: 0.017-21 mg/L
			HMX	$K = 0.0220 \text{ (L/mg)}^{1/n}$ $n = 3.690$	$R^2 = 0.721$; linearizing 5 out of 5 data points $C_{o_HMX} = 4.53 \text{ mg/L}$; C_{e_HMX} range: 0.003-3.95 mg/L
			DNT	$K = 0.0133 \text{ (L/mg)}^{1/n}$ $n = 3.109$	$R^2 = 0.923$; linearizing 5 out of 5 data points $C_{o_DNT} = 0.763 \text{ mg/L}$; C_{e_DNT} range: 0.00007-0.525 mg/L
			TNT	$K = 0.274 \text{ (L/mg)}^{1/n}$ $n = 5.936$	$R^2 = 0.844$; linearizing 4 out of 5 data points $C_{o_TNT} = 59 \text{ mg/L}$; C_{e_TNT} range: 0.024-47.9 mg/L This set of isotherm was run at 40°F
	Witcarb 950 (PAC)	Freundlich	RDX	$K = 0.0497 \text{ (L/mg)}^{1/n}$ $n = 5.067$	$R^2 = 0.930$; linearizing 4 out of 5 data points $C_{o_RDX} = 23.7 \text{ mg/L}$; C_{e_RDX} range: 0.0009-16.5 mg/L
			HMX	$K = 0.0258 \text{ (L/mg)}^{1/n}$ $n = 3.099$	$R^2 = 0.85$; linearizing 4 out of 5 data points $C_{o_HMX} = 4.71 \text{ mg/L}$; C_{e_HMX} range: 0.00193-2.07 mg/L
			DNT	$K = 0.0151 \text{ (L/mg)}^{1/n}$ $n = 3.994$	$R^2 = 0.984$; linearizing 4 out of 5 data points $C_{o_DNT} = 0.773 \text{ mg/L}$; C_{e_DNT} range: 0.000147-0.467 mg/L
			TNT	$K = 0.380 \text{ (L/mg)}^{1/n}$ $n = 6.465$	$R^2 = 0.997$; linearizing 4 out of 5 data points $C_{o_TNT} = 59.7 \text{ mg/L}$; C_{e_TNT} range: 0.0006-43.3 mg/L This set of isotherm was run at 120°F
	Witcarb 950 (PAC)	Freundlich	RDX	$K = 0.122 \text{ (L/mg)}^{1/n}$ $n = 2.234$	$R^2 = 0.961$; linearizing 5 out of 5 data points $C_{o_RDX} = 22.6 \text{ mg/L}$; C_{e_RDX} range: 0.0103-16.3 mg/L
			HMX	$K = 0.0921 \text{ (L/mg)}^{1/n}$ $n = 2.369$	$R^2 = 0.949$; linearizing 5 out of 5 data points $C_{o_HMX} = 4.42 \text{ mg/L}$; C_{e_HMX} range: 0.000416-2.5 mg/L This set is a 2-component adsorption system run at ambient temperature.

Table 3b (Continue)

Reference	Carbon Type	Isotherm	Explosives	Parameters ^a	Remarks
	Witcarb 950 (PAC)	Freundlich	RDX	K = 0.0505 (L/mg) ^{1/n} n = 3.487	R ² = 0.877; linearizing 5 out of 5 data points C _{o,RDX} =22mg/L; C _{e,RDX} range:0.0132-20.3mg/L
			HMX	K = 0.0226 (L/mg) ^{1/n} n = 3.799	R ² = 0.861; linearizing 5 out of 5 data points C _{o,HMX} =4.02mg/L; C _{e,HMX} range:0.000491-3.57mg/L
			DNT	K = 0.00237 (L/mg) ^{1/n} n = 4.47	R ² = 0.997; linearizing 3 out of 5 data points C _{o,DNT} =0.0663mg/L; C _{e,DNT} range: 0.000893-0.043mg/L
			TNT	K = 0.295 (L/mg) ^{1/n} n = 4.780	R ² = 0.950; linearizing 4 out of 5 data points C _{o,TNT} =49.4mg/L; C _{e,TNT} range: 0.012-37.9mg/L This set used KAAP's actual pink water instead of synthetic pink water.
	Witcarb 950 (PAC)	Freundlich	RDX	K = 0.0151 (L/mg) ^{1/n} n = 3.814	R ² = 0.81; linearizing 4 out of 4 data points C _{o,RDX} =23.1mg/L; C _{e,RDX} range:0.0363-22.8mg/L
			HMX	K = 0.00695 (L/mg) ^{1/n} n = 4.408	R ² = 0.802; linearizing 4 out of 4 data points C _{o,HMX} =4.35mg/L; C _{e,HMX} range:0.0007-4.28mg/L
			DNT	K = 0.0107 (L/mg) ^{1/n} n = 3.365	R ² = 0.998; linearizing 3 out of 4 data points C _{o,DNT} =0.776mg/L; C _{e,DNT} range:0.000163-0.677mg/L
			TNT	K = 0.206 (L/mg) ^{1/n} n = 6.231	R ² = 0.979; linearizing 3 out of 4 data points C _{o,TNT} =61.3mg/L; C _{e,TNT} range: 0.00055-57.6mg/L This set used synthetic pink water with acetone concentration of 2% by volume
Vlahakis, 1974	Filtrisorb 400 (PAC)	Freundlich	RDX	K = 0.043 (L/mg) ^{1/n} n = 5.56	C _{o,RDX} =21mg/L; C _{e,RDX} range:0.5-10mg/L C _{o,TNT} =57.5mg/L
			TNT	N.A.	Literature did not include the Freundlich parameters for TNT.

Notes:

- a. All work cited above used monocomponent Freundlich isotherm to explain single component adsorption and multicomponent adsorption; there is no parameter accounting for the competitive effect existing in the

Table 3b (Continue)

Notes (continue):

multicomponent system.

- b. All isotherm tests were performed with 5 different carbons and used samples containing 0.0149mg/L Tetryl, 0.0076mg/L 2,4-DNT, 0.00352mg/L 2,6-DNT, 0.00311mg/L 1,3-DNB, 0.0142mg/L 1,3,5-TNB, <0.00113mg/L NB, and 0.00275mg/L HMX, in addition to 0.486mg/L RDX and 0.493mg/L TNT; only RDX and TNT were detected in solution after adsorption.
- c. The Freundlich parameters listed for Hinshaw et. al.'s data were extrapolated by the writer according to the linear plots shown in the original reference.
- d. The R^2 from the Remarks column indicates how well linearization fits Hinshaw et al.'s data.

3. EXPERIMENTAL METHODS

Developing a comprehensive multicomponent isotherm requires experiments that will give a wide equilibrium concentration range. Some of these experiments will involve very low liquid phase concentration which requires a very sensitive equipment or an analytical technique that enhances the sensitivity of an instrument. In order to perform experiments that will give a good distribution of RDX-HMX equilibrium concentration ratio, a method that helps select experimental conditions and predict the end results will save a lot of time and resources. Another consideration is to examine the error introduced by analytical instruments and other apparatus so that the author can select the experimental conditions which will not magnify the error.

The analytical techniques chosen for examining the experimental results for this thesis are the High Performance Liquid Chromatography (HPLC) and solid phase extraction (SPE). This chapter first describes the HPLC analytical method and the SPE procedures, then it explains the process of selecting experimental conditions. The chapter concludes with an error analysis.

3.1 Analytical Techniques

3.1.1 High Performance Liquid Chromatography (HPLC)

The Hewlett Packard 1050 Series HPLC was used for analyzing liquid phase concentration of RDX and HMX for all isotherm experiments. The HP 1050 was equipped with a variable wavelength detector and autosampler. All the results from the HPLC analysis were processed and presented by the Hewlett Packard 3396 Series II

Integrator. The analytical column for the HPLC was a 10 μ Adsorbosphere, C18 (12% C) reversed phase column which had an inner diameter of 4.6 mm and a length of 250 mm. A 5 μ C18 guard column was connected to the front of the analytical column to filter particles which might otherwise have entered the main column. Both of these columns were manufactured by Alltech.

The analytical method used was a mobile phase of 50% methanol and 50% water, and the flowrate was 1.5 mL/min. The retention time for RDX and HMX were approximately 4.3 minutes and 2.7 minutes respectively. The wavelength of the detector was set at 236 nm.

Four calibration standards were prepared for RDX and HMX: 40 mg RDX/L in deionized water, 40 mg RDX/L in HPLC grade acetonitrile, 4 mg HMX/L in deionized water, and 4 mg HMX/L in HPLC acetonitrile. Each of these standards was injected six times, with the injection volume being 1, 2, 5, 10, 20, and 40 μ L. As shown in Appendix A, the calibration curves for all four standards were linear. Note that the average area code for each injection volume corresponded to a specific RDX or HMX concentration in water or acetonitrile.

3.1.2 Solid Phase Extraction (SPE)

Since the HPLC has a detection limit of 0.1 mg/L for both RDX and HMX, isotherm samples with concentrations below this limit must be preconcentrated using the SPE procedures prior to the HPLC analysis. This section first reviews some SPE research

that is related to extracting explosives, then it describes the process of developing the appropriate SPE procedures and the procedures themselves.

3.1.2.1 Previous Work on SPE and Other Extraction Methods

Several researchers have used SPE to concentrate liquid samples containing explosives for analysis. Richard and Junk (1986) performed recovery studies of RDX using XAD-2, XAD-4, and XAD-7 macroreticular resins as sorbents. No conclusive results could be reached from their experiments because the recovery varied with different resins and different mesh sizes. The researchers suspected that the low recoveries were caused by short-circuiting due to the formation of resins' microparticles.

Winslow et al. (1991) compared the SPE recovery with that of salting-out solvent-extraction (SOE). The SPE sorbent they used was Porapak R, and for SOE, they used NaCl and acetonitrile followed by a Kuderna-Danish evaporator. The average SPE recoveries for RDX and HMX were 95.5% and 97.8% respectively; the SOE yielded slightly lower recoveries: 86.7% for RDX and 91.8% for HMX. They also reported that the Certified Reporting Limits (CRLs) for the SPE method were lower than that for the SOE. With the experimental results stated above, and the fact that the SOE was more labor-intensive, the researchers recommended SPE using hydrophilic resin Porapak R over SOE.

Major et al. (1992) used J.T. Baker 40 μm Sep-Pak Octadecyl C18 cartridges to analyze aqueous leachates contaminated with nitroaromatics and nitramines. Prior to the SPE procedures, pH adjustment and salting-out were performed on the samples.

Although this method was very effective in recovering nitroaromatics, such as TNT, it was very poor in recovering nitramines, such as RDX and HMX. The recoveries of RDX and HMX were only 38% and 29% respectively. It seemed that leachate exceeding 30 mL had the effect of rinsing part of the nitramines out of the cartridges; therefore, they suggested using vinyl-divinyl benzene resins for recovering nitramines.

From Winslow et al.'s and Major et al.'s work, Jenkins et al. (1994) noticed that the SPE using organic polymeric resin sorbent provided better recoveries for RDX and HMX than those using reversed-phase silicas. They also compared resin-based cartridge-SPE, resin-based membrane-SPE, and SOE. For cartridge-SPE, they packed Supelco's Porapak R into cartridges; for membrane-SPE, they used 47 mm Empore styrene-divinyl benzene disks; for SOE, they used NaCl and acetonitrile; no evaporative preconcentration was used for the SOE. Over 80% recoveries for RDX and HMX were obtained using cartridge-SPE and SOE. HMX had the poorest recovery (68%) using the membrane-SPE. Both SPE methods were more prone to interferences than the SOE method. The interferences could be due to matrix interaction of polymeric resins with low-pH groundwater; they believed that the low pH samples interacted with the solid phases to either degrade the polymer or release contaminants from within polymer by swelling or reorienting the polymer matrix. They claimed that the interferences peaks might be drastically reduced if the samples were neutralized by NaOH. After performing blank tests using the SPE cartridges, Jenkins et al. concluded that the resins were not adequately cleaned. Since the dirty resins might have led to positive interferences, hence higher

recoveries, for pre-concentrated RDX samples, cleaner Porapak R might result in lower interferences or lower recoveries than what was observed from Jenkins et al.'s research.

Among the three methods, the SOE had the lowest CRLs for both RDX and HMX; the cartridge-SPE had lower CRLs for HMX than the membrane-SPE, but the membrane-SPE had lower CRLs for RDX than the cartridge-SPE. The membrane-SPE did not appear to be a very attractive method for pre-concentrating samples because of poor recoveries and cumbersome cleaning procedures for the membranes.

3.1.2.2 SPE Method Development

The most important and difficult step in developing an SPE method for pre-concentrating the isotherm samples was to find a sorbent bed which could pre-concentrate samples of up to 500 mL without reaching breakthrough. The nonpolar nature of RDX and HMX called for nonpolar SPE. The first two candidates for SPE sorbent were C18 and C8. C18 is commonly used as packing material for reversed phase analytical columns, and C8 SPE cartridges have been used by the author for extracting RDX and HMX from biological samples in the Water Lab at UCLA. Varian's Bond Elut C18 cartridges (Harbor City, CA) were used, and the results confirmed Major et al.'s finding. Less than 10% recovery was found for RDX when 500 mL of 0.45 mg/L RDX sample were passed through the sorbent bed. The same result was found for the C8 cartridges. While C8 gave over 90% recovery for extracting 5 to 20 mL of samples, the recovery dropped to below 25% when the sample volume increased. Previous researchers suggested that adding salt to samples might increase the recoveries of isolates; therefore,

another C18 SPE study was performed using salted RDX samples (Winslow et al., 1991; Major et al., 1992; Jenkins et al., 1994). Although the recovery was improved by approximately 10%, it was still unacceptable.

The manufacturer (Varian) was contacted, and the representative suggested using SPE cartridges developed for pesticide analysis. Pesticide cartridges were successful in recovering pesticides which contained triazine. Since RDX is a triazine, the SPE cartridges may be able to recover RDX. Unfortunately no RDX was recovered using the pesticide SPE cartridges.

The author next performed recovery studies using Supelco's Porapak R (Bellefonte, PA). Inconsistent and unrealistic (over 100%) recoveries were obtained. The recovery of RDX varied from 109% to 194%. The sorbent was clearly too dirty, and using up to 60 mL of acetonitrile to prewash the column was not enough to remove the interferences. Jenkins et al. had only 90% to 110% recovery for the same SPE tests and they did not notice as many interferences from Gas Chromatography (GC) because GC is generally less sensitive than HPLC, which is the analytical instrument used by the author. Supelco then supplied samples of Hayesep R cartridges which the manufacturer claimed to be cleaner than Porapak R; however, using up to 100 mL of acetonitrile did not remove the interferences which appeared in blank experiments. Due to the amount of solvent potentially required to clean the sorbent bed and the inconsistent recovery, Porapak R and Hayesep R were removed from further consideration.

The last SPE sorbent tested was styrene divinylbenzene (SDVB), and it gave acceptable recoveries for both RDX and HMX. The recovery studies using various batches of SDVB cartridges for both RDX and HMX are listed in Appendix B. Overall the recoveries for RDX and HMX were about 100% and 80% respectively; however, recoveries varied from batch to batch of SPE cartridges. Pre-market SDVB SPE cartridges were supplied by Varian (Harbor City, CA). The product's official name is BondElut-ENV. The polymer was not functionalized, but purity was established for it. The SDVB had a surface area of 500 m²/g, and the particle size was between 75 to 150 micron. According to Varian's representative, these particles were larger than the silica-based sorbent particles.

3.1.2.3 The SPE Method

The SPE setup included 400 mg semi-dry or 200 mg dry SDVB sorbent packed between two fritted discs in each polypropylene SPE cartridge, vacuum supply, a Bond Elut/Vac Elut System with a 10-place molded cover that fitted the top of a vacuum basin, a 1/8" NPT hose fitting used for vacuum application, and a metal vial rack which was used for collecting eluant. With the developed SPE method, the detection limit of RDX and HMX increased from 0.1 mg/L to 0.0001 mg/L, which was a 1000-fold improvement in sensitivities.

The SPE procedures began with passing 12 mL of HPLC grade acetonitrile through a 3cc-SPE cartridge by applying a vacuum that provided a flowrate of approximately 5 mL/min. This was equivalent to about 1" Hg vacuum pressure. The

Figure 2 Solid Phase Extraction Setup

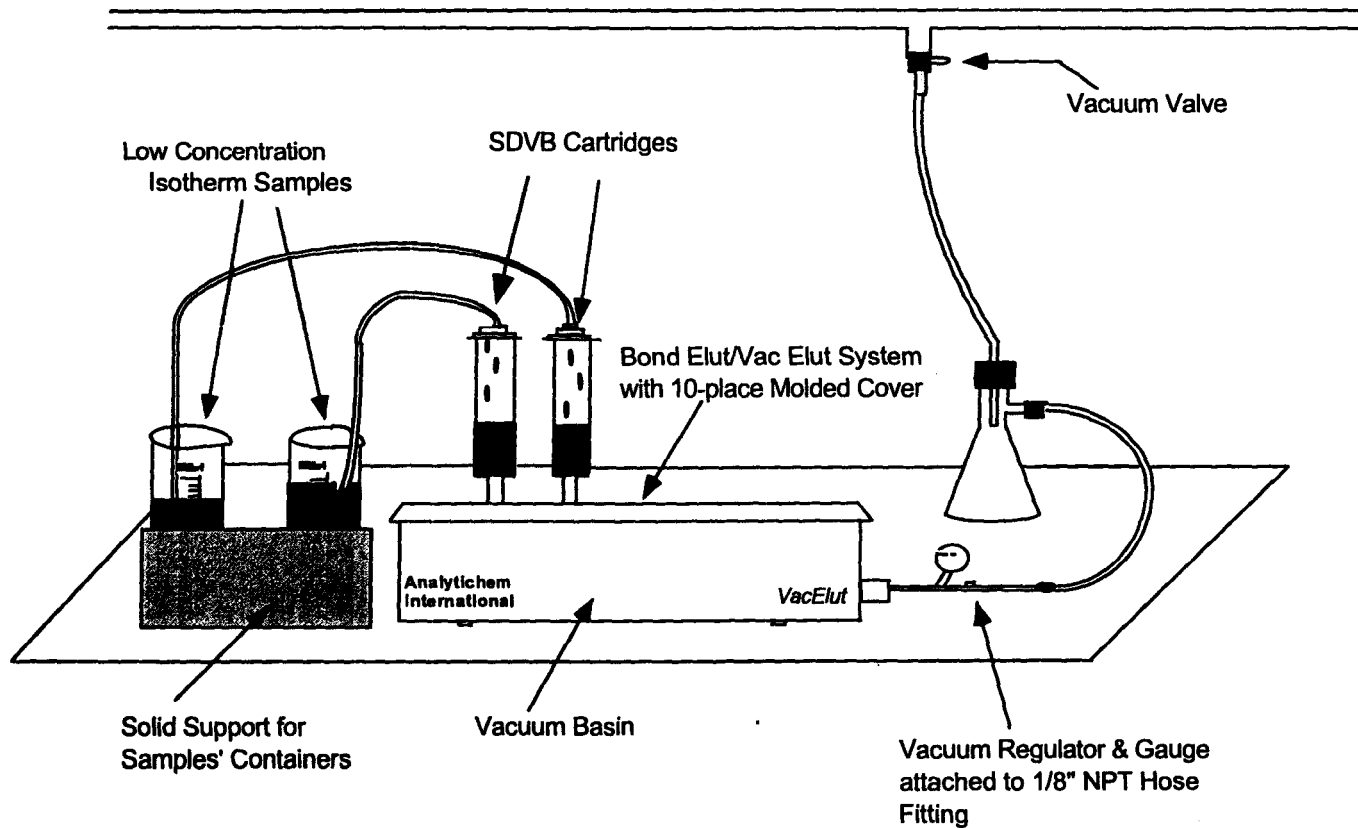


Table 4 Solid Phase Extraction Procedures

Equipments/Chemicals Required

- SPE Manifold
- Vacuum Outlet
- 2-mL Sampling Vials
- HPLC Grade Acetonitrile
- HPLC Grade Water
- 3-mL SPE cartridges containing 200mg StyreneDivinyl Benzene (SDVB) sorbent

Procedures

1. Condition the SDVB sorbent bed with 3mL of HPLC grade acetonitrile (i.e. one cartridge volume) and wait for 5 minutes.
2. Apply vacuum pressure (about 1 inch Hg) such that the solvent will be drawn out of the cartridge at a rate of about 5mL/min.
3. Continue adding 9mL of acetonitrile (3 cartridge volumes) and then rinse the sorbent bed with 12mL (4 cartridge volumes) of HPLC Grade water. Leave vacuum on and do not let sorbent bed dry.
4. Before all the water finishes passing through the sorbent bed, apply the desired volume of sample to the SPE cartridge while the vacuum is still drawing liquid at 5mL/min.
5. Use 3mL of water (one cartridge volume) to rinse the cartridge when all the sample has passed through the sorbent bed. Vacuum pressure may be increased at this time to draw all the water faster.
6. Allow the cartridge dry for about 20-30mins. under full vacuum pressure (about 20-25 inches Hg).
7. Turn off the vacuum and put a sampling vial on the vial rack. Add 0.5mL of acetonitrile into the SPE cartridge. Let sit for 1min. and then turn on vacuum for one second and turn off quickly. This is to allow acetonitrile to soak through the sorbent bed.
8. Add another 0.5mL of acetonitrile into the cartridge and let sit for another minute. Turn on the vacuum slowly and let the acetonitrile come out of the cartridge's tip drop by drop. Increase the vacuum pressure very slowly until no more acetonitrile can be drawn. Be careful not to increase the vacuum so high that it will splash the eluant out of the sampling vial. Pressure can be increased up to 10 inches Hg without splashing eluant out of a 2-mL vial.

sorbent bed was then washed by 12 mL of HPLC grade water. Before the sorbent bed dried, liquid sample was added to the cartridge while the vacuum was still drawing liquid at about 5 mL/min. When all the sample had passed through the sorbent bed, 4 mL of HPLC grade water were used to rinse the cartridge and to remove interferences. The SPE cartridge was then dried under full vacuum (25" Hg) for 30 minutes. For eluting the isolate, 1 mL of HPLC grade acetonitrile was used. The eluant was then collected in a vial and analyzed by the HPLC. A schematic of the SPE setup is shown in Figure 2, and Table 4 outlines the step-by-step SPE procedures.

3.2 Experimental Design and Methods

3.2.1 Isotherm Experimental Design

The goal of doing the bisolute isotherm experiments was to provide adsorption equilibrium data from which a multicomponent isotherm could be derived. Since a good isotherm would account for all the practical concentration ranges, the experimental conditions must be designed such that they would provide a wide distribution of experimental endpoints. A Pascal computer program which employed the Langmuir Multicomponent Isotherm was written to predict the experimental outcome by using a trial and error method called the Complex Method of Box (Box, 1965). The flowchart in Figure 3 outlines the procedures of the program, and a copy of the program is in Appendix C-1.

3.2.1.1 Program's Results & Usage

All the endpoints predicted from the initial experimental conditions are displayed

Figure 3 Flowchart for the Pascal Program

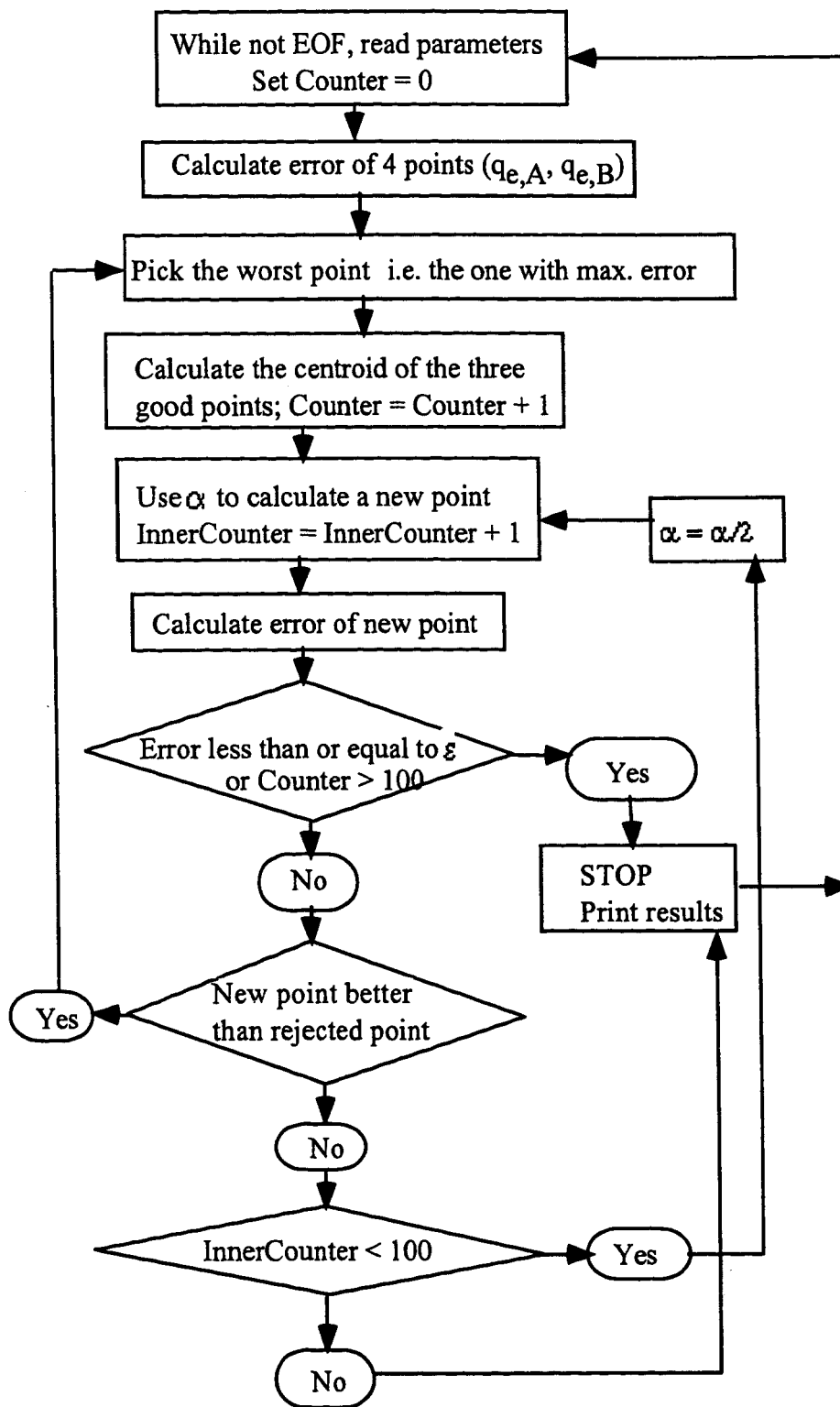


Figure 4 Computer Program Prediction for RDX

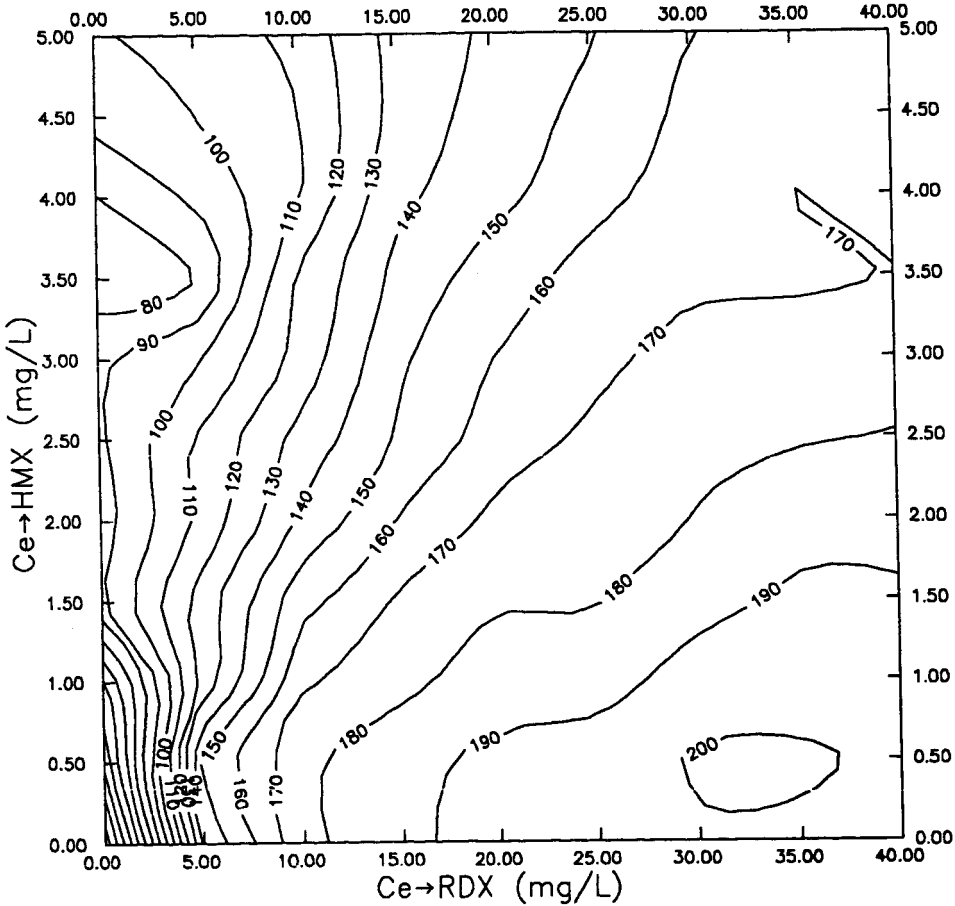
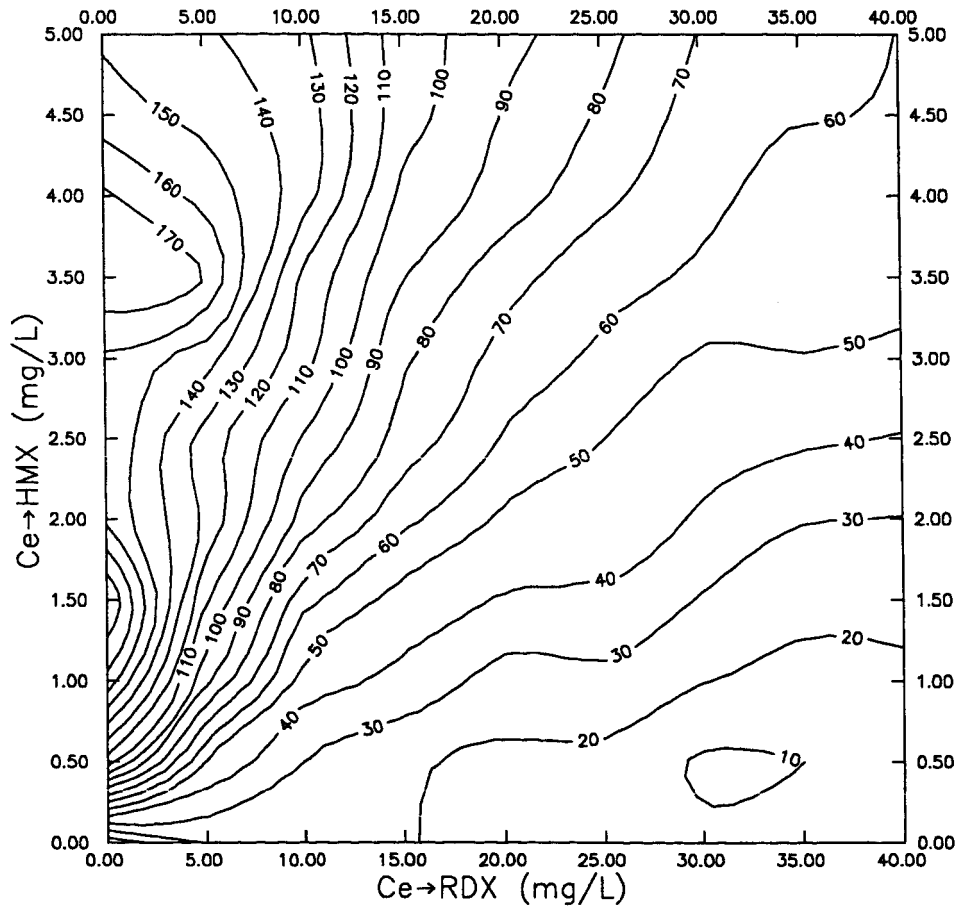


Figure 5 Computer Program Prediction for HMX



using two-dimensional contour graphs. Figure 4 and 5 show the isotherm predictions for RDX and HMX sorbed concentration as functions of RDX and HMX equilibrium concentration. The desired experimental endpoints or equilibrium concentrations were first selected from the contours; knowing the corresponding sorbed concentration of RDX and HMX, the required initial experimental conditions could be calculated.

Sometimes the same experimental endpoint could be attained using different initial experimental conditions. These conditions could be found using the contours and backcalculations. This process offered the author the freedom to choose from various carbon dosages, volumes of mixtures, and compounds' concentrations. Generally the goal was to minimize the amount of resources used for reaching a certain experimental endpoint and to select conditions which had the least experiment error (to be discussed last in this chapter). Without the program, experiments would be done blindly and there would be no guarantee that all experiments performed would produce a unique point on an isotherm.

Another advantage of this program was related to the experimental data analysis. The SPE method was necessary for preconcentrating isotherm samples that had extremely low concentrations. Since the program predicted the RDX and HMX equilibrium liquid concentrations, isotherm samples which required preconcentration prior to the HPLC analysis could be identified. Furthermore, the SPE concentration factors could easily be estimated from the program's predicted equilibrium concentrations and the HPLC detection limits for both RDX and HMX.

3.2.1.2 Experimental Conditions

The first set of experimental conditions were designed to cover a broad initial concentration ratio between RDX and HMX. They varied from 40 mg/L RDX and 5 mg/L HMX to 40 mg/L RDX and 0.5 mg/L HMX. In order to ensure a systematic procedure for all isotherm experiments, the carbon dosages of 0.5 g, 0.23 g, 0.1 g, 0.05 g, and 0.023 g, and the volume of 1 liter were selected. Using the computer program prediction, a general trend of how the sorbed RDX and HMX concentration varied with the equilibrium RDX and HMX concentration could be obtained. Subsequent isotherm experimental conditions were backcalculated from the endpoints selected on the contour graphs which are generated by the first set of predicted data. Endpoints that covered all ranges of end concentration and various end concentration ratios between the two compounds were selected for future experiments. While the carbon dosages were set to the 5 previously cited values, the volume and the initial concentrations were adjusted to obtain the desired results. Overall the predicted end concentrations for all the experiments varied from 0.0061 mg/L to 39.8 mg/L for RDX and 0.0023 mg/L to 5 mg/L for HMX. Notice that the predictions and calculations assumed 40 mg/L and 5 mg/L to be the saturated concentrations for RDX and HMX respectively. An example of the program's input and output can be found in Appendix C-2 and C-3.

3.2.1.3 Isotherm Experiments: Materials & Methods

About 90 g of granular Calgon's F400 was measured and rinsed with deionized water. After overnight pretreatment using deionized water heated at 80°C, the carbon

was stored in an oven which was set at 100°C. All the multicomponent isotherm experiments were performed using the same batch of carbon, and the carbon was pulverized at least a day before the experiments. The pulverized carbon was then left overnight in the same oven.

Technical grade RDX and HMX were used for all the multicomponent isotherm experiments presented in this thesis. Generally the explosives were heated and stirred in deionized water for about 16 hours to ensure that all RDX and HMX were dissolved. When the stock solution was cooled to room temperature, aliquots of carbon and the explosive solution were measured and put in the appropriate Erlenmeyer flasks. The carbon dosages were fixed at 0.5 g, 0.23 g, 0.1 g, 0.05 g, and 0.023 g, and the volume of solution used varied from 1 L, 1.8 L, 4 L, to 6 L at most. The flasks were stoppered and shaken on an orbital shaker table at about 90 rpm. The 1-L isotherm mixtures were shaken for at least 4 days, and the rest were shaken for 5-7 days, depending on the size of the volume. Samples of stock solution and isotherm mixtures were collected and filtered using 0.2 µm ACRODISC filters prior to injection into the HPLC. If the sample's concentration was expected to be below detection limit, they would be preconcentrated using the SPE procedures.

3.2.2 Solubility Tests: Materials & Methods

Although various literature sources have established the aqueous solubility limits for both RDX and HMX at 20°C, a different laboratory setting and technique might affect the solubility limits; therefore, saturated concentration tests using technical grade RDX

and HMX were conducted. Approximately 83 mg RDX and 12 mg HMX were put in separate 1-L Erlenmeyer flasks, and they were heated and stirred overnight in deionized water. The RDX and HMX mixtures were allowed to cool to room temperature before they were transferred to separate 225-mL Erlenmeyer flasks; these flasks were then left in an incubator which was set at 20°C. Samples were periodically collected from both mixtures, and their concentrations were determined using the HPLC analysis.

3.3 Error Analysis

During the course of experiments, errors are introduced from measurements and analytical instruments. These errors cannot be overlooked because they can greatly influence the accuracy or interpretation of the experimental data. This section is devoted to analyzing the uncertainties in the experimental results due to various sources of error. For the purpose of simplicity, only pure RDX and HMX isotherms are considered; however, similar error analysis is applicable to the bisolute adsorption case.

An adsorption isotherm experiment is governed by the mass balance equation

$$q_e = \frac{V(C_o - C_e)}{M} \quad (3.1)$$

where q_e = adsorbed phase concentration, mg of sorbates/g of carbon

V = volume of isotherm mixture, L

C_o = initial liquid phase concentration, mg/L

C_e = equilibrium liquid phase concentration, mg/L

M = mass of carbon, g

Using the Freundlich isotherm for data interpretation, the value of q_e should be related to the equilibrium concentration as follows:

$$q_e = KC_e^{1/n} \quad (2.5)$$

or

$$C_e = \left(\frac{q_e}{K}\right)^n \quad (3.2)$$

where

$$q_e = \frac{X}{M} \quad (3.3)$$

X = the amount of sorbate adsorbed in milligrams.

After substituting equation (3.2) and (3.3) into equation (3.1), the mass balance equation can be rewritten as

$$q_e = \frac{V(C_o - (\frac{X/M}{K})^n)}{M} \quad (3.4)$$

In order to examine the different variables' effects on the values of q_e , the author uses the software Maple to take the derivative of q_e with respect to each experimentally measured parameters; for example, the derivative of q_e with respect to carbon mass is:

$$\frac{\partial q_e}{\partial M} = \frac{V(\frac{X}{MK})^n n}{M^2} - \frac{V(C_o - (\frac{X}{MK})^n)}{M^2} \quad (3.5)$$

This derivative shows how q_e varies with a unit change of mass M . Since the laboratory balance (Sartorius Balance Model 1712 MP8, Silver Edition) measured up to 10^{-6} g, and the mass reading fluctuated during the measurement of powdered carbon, a precision of

Figure 6a: Estimated Error for q_e _RDX Subject to 0.00025g error in Measuring Carbon Dosages

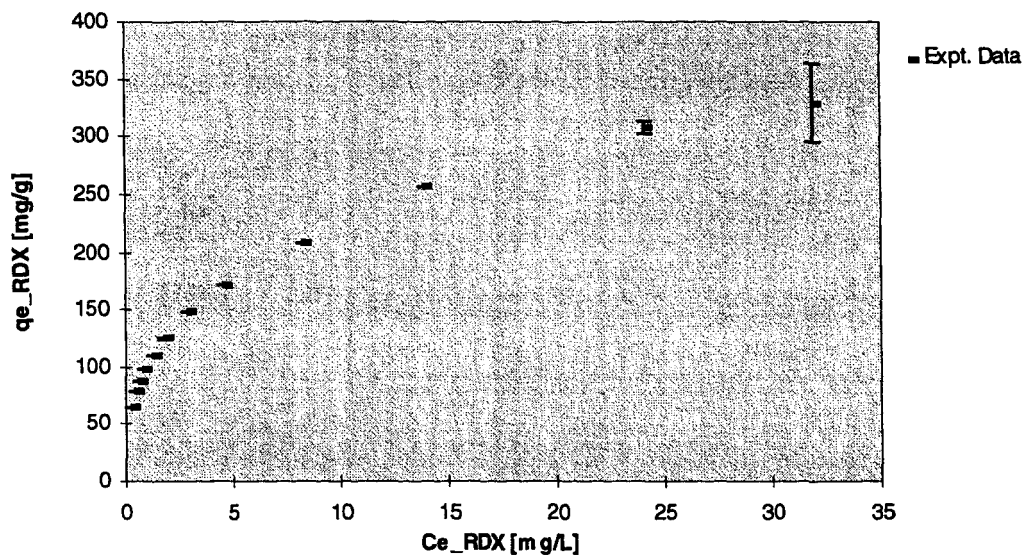
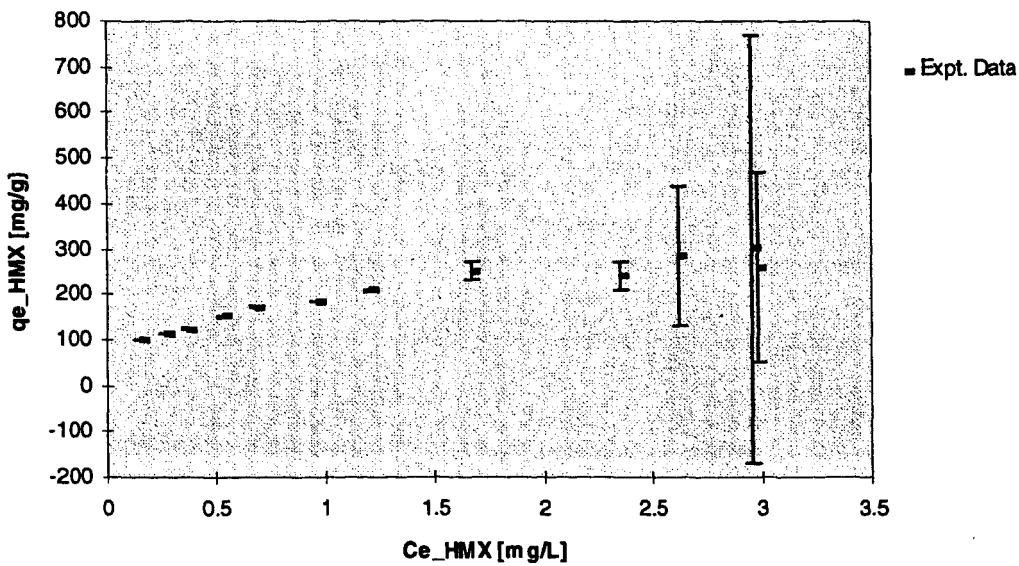
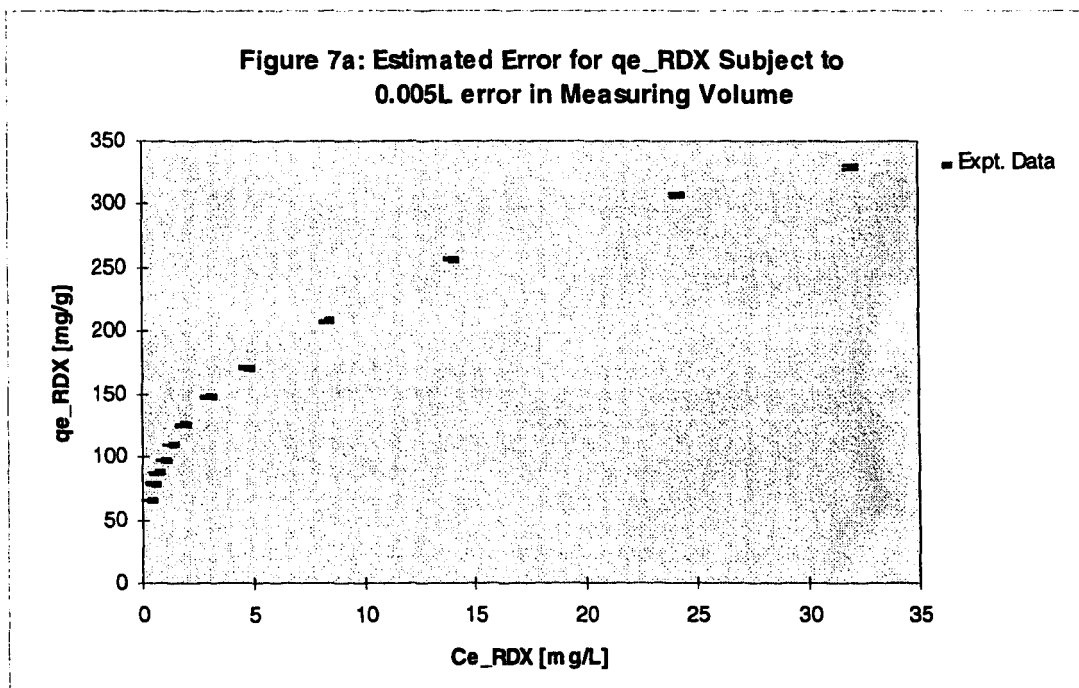


Figure 6b: Estimated Error for q_e _HMX Subject to 0.00025g error in Measuring Carbon Dosages



± 0.00025 g was established for each carbon measurement. Using equation (3.5), the effect of the error in M on q_e can be calculated. Figures 6a and b illustrate the error in q_e for RDX and HMX at various equilibrium concentrations. All the points shown in the error analytical graphs are actual experimental data. Notice that as the carbon dosages decrease, the error increases because the same uncertainty has a more significant effect on a small carbon mass than on a large carbon mass. The last three points in Figure 6b show large experimental error; therefore, experiments are not performed for these conditions. The extremely low carbon dosage, such as 0.002205 g for the most erroneous point in Figure 6b, increase the sensitivity of each error tremendously because mass M plays an important role in the $\partial q_e / \partial M$ expression. The smaller the M value, the larger the error becomes.

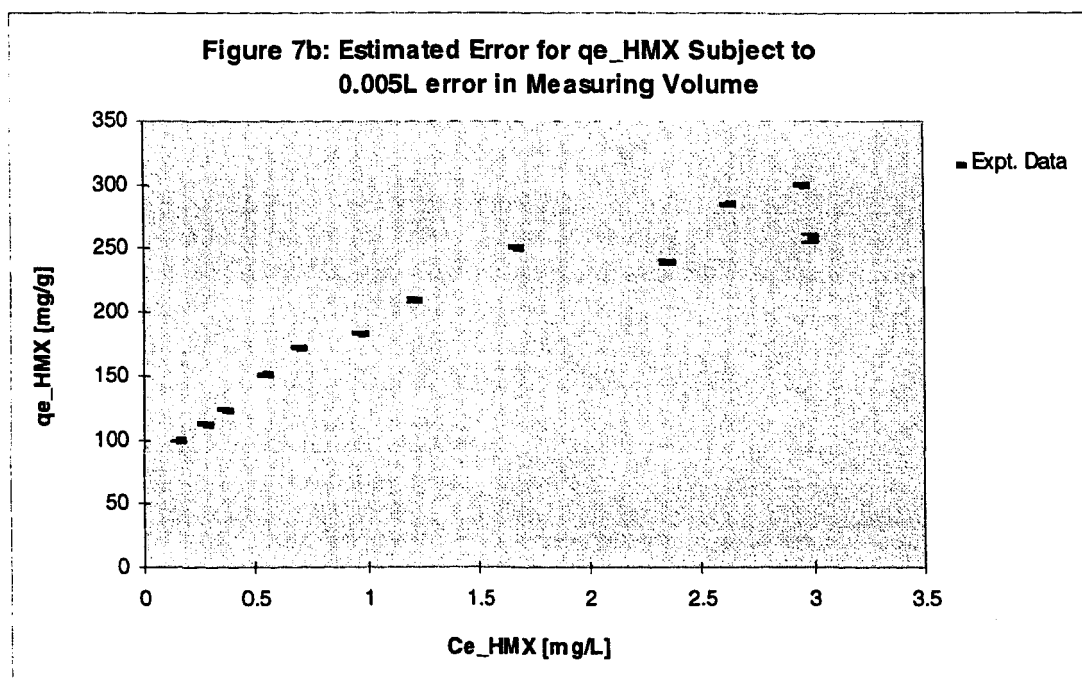
Figure 7a: Estimated Error for q_{e_RDX} Subject to 0.005L error in Measuring Volume



Differentiating q_e with respect to volume V gives

$$\frac{\partial q_e}{\partial V} = \frac{C_0 - \left(\frac{X}{MK}\right)^n}{M} \quad (3.6)$$

Higher accuracy in measuring volume can be obtained by using volumetric flasks than graduate cylinders. Since the single-solute isotherm mixtures were measured with volumetric flasks, and the multicomponent isotherm mixtures were measured with both graduate cylinders and volumetric flasks, a conservative estimation of 5 mL was assumed for the error in measuring volume V . After substituting in the appropriate values for the above equation, q_{e_RDX} and q_{e_HMX} are plotted with error bars in Figure 7a and b. Since



5 mL is only 0.5% of 1L, the fixed volume of the pure isotherm mixtures and the minimum volume for the bisolute isotherm mixtures, it has a negligible impact on the measured sorbed concentration for both species. For higher volume mixtures in the

multicomponent adsorption experiments, the error will be more insignificant.

Another source of inaccuracy in calculating q_e is from measuring C_o and C_e using the HPLC as the analytical instrument. The HPLC's integrator prints out area codes which correspond to the area under each peak in the chromatograph. The translation from area codes to liquid concentrations relies on the standard solutions' data shown in Appendix A. Linear regression of the area codes provides values for each standard's slope and intercept from which liquid concentrations are calculated. The accuracy of the calculated concentration depends on the consistency of the HPLC integration and the precision of the linear regression.

Differentiating the sorbed concentration q_e with respect to C_o and C_e individually results in the following expressions:

$$\frac{\partial q_e}{\partial C_o} = \frac{V}{M} \quad (3.7)$$

$$\frac{\partial q_e}{\partial C_e} = -\frac{V}{M} \quad (3.8)$$

The errors for calculating C_{e_RDX} and C_{e_HMX} from linear regression data are 0.000339 mg/L and 0.0255 mg/L respectively. Since the change of q_e with respect to C_o and C_e differs only by the sign, the error bars for both cases should be the same. Figure 8a shows that for the RDX data, the errors introduced by the HPLC are as insignificant as the ones introduced by the volumetric measurements; however, Figure 8b shows that the HMX data are subject to noticeable error at low carbon dosages. This is expected

Figure 8a: Estimated Error for q_e _RDX Subject to 0.000339mg/L Error in Measuring Concentration

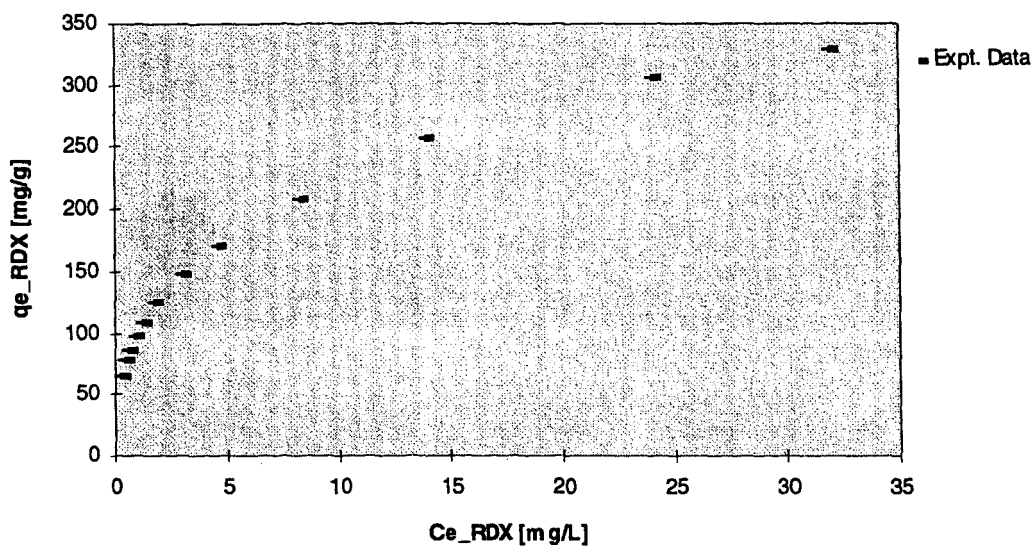
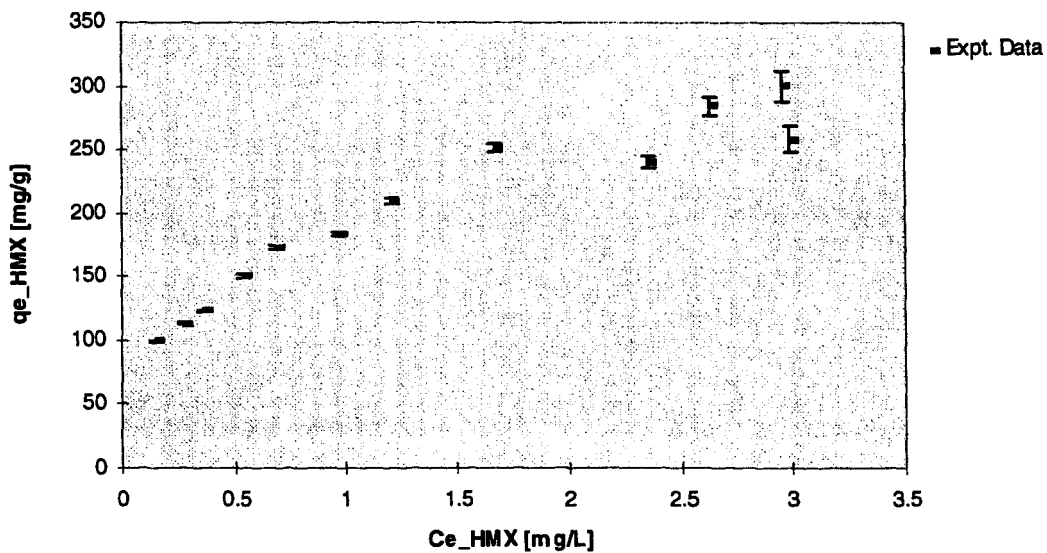


Figure 8b: Estimated Error for q_e _HMX Subject to 0.0255mg/L Error in Measuring Concentration



because the uncertainty for measuring HMX concentration is about 75 times larger than that of RDX. In addition, higher inaccuracies at extremely low carbon dosages for the pure HMX isotherm can be explained by the denominator of the $\partial q_e / \partial C_e$ expression.

The error analysis thus far concentrates on the experimental measurements. As shown in the first few equations in the beginning of this section, the Freundlich isotherm parameters K and n also contribute to certain amount of error in the sorption data because they are derived from the experimental data. From the Freundlich isotherm

$$q_e = KC_e^{1/n} \quad (2.5)$$

one can examine how K and n affect the value of q_e by taking the following derivatives:

$$\frac{\partial q_e}{\partial K} = C_e^{(1/n)} \quad (3.9)$$

$$\frac{\partial q_e}{\partial n} = -\frac{KC_e^{1/n} \ln C_e}{n^2} \quad (3.10)$$

A 1% error in both K and n is assumed. The effect of 1% error in K and n on q_e is illustrated in Figures 9a & b to 10a & b. Figures 9a and 10a are for the RDX data; Figures 9b and 10b are for the HMX data. All four graphs imply that there is at most 1.2% error in q_e subject to the 1% uncertainty in the Freundlich parameters; nevertheless, the impact on q_e 's values is mild.

Figure 9a: Estimated Error for q_{e_RDX} Subject to 1% Error in Freundlich Parameter K

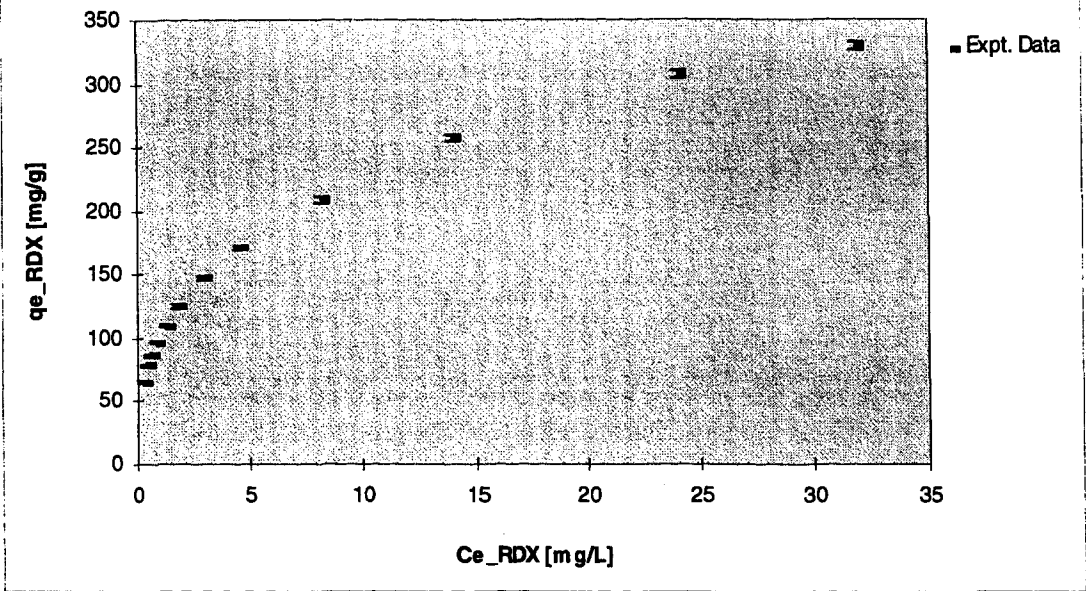


Figure 9b: Estimated Error for q_{e_HMX} Subject to 1% Error in Freundlich Parameter K

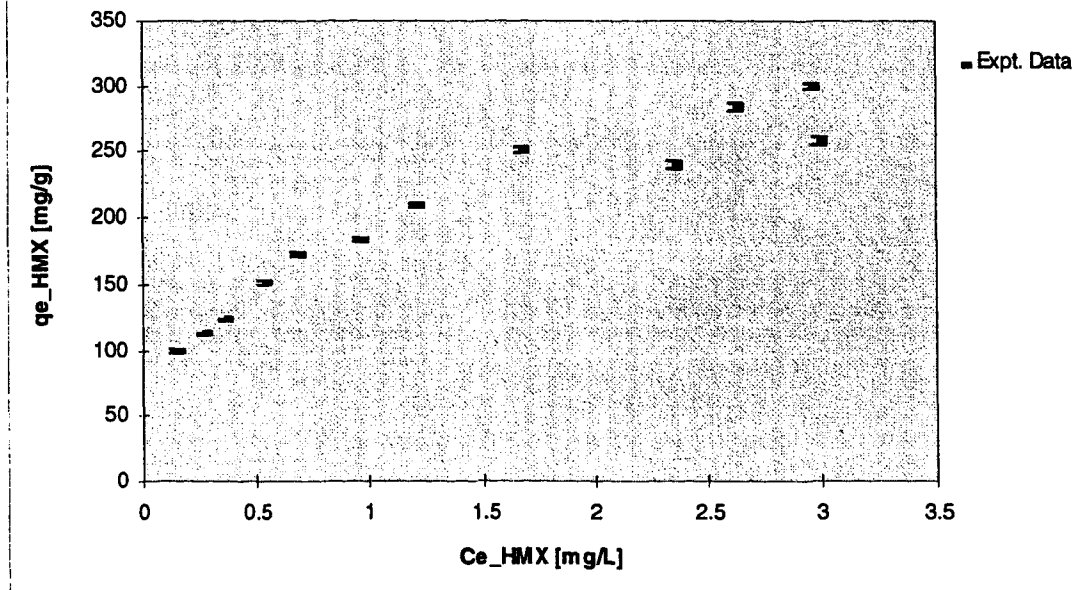


Figure 10a: Estimated Error for q_{e_RDX} Subject to 1% Error in Freundlich Parameter n

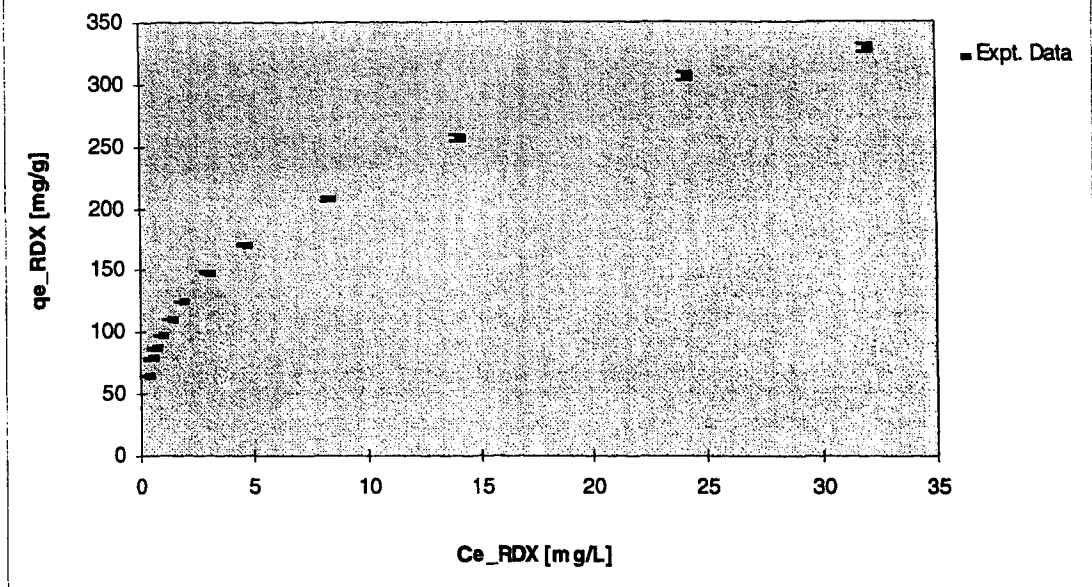
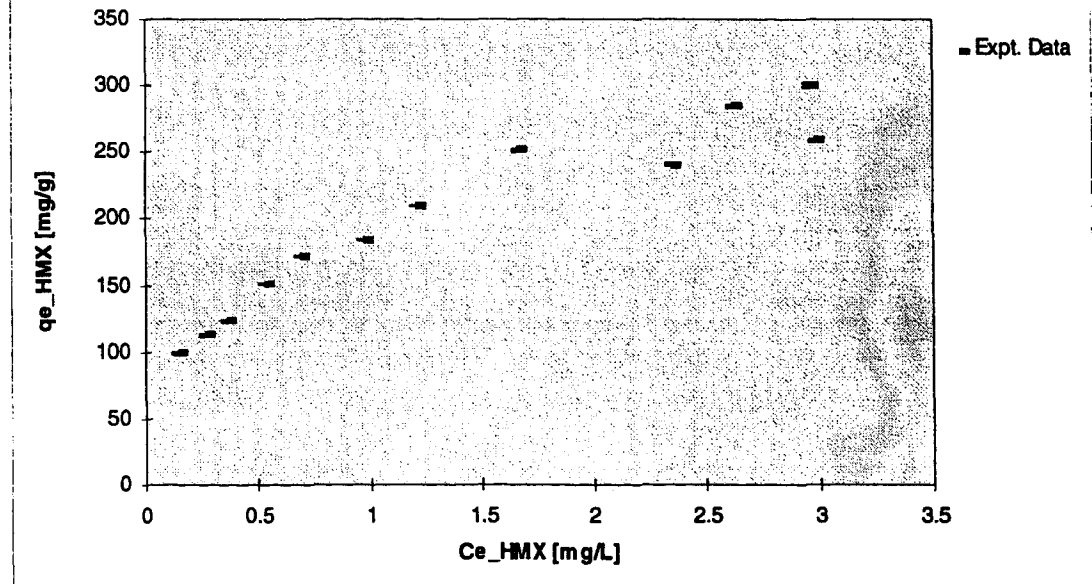


Figure 10b: Estimated Error for q_{e_HMX} Subject to 1% Error in Freundlich Parameter n



From the above discussion, one can conclude that the major source of error in the adsorption experiments is from measuring carbon mass. This is especially true for low carbon doses. By selecting experimental conditions that avoid large error, more precise isotherms can be obtained. The conditions with large error, shown in Figure 6b, are avoided. Values of q_e and C_e can be obtained by selecting different experimental conditions. The multicomponent isotherm carbon dosages are fixed at 0.5 g, 0.23 g, 0.1 g, 0.01 g, and 0.023 g. The error in HMX sorbed concentration are negligible for those dosages because they correspond to earlier data points with equilibrium concentration less than 0.4 mg/L. Conversely, the last two points in Figure 6a are problematic because the two points with noticeable errors correspond to 0.05 g and 0.023 g of carbon. Since many multicomponent isotherms are done with 0.023 g of carbon, the corresponding experimental data for RDX may be unreliable; it may lead to an error as high as 10% for the RDX sorption data. For the HMX sorption data, the error is about 0.65% for 0.020 g of carbon; therefore, dosages above this value will have less error. As for the rest of the factors, such as isotherm mixtures' volume and liquid-phase concentrations, they will not introduce as much error as the carbon dosages; therefore, they are not of major concern.

4. RESULTS AND DISCUSSIONS

Before examining the bisolute adsorption of RDX and HMX onto activated carbon, it is important to first understand the independent adsorption behavior of each component. Single-solute adsorption can provide a basis for comparing adsorption behavioral change in a 2-component system, and fitting the single-solute adsorption data to classical isotherms will help eliminate inapplicable isotherms. If a monocomponent isotherm cannot fit the single-solute data well, its corresponding multicomponent form will also not fit well.

4.1 *RDX and HMX Adsorption*

As mentioned in Chapter 2, the Langmuir, the BET, and the Freundlich isotherms are the three classical isotherm models. At least one of these models can fit most monocomponent isotherm data. Independent adsorption isotherm experiments were conducted for RDX and HMX, and the data were used to fit the linearized form of the three isotherms. Figure 11 compares the linear fit of the three isotherms using the RDX adsorption data, and Figure 12 is a similar illustration for HMX. The results indicated that the Freundlich isotherm fitted data the best for the given equilibrium concentration range, and the BET isotherm gave moderate fit for the same concentration range. It was not surprising that the Langmuir isotherm did not fit the data well because its assumptions are too ideal; however, the Langmuir isotherm is used as a reference for the discussion in this chapter because of its widespread acceptance.

Figure 11 Linearized Langmuir, BET, Freundlich Isotherms for RDX

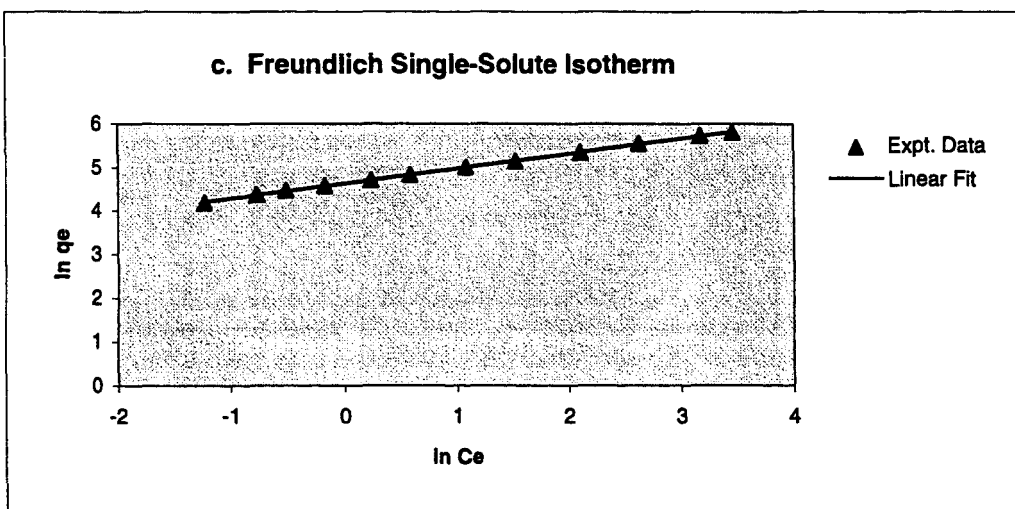
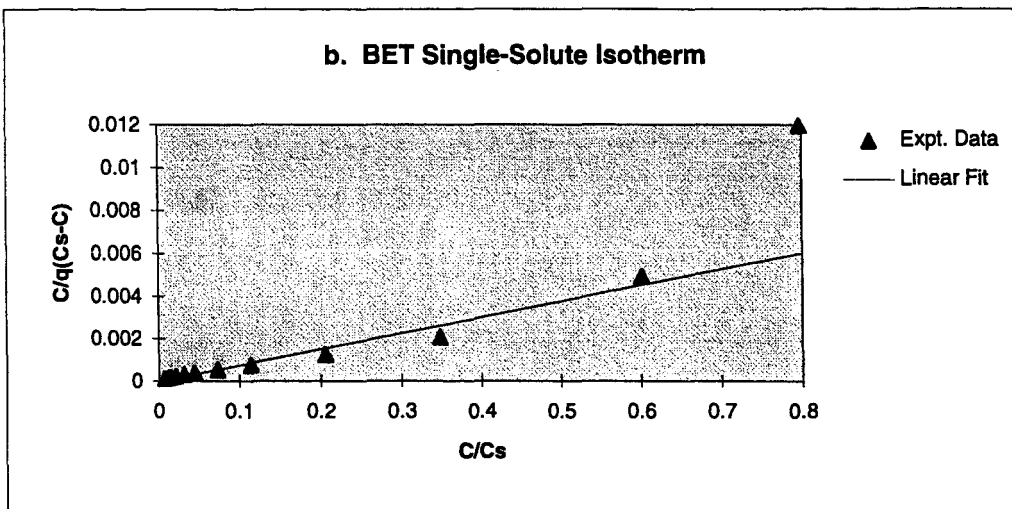
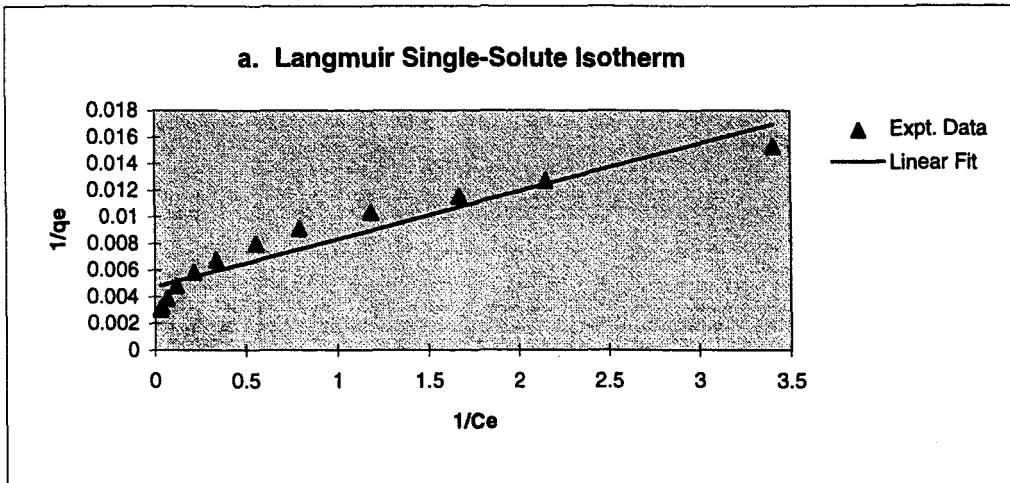
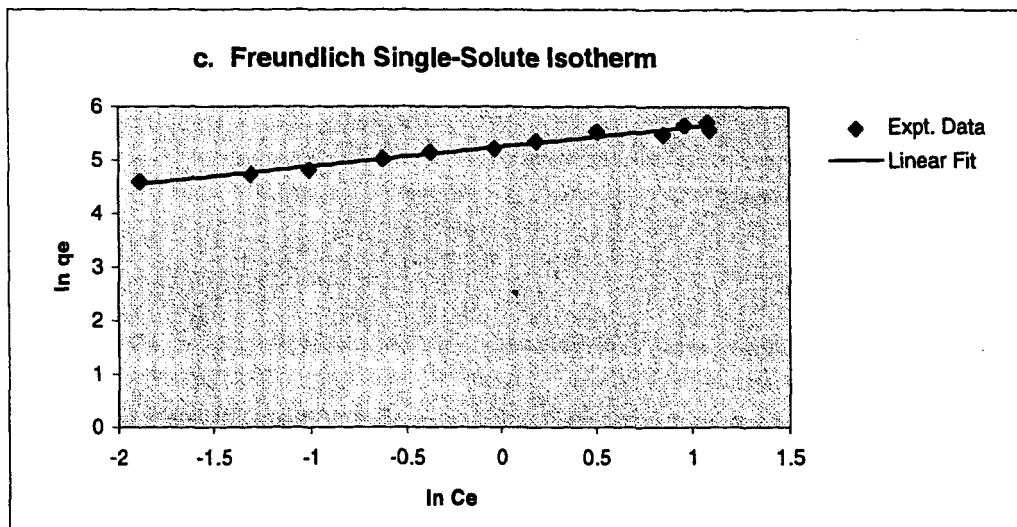
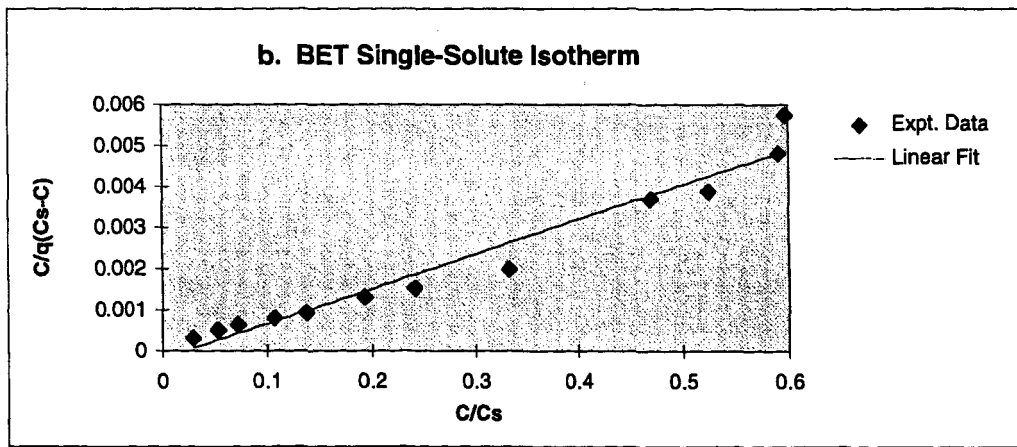
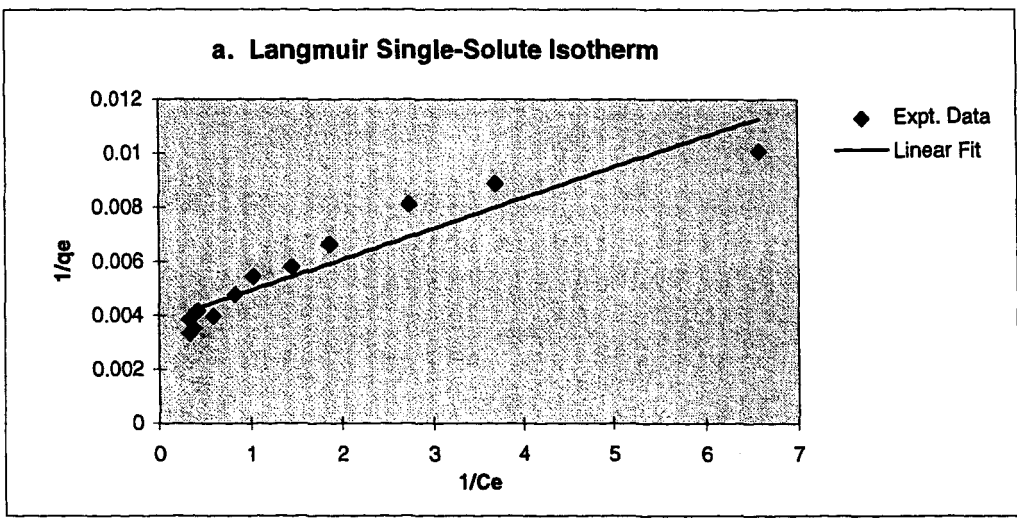


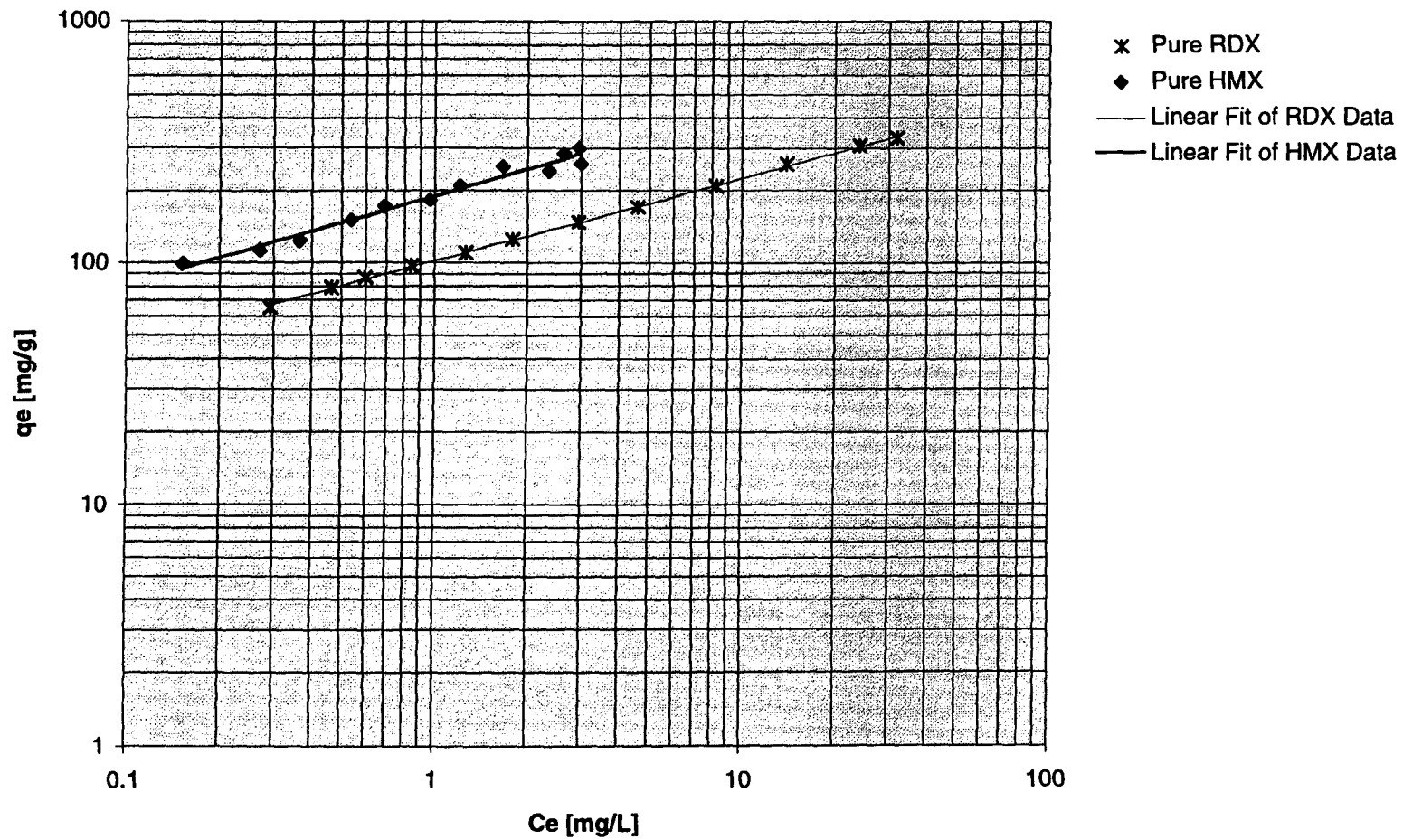
Figure 12 Linearized Langmuir, BET, Freundlich Isotherms for HMX



Since the Freundlich isotherm represent the RDX and HMX adsorption data very well, further study of the two linear plots should give more information about their adsorption behavior. As shown in Figure 13, both linearized Freundlich isotherms for RDX and HMX have similar slopes, but the intercept of the HMX isotherm is clearly higher than that of the RDX. Recall that the slope and the intercept of a linearized Freundlich isotherm represent roughly the adsorption intensity and the adsorption capacity respectively; HMX must have a higher adsorption intensity and capacity than RDX. This indicates that HMX should be more efficiently removed than RDX at all concentration ranges. RDX's adsorption intensity ($1/n$) was found to be 0.343 ± 0.006 , and HMX's was 0.369 ± 0.042 . The numeric similarity implies that their adsorption intensities are quite comparable. Conversely, the clear differences between the two intercepts indicates that F400 definitely has higher capacity for HMX than for RDX. The K parameter (or equivalently the exponential factor of the intercepts) was 101.87 ± 1.10 $(\text{mg/g})(\text{L/mg})^{1/n}$ for RDX and 190.12 ± 7.92 $(\text{mg/g})(\text{L/mg})^{1/n}$ for HMX respectively. It is important to note that the relative differences between these numbers play a more significant role than the absolute values.

The same conclusion regarding the carbon's capacity for both species can be drawn from the Langmuir isotherm as well. The maximum sorption capacity for RDX and HMX were found to be 212.20 mg/g and 305.90 mg/g. Despite the numeric differences calculated from the two isotherms, the two isotherms agreed that there were more adsorption sites for HMX than for RDX on the F400. Since HMX has higher

Figure 13 Freundlich Monocomponent Isotherm for RDX & HMX



adsorption capacity and slightly higher adsorption intensity, it is logical to assume that HMX should be preferentially adsorbed in the bisolute system; however, HMX should not suppress RDX adsorption too much because the adsorption intensities for both are quite similar.

In general when two species are present at the same time during adsorption, they either mutually enhance each other's adsorption, or they adsorb onto the surfaces independently, or they interfere with each other by competing for the same adsorption sites. The RDX-HMX adsorption behavior resembles the third behavior. Figure 14 compares bisolute adsorption behavior with the independent adsorption behavior using the Freundlich Monocomponent Isotherm. Adsorption of both RDX and HMX individually was worse in the bisolute system than in the single-solute systems; nevertheless, the overall adsorption efficiency did not seem to change significantly. RDX and HMX must have competed for at least part of the activated sites on the carbon surfaces.

Generally speaking, the degree of inhibition during adsorption depends partially on the initial concentration ratio of the two explosives. In Figure 14's "40/5" series, meaning initial concentration of RDX and HMX being 40 mg/L and 5 mg/L respectively, RDX adsorption was barely affected by the presence of HMX, but the reverse was true for HMX. Although HMX should generally be preferentially adsorbed, there was higher RDX sorption and lower HMX sorption for this series because the amount of RDX was 8 times larger than HMX. This is an example of unfair competition. Unfair competition means one of the two explosives are initially present at a significantly higher

concentration than the other; therefore, the explosive with higher concentration dominates the adsorption and is favorably adsorbed. A closer look at the isotherms revealed that the competitive HMX's slope (adsorption intensity) actually increased slightly compared to the independent HMX's, and the competitive RDX's slope (adsorption intensity) decreased slightly compared to the independent RDX's. Although HMX in a competitive adsorption system may not be as efficiently removed as the HMX in a non-competitive adsorption system, HMX is still capable of inhibiting the RDX adsorption. The adsorption capacities for both RDX and HMX were slightly decreased in the multicomponent adsorption mode.

More informative comparisons can be performed from the "5/5" and "1/1" series in Figure 14. Since the amount of RDX and HMX initially present in the solution were about the same, there was no overshadowing or dominating effect of one explosive over the other, and hence, the competition was fair. Throughout the discussion in this chapter, fair competition means the initial concentration of RDX and HMX are similar; therefore, there is no preferential sorption subject to large concentration differences. The linear plots for the two series' isotherms clearly showed that both RDX and HMX adsorption was inhibited when they were present in the adsorption system simultaneously. The increase in slopes or intensities could also be observed from both RDX and HMX linear plots, but HMX's increasing factor was consistently higher than RDX's. The change of intensities could be induced by the competition between the two. Since HMX was slightly more competitive than RDX, HMX's increasing factor was higher than that of

RDX. As the competition became more intense, the carbon adsorption capacities for both compounds decreased accordingly, but HMX's sorption capacity was consistently higher than RDX's under fair competition.

The Freundlich linear isotherm's slope is also an indication of the adsorption energy. Given the linearized Freundlich isotherm (see equation 2.6), a steeper slope (lower n) means lower adsorption energy, and a flatter slope (larger n) means higher adsorption energy. Since the n for RDX is consistently higher than that of HMX, RDX may be attracted to high energy sites while HMX is attracted to low energy sites.

The degree of mutual inhibition between two competing adsorbates is also governed by the relative molecular sizes of the sorbates and the relative adsorptive affinities. Lindelius's Rule states that an increase in a sorbate's molecular weight makes the compound less soluble, and the less soluble the compound is, the more likely it is to move to the carbon surfaces than to stay in the liquid phase. The lyophobic (solvent-disliking) or hydrophobic (water-disliking) nature of HMX can explain the preferential adsorption of HMX over RDX. HMX does not only have greater molecular weight than RDX, it is less soluble than RDX. Since HMX is less soluble, it has less affinity towards water than RDX, and hence, HMX's tendency for being adsorbed onto the carbon surfaces will be higher than RDX's. Not all the multicomponent systems obey Lindelius's Rule; for example, TNT-RDX system does not obey this rule; however, the RDX-HMX system does obey it.

Another factor affecting multicomponent adsorption is the relative concentration of the compounds. As discussed earlier, the adsorption behavior can be biased by large RDX-HMX concentration ratio. When C_{o_RDX}/C_{o_HMX} is larger than one, the adsorption phenomenon is not very interesting because the excess amount of RDX will make the competition unfair, leading to higher RDX sorption and lower HMX sorption. Conversely, when C_{o_RDX}/C_{o_HMX} approaches 1 or less than one, more phenomenal competition takes place; HMX's more competitive nature can be observed more easily, but it does not lead to one species dominating the adsorption process because both compounds are still quite comparable under fair competition.

The number of nitro groups in each explosive may also have significant effect on adsorption. Haberman et al. (1982) explained that the nitro groups in the explosives can act as electron-withdrawing groups which directly increase the sorbate-carbon adsorption. Haberman et al. (1982) compared the carbon adsorption of a compound with two nitro groups (2,4-dinitrophenol) with a compound with only one nitro group (p-nitrophenol). There was better sorption of 2,4-dinitrophenol than p-nitrophenol because there was larger electron-withdrawal for 2,4-dinitrophenol than p-nitrophenol. The higher number of nitro groups led to more electron-withdrawing groups reacting with the reducing carbon surfaces, leading to better sorption. Since HMX has four nitro groups and RDX only has three, HMX should react better with the carbon than RDX, hence HMX is preferentially adsorbed.

Apart from ion-exchange adsorption explained above, it is possible that physical adsorption and chemical adsorption also contribute to RDX and HMX adsorption because these three types of adsorption are commonly known for taking part in carbon adsorption simultaneously. Physical adsorption or ideal adsorption usually refers to adsorption subject to van der Waals forces. Solutes or molecules undergoing this type of adsorption are free to undergo translational motion along the surfaces. Since physical adsorption is characterized by a relatively low energy of adsorption, the adsorbate is not held very strongly to the adsorbent and the process is reversible. Conversely, molecules that undergo chemical adsorption, or activated adsorption, or chemisorption are not free to move along the adsorbent surfaces. Since the adsorbates form strong bonds and react with the adsorbent during chemisorption, the process involves high energies of adsorption and the process is irreversible. While chemisorption can be enhanced by higher temperature, physical adsorption is favored by lower temperature.

The discussion thus far argues that RDX-HMX concurrent adsorption is a competitive process; however, it is difficult to decide whether the two explosives are partially competing or fully competing for all adsorption sites. Studying various multicomponent isotherms may lead to further insights on the bisolute system.

4.2 Multicomponent Adsorption Isotherms

Previous researchers have tried to use single-component isotherms to account for multicomponent adsorption data. While the isotherms might provide adequate fit for the data, this method of data analysis is not sufficiently accurate because it fails to account

for the interaction between the sorbates. In order to develop an appropriate isotherm for the RDX-HMX adsorption system, the author establishes a few criteria for choosing the best isotherm. First, the isotherm must be able to predict or model adsorption over a wide concentration range; second, it must be simple to apply mathematically; third, it must account for nonidealities, such as heterogeneous and irreversible adsorption. It is also preferable that this isotherm can be derived from the single-solute data.

A common criterion for applying classical multicomponent isotherms to interpret bisolute data is that the corresponding monocomponent isotherm must fit the single-solute adsorption data well. Upon examining the three classical isotherms which are the BET isotherm, the Langmuir isotherm, and the Freundlich isotherm, the possibility of using the BET isotherm was eliminated for two reasons. First, it did not give satisfactory linear fit for both RDX and HMX adsorption; second, a bisolute or multicomponent BET isotherm for liquid mixtures was not found. Although the Langmuir isotherm was not able to fit the single-solute RDX and HMX data well at low concentration range, its multicomponent isotherm was helpful in estimating experimental results. In addition, the Langmuir isotherm was the most well-known multicomponent isotherm; therefore, it would be informative to include the Langmuir Multicomponent Isotherm for comparing various multicomponent isotherms. The Freundlich Monocomponent Isotherm fitted the data the best among the three, and it has been widely used for describing multicomponent data (Table 3b). Consequently the Freundlich Multicomponent Isotherm appeared to be the best candidate among the three classical isotherms.

There are also a few additional isotherms which prove to be promising. Among the ten multicomponent isotherms discussed in the literature review, the applicable ones consist of the Langmuir Partially Competitive Isotherm, the SIAS Isotherm, and the ISIAS Isotherm. The rest of the isotherms were not chosen for further study for various reasons; some were too complicated mathematically, some required too many parameters that needed to be derived from the experimental data, some provided extremely poor fit for the experimental data, and some were simply inapplicable to the adsorption system of interest.

4.2.1 Langmuir Multicomponent Isotherm

The Langmuir Multicomponent Isotherm

$$q_{e,i} = \frac{Q_i^{\circ} b_i C_i}{1 + \sum_{j=1}^n b_j C_j} \quad (2.8)$$

has proved to be extremely helpful in estimating the experimental results despite the discrepancies between the calculated and the experimental data. The bisolute form of the isotherm is as follows:

$$q_{e,1} = \frac{Q_1^{\circ} b_1 C_1}{1 + b_1 C_1 + b_2 C_2} \quad (4.1a)$$

$$q_{e,2} = \frac{Q_2^{\circ} b_2 C_2}{1 + b_1 C_1 + b_2 C_2} \quad (4.1b)$$

The subscript 1 represents RDX, and 2 represents HMX. Q_1° , Q_2° , b_1 , b_2 are 212.204 mg/g, 305.899 mg/g, 1.312, and 2.576 respectively and they are derived from the single-

Figure 15 Langmuir Multicomponent Isotherm Contour for RDX

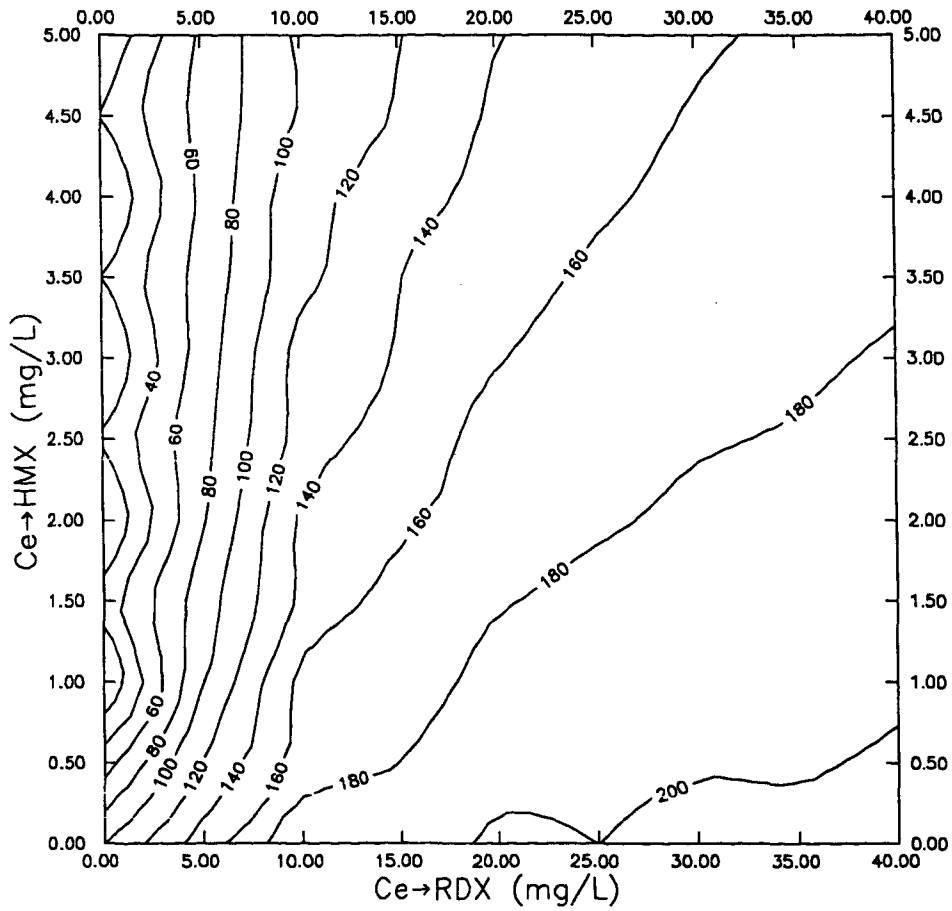


Figure 16 Langmuir Multicomponent Isotherm Contour for HMX

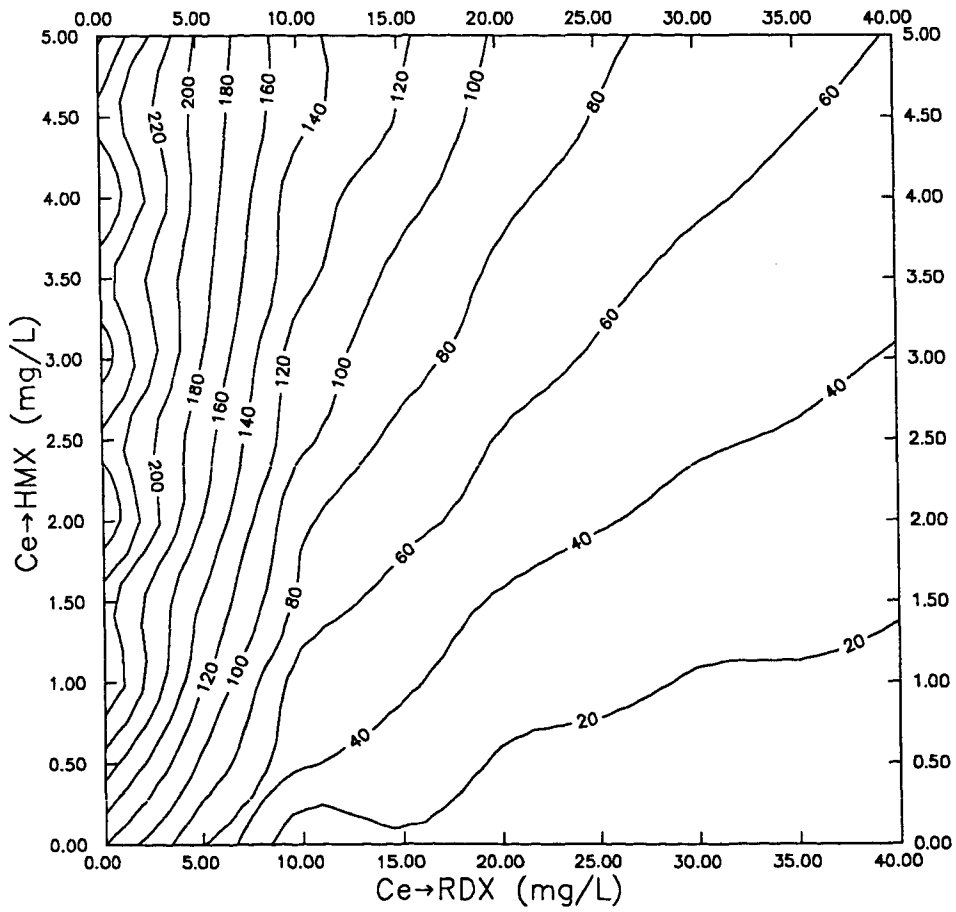


Figure 17 Experimental Results for RDX

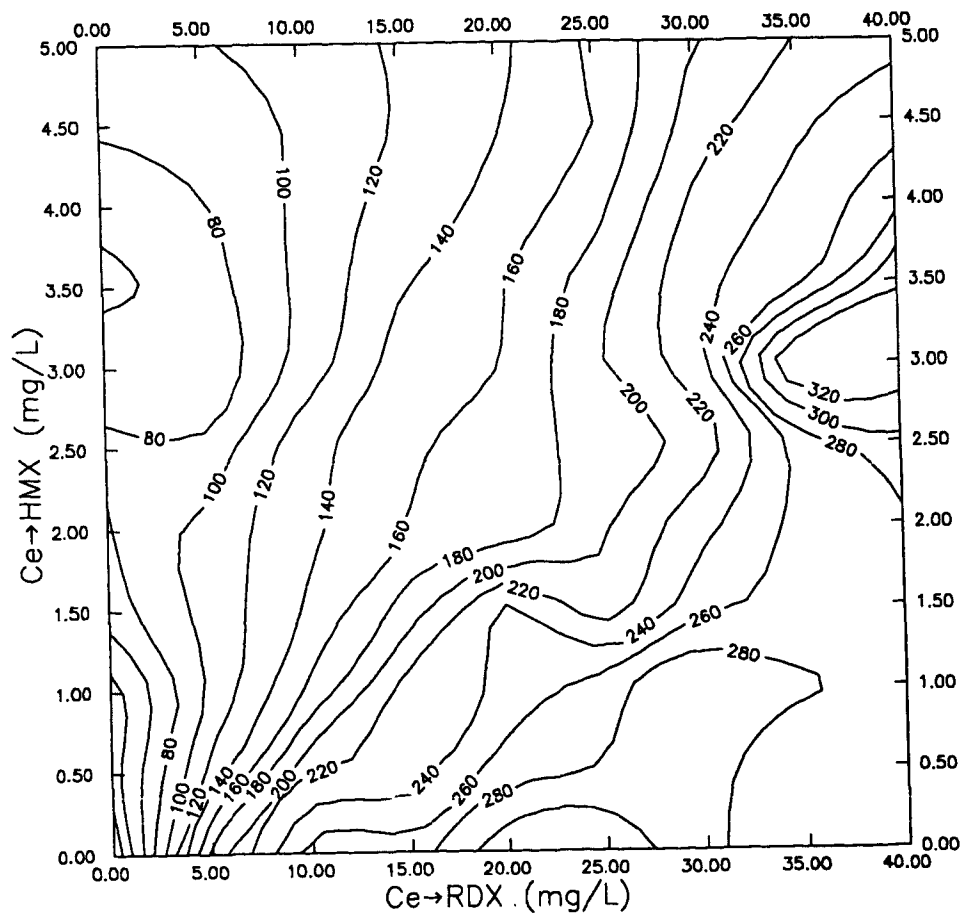
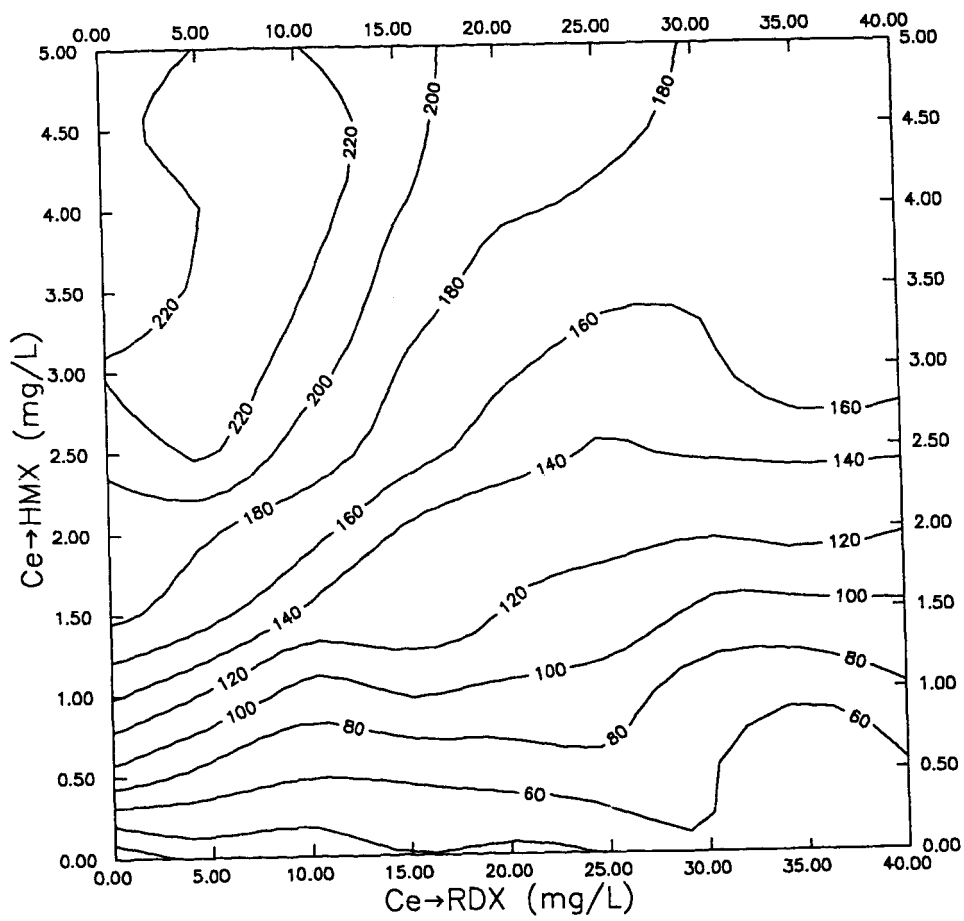


Figure 18 Experimental Results for HMX



solute isotherm experiments.

This isotherm does not fit the experimental data very well. The root mean squares (RMS) errors for the RDX and the HMX sorption values are ± 54.37 mg/g and ± 61.70 mg/g. Figure 15 and 16 show the contour graphs for the RDX and the HMX sorption respectively. The explosives' sorption values are generated by the Langmuir Multicomponent Isotherm from substituting wide range of RDX and HMX equilibrium concentrations. Figure 17 and 18 show the contour graphs generated from the experimental data alone. There is no modeling or isotherm-fitting involved. Overall the Langmuir Multicomponent Isotherm tends to underestimate the RDX sorption data. The maximum experimental RDX sorbed concentration was above 300 mg/g, but the isotherm calculated a maximum value of about 200 mg/g only. One will also notice that the isotherm is overestimating the HMX sorption if one compares the contours on Figure 16 and 18. Figure 15's and 16's contours are also too wide in the intermediate and high RDX equilibrium concentration ranges, meaning that the isotherm is misrepresenting the adsorption trend in these areas.

The main reason which contributes to the poor fit is that the Langmuir Monocomponent Isotherm does not fit the RDX and the HMX single-solute isotherm data very well (please refer to Figure 11 and 12). In addition, the competitive adsorption violates most of the Langmuir assumptions. Activated carbon's heterogeneous surfaces do not allow homogeneous adsorption, and carbon adsorption is an irreversible process. Researchers have proved that RDX adsorption is an irreversible process (Haberman et al.,

1982). Although no tests have been done to identify the reversibility of HMX adsorption, HMX adsorption is likely to be irreversible as well because both RDX and HMX have similar characteristics. Since RDX-HMX adsorption is competitive, adsorption without interaction between the adsorbates is not likely; this is another violation of Langmuir assumptions.

4.2.2 Langmuir Partially Competitive Isotherm

A modification of the Langmuir Bisolute Competitive Isotherm is the Langmuir Partially Competitive Isotherm:

$$q_1 = \frac{(Q_1^o - Q_2^o)b_1C_1}{1 + b_1C_1} + \frac{Q_2^ob_1C_1}{1 + b_1C_1 + b_2C_2} \quad (2.11a)$$

$$q_2 = \frac{Q_2^ob_2C_2}{1 + b_1C_1 + b_2C_2} \quad (2.11b)$$

where $Q_1^o > Q_2^o$.

The subscript 1 denotes HMX, and the subscript 2 denotes RDX in this particular isotherm because the HMX maximum sorption capacity is higher than RDX's. The constants Q^o and b are derived from the single-solute data and the numerical values are the same as before.

Figure 19 and 20 are the contour graphs generated by the Langmuir Partially Competitive Isotherm from using the equilibrium concentration values similar to the experiments'. It is no surprise that Figure 15 and Figure 19 are identical because the RDX sorption equation (2.11b & 4.1b) for both isotherms are the same. Figure 16 differs from Figure 20 because the isotherm is modified for the more competitive sorbate. The

Figure 19 Langmuir Partially Competitive Isotherm Contour for RDX

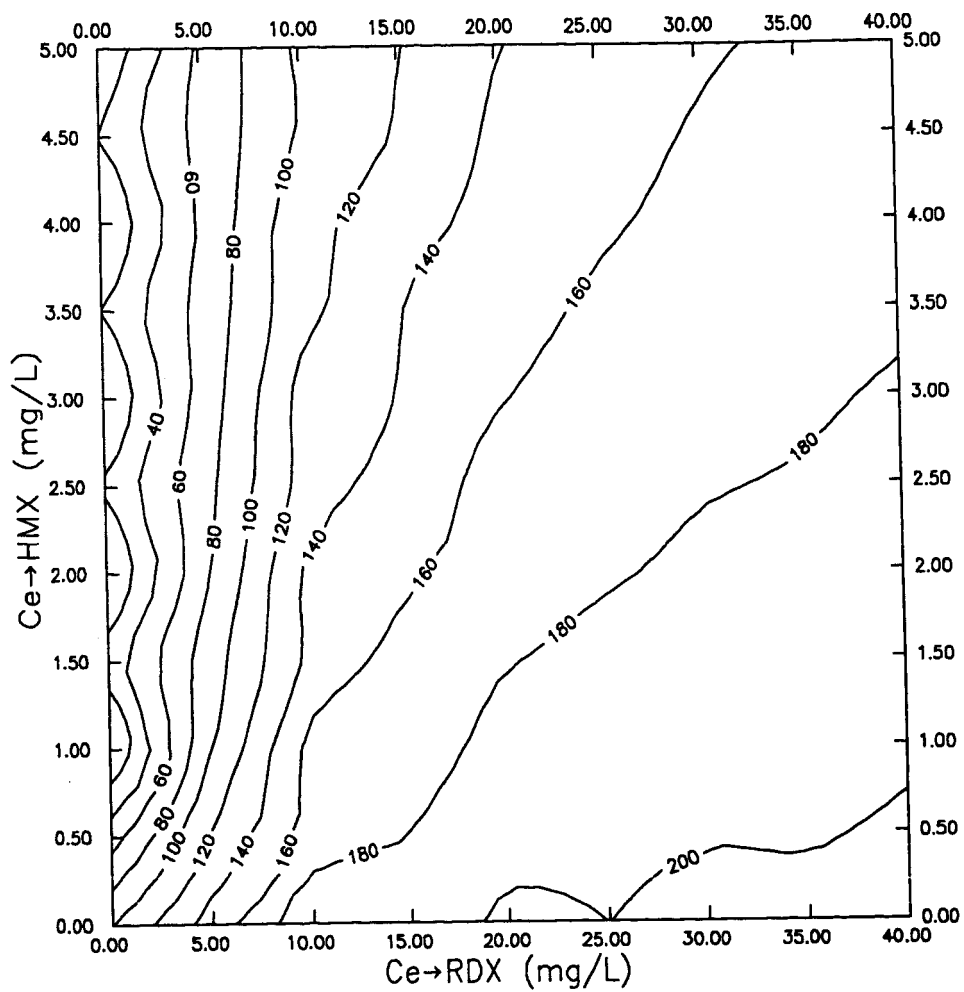
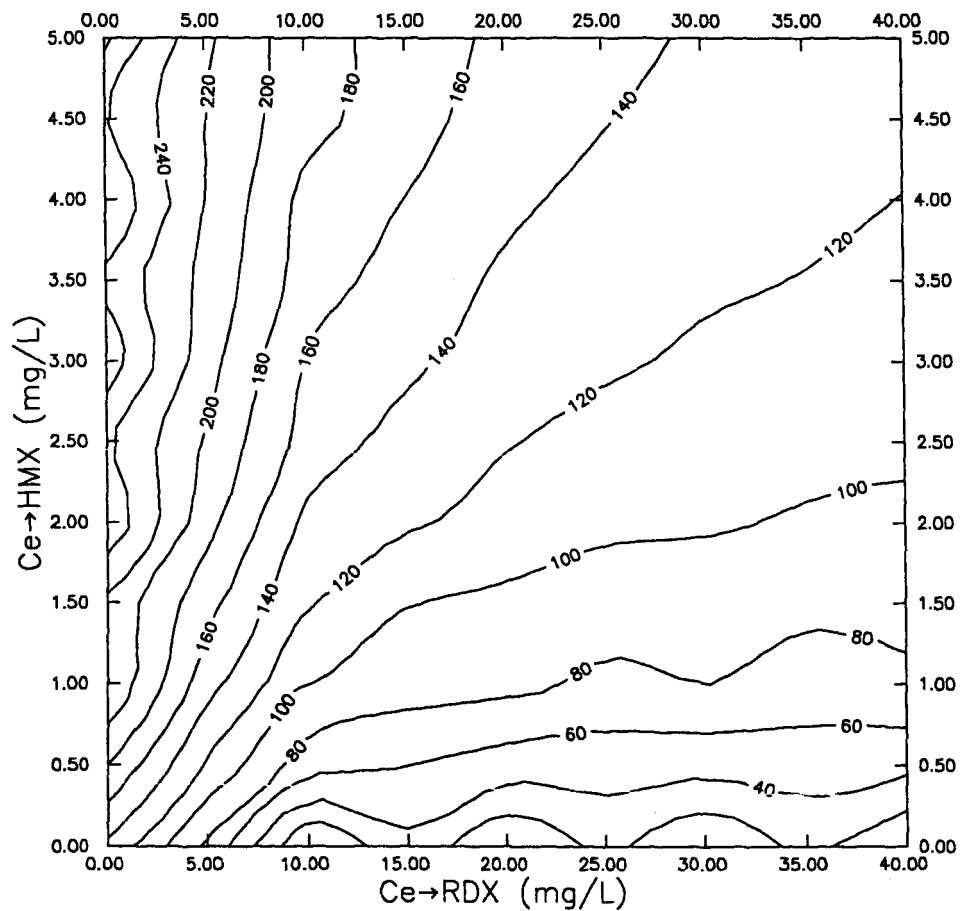


Figure 20 Langmuir Partially Competitive Isotherm Contour for HMX



Langmuir Partially Competitive Isotherm has improved Langmuir Multicomponent Isotherm's ability in portraying the contours for the HMX adsorption data. While the RMS error for the RDX data stays at 54.37 mg/g, the RMS error for the HMX data improves by 50 percent, to 29.56 mg/g.

The modified Langmuir isotherm is unique in that no other isotherms explicitly consider partial competition between the two adsorbates. Most isotherms usually assume the bisolute adsorption process to be fully competitive. The Langmuir Partially Competitive Isotherm's general assumptions are the same as that of the Langmuir Multicomponent Isotherm, but the assumption of partial competition has improved the isotherm's ability to predict the HMX sorption values. Since the isotherm equations for RDX in the Langmuir Multicomponent Isotherm and the Langmuir Partially Competitive Isotherm are the same, there is no improvement in predicting the RDX sorption values.

4.2.3 Freundlich Multicomponent Isotherm

The Freundlich bisolute isotherm has various forms, and the common linear expressions are as follows:

$$\frac{C_1}{C_2} = \frac{1}{C_2} \beta_1 - a_{12} \quad (2.13a)$$

$$\frac{C_2}{C_1} = \frac{1}{C_1} \beta_2 - a_{21} \quad (2.13b)$$

where $\beta_i = \left(\frac{K_i C_i}{q_i} \right)^{\frac{1}{1-n_i}}$

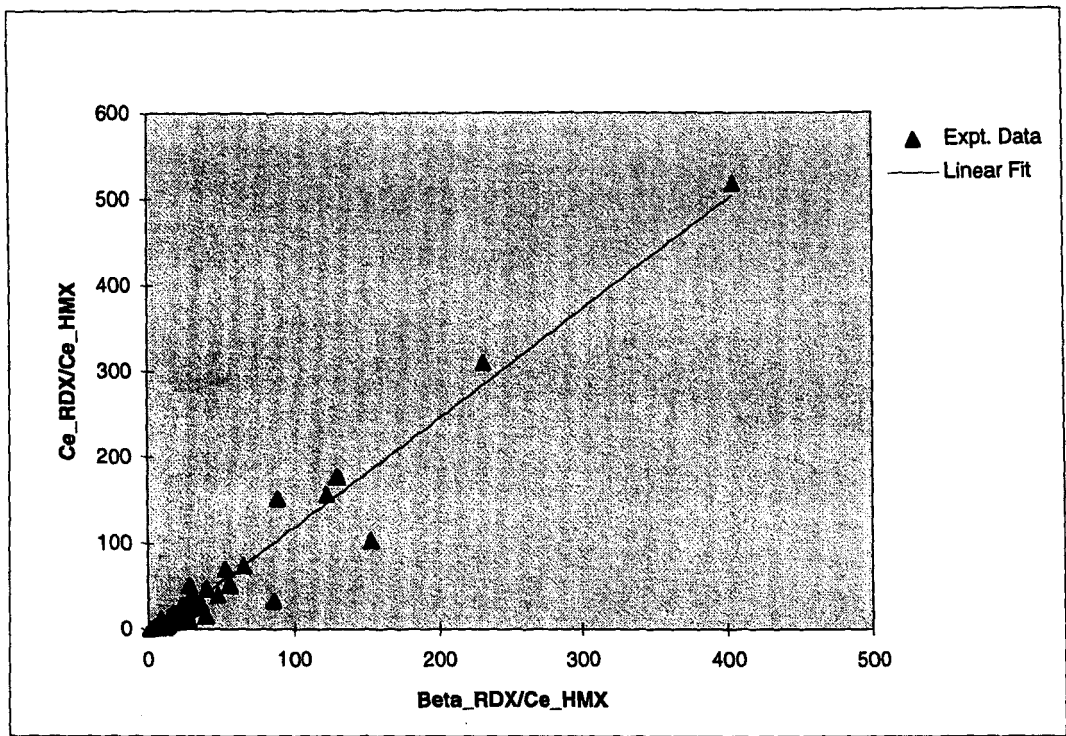


Figure 21 Freundlich Linearized Bisolute Isotherm for RDX

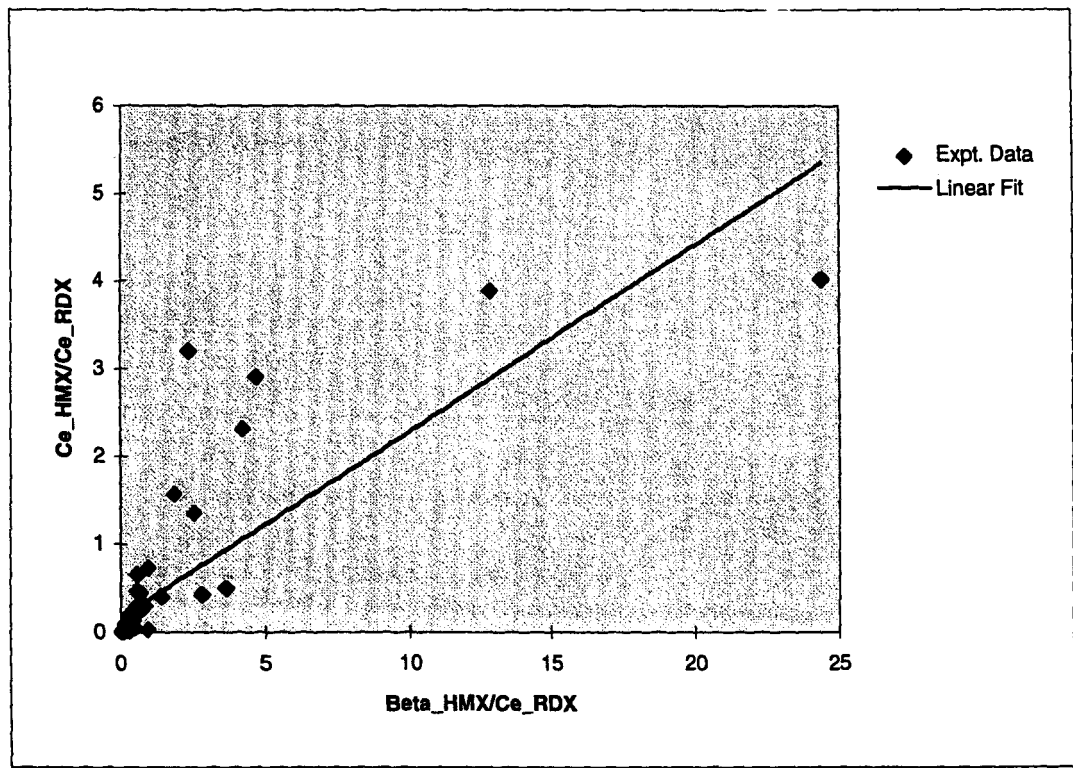


Figure 22 Freundlich Linearized Bisolute Isotherm for HMX

Figure 23 Freundlich Multicomponent Isotherm
Contour for RDX

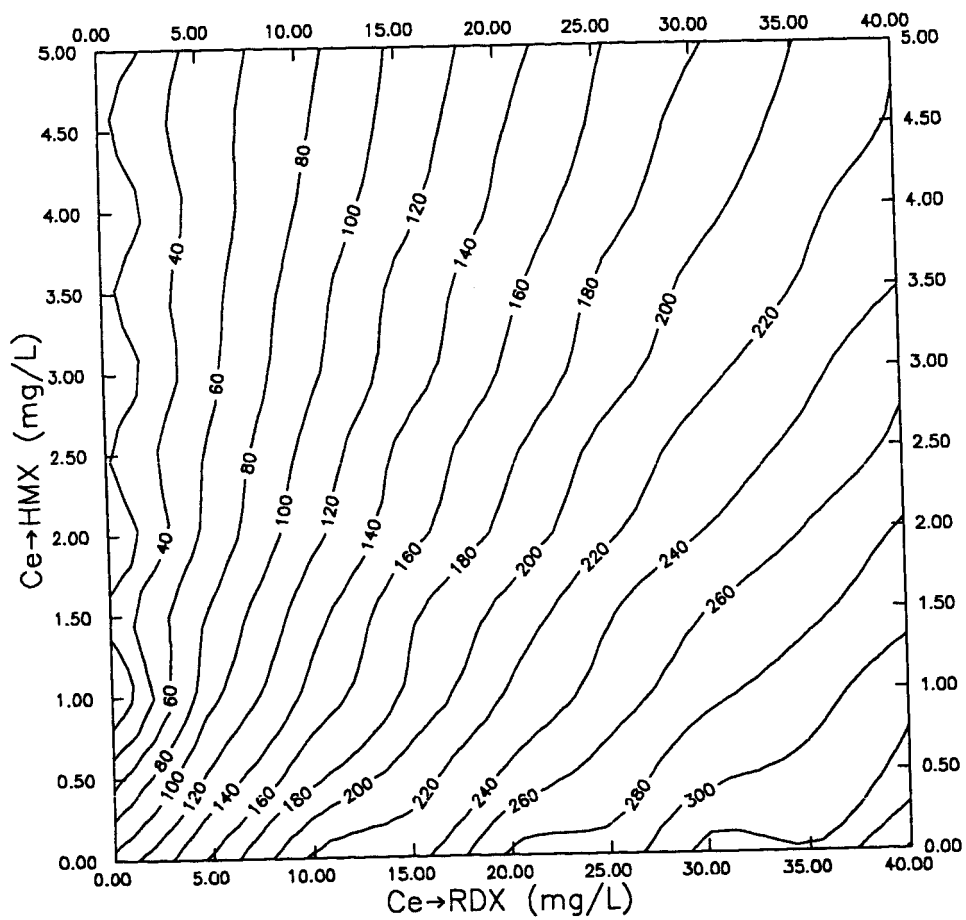
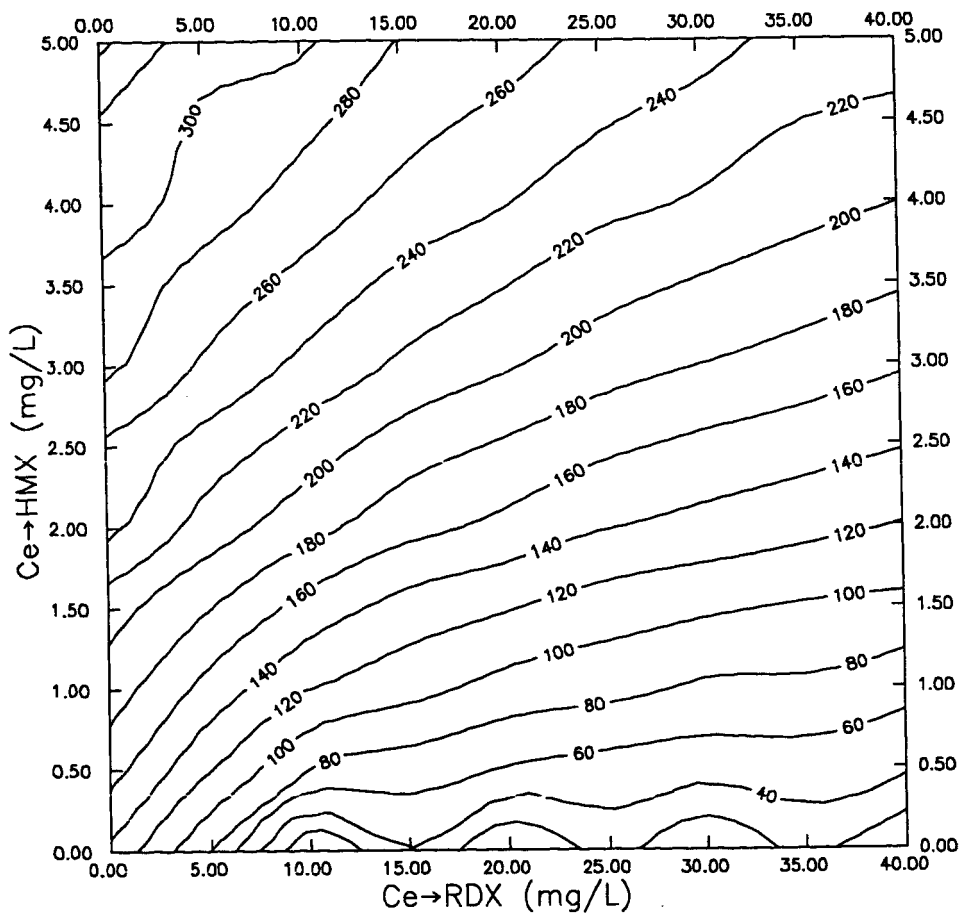


Figure 24 Freundlich Multicomponent Isotherm Contour for HMX



Figures 21 and 22 are the linear plots of the RDX and the HMX data. The straight line shown in Figure 21 has a y-intercept of -9.31, which is also the competition factor $-a_{12}$. The other competition coefficient a_{21} , which is the inverse of a_{12} by definition, is 0.107. Nevertheless, the HMX data give a line with y-intercept being 0.155 (Figure 22).

Although the linearized Freundlich Multicomponent Isotherm defines the slope of the line to be unity, Figures 21 and 22 do not have lines with slopes equal one. The rest of the parameters K_i and n_i are derived from the single-solute data and are mentioned earlier in this chapter. A slight modification of the single-solute parameter n is necessary because Sheindorf et al. defined q_e as KC^n instead of $KC^{1/n}$. After taking the reciprocal of the original n values, n_{RDX} and n_{HMX} are 0.344 and 0.369 respectively.

The Freundlich Multicomponent Isotherm is by far the best, among the three isotherms discussed, at modeling both the RDX and the HMX data if one neglects part of the isotherm parameter's definition. The RMS error for the RDX data is 40.13 mg/g, and it is 25.11 mg/g for the HMX data, but these RMS errors are based on the competition coefficient ($a_{12}=9.31$) which gives a line with slope equals to 1.27 instead of 1. Since the Freundlich isotherm is empirical, one can probably add a constant (slope equals 1.27) to improve the bisolute isotherm.

Figures 21 and 22 may give one the impression that the Freundlich Multicomponent Isotherm fits the RDX data better than the HMX data; however, the illustrations are quite misleading. One should note the difference in scales between the two linear plots. In fact, this isotherm is better at fitting the HMX data than the RDX

data. Figures 23 and 24 are the two-dimensional contours generated by this isotherm. Notice the narrower gaps between the contours on these two graphs suggest the isotherm is improving. While the Freundlich Multicomponent overestimates the HMX sorbed concentration, it underestimates the RDX sorbed concentration.

4.2.4 Simplified Ideal Adsorbed Solution (SIAS) Isotherm

The IAS Model is well-known for its accuracy in accounting for multicomponent adsorption data, but its mathematical complexity discourages researchers from fitting isotherm data to the IAS Model. A good alternative is the SIAS Isotherm which incorporates the Freundlich isotherm into the IAS theory. The SIAS Isotherm for n components is governed by n equations. For component i,

$$q_i = K' \left(\frac{n'-1}{n'} \right) \left[K_i C_i^{n'} \right]^{\frac{1}{n'}} \left[\sum_N \left(\frac{K_i}{K'} C_i^{n'} \right)^{\frac{1}{n'}} \right]^{(n'-1)} \quad (2.22)$$

All the parameters are defined in Chapter 2, and for the specific RDX-HMX bisolute adsorption system, K' is $145.997 \text{ (mg/g)(L/mg)}^n$ and n' is 0.357. The single-solute parameters and the Freundlich isotherm are defined in the same way as the previous isotherm.

The SIAS Isotherm is by far the best in modeling the RDX and the HMX sorption data among the four isotherms. The RMS error for the RDX data is 36.07 mg/g, and it is 21.85 mg/g for the HMX data. Like the Freundlich Multicomponent Isotherm, the SIAS

Figure 25 SIAS Isotherm Contour for RDX

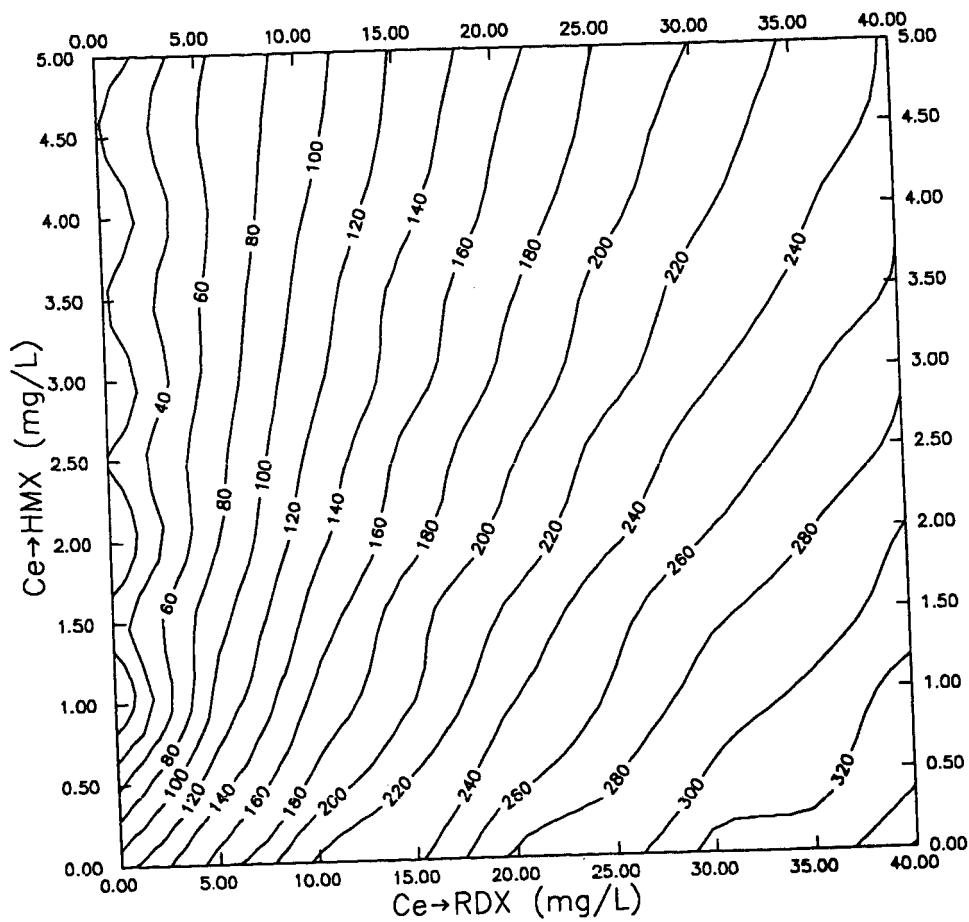
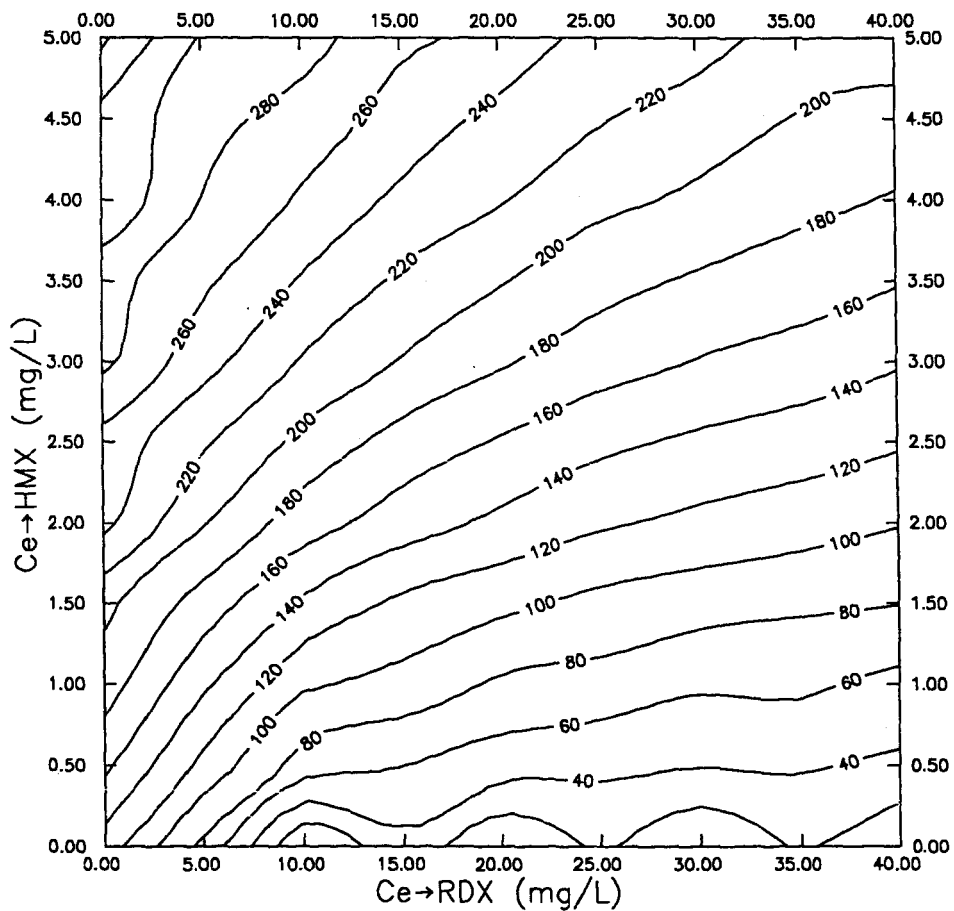


Figure 26 SIAS Isotherm Contour for HMX



Isotherm underestimates the RDX sorption and overestimates the HMX sorption. This observation is made from comparing the maximum contour lines shown in Figure 25 and 26 with the experimental data. Figure 25 and 26 are the contours generated by this isotherm, and they are very similar to Figure 23 and 24; however, Figure 25 and 26 should be closer in illustrating the modeling results.

Although the SIAS Isotherm is very good at describing the RDX-HMX sorption quantitatively, its assumption of ideal competition does not make the isotherm very realistic. Fortunately there is the ISIAS Isotherm which takes nonideal competition into consideration.

4.2.5 Improved Simplified Ideal Adsorbed Solution (ISIAS) Isotherm

The ISIAS isotherm is very similar to the previous one, except this isotherm includes a competition factor η_i which allows the isotherm to account for nonideal competition. The other dissimilarity between the two is the way K' is defined:

$$q_i = K' \left(\frac{n'-1}{n'} \right) \left[\frac{K_i}{\eta_i} C_i^{n_i} \right]^{\frac{1}{n'}} \left[\sum_N \left(\frac{K_i / \eta_i}{K'} C_i^{n_i} \right)^{\frac{1}{n'}} \right]^{(n'-1)} \quad (2.23)$$

$$K' = \frac{\sum (K_i / \eta_i)}{N}$$

where

Figure 27 Sum of Least Squares vs. η^2

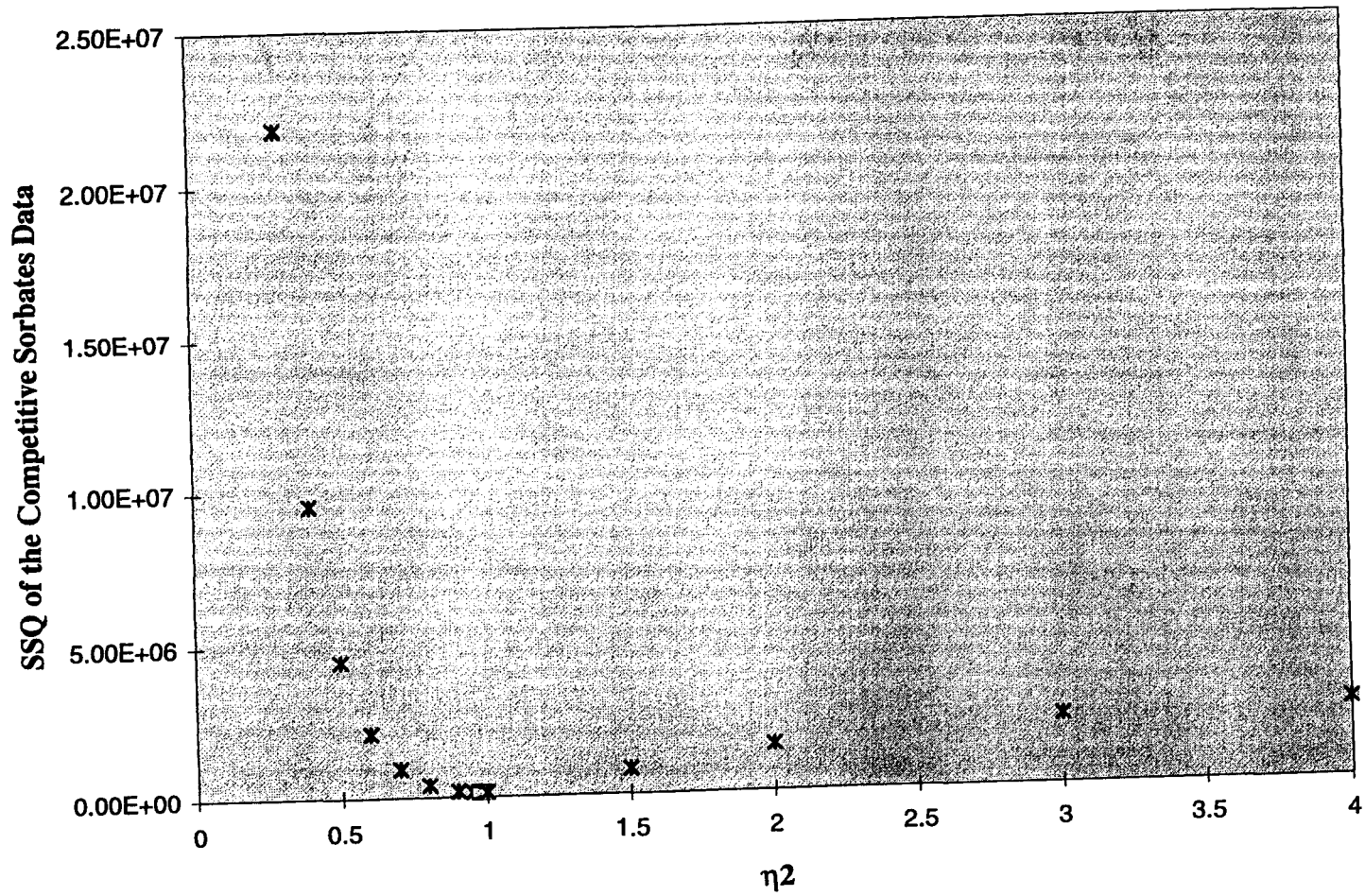


Figure 28 ISIAS Isotherm Contour for RDX

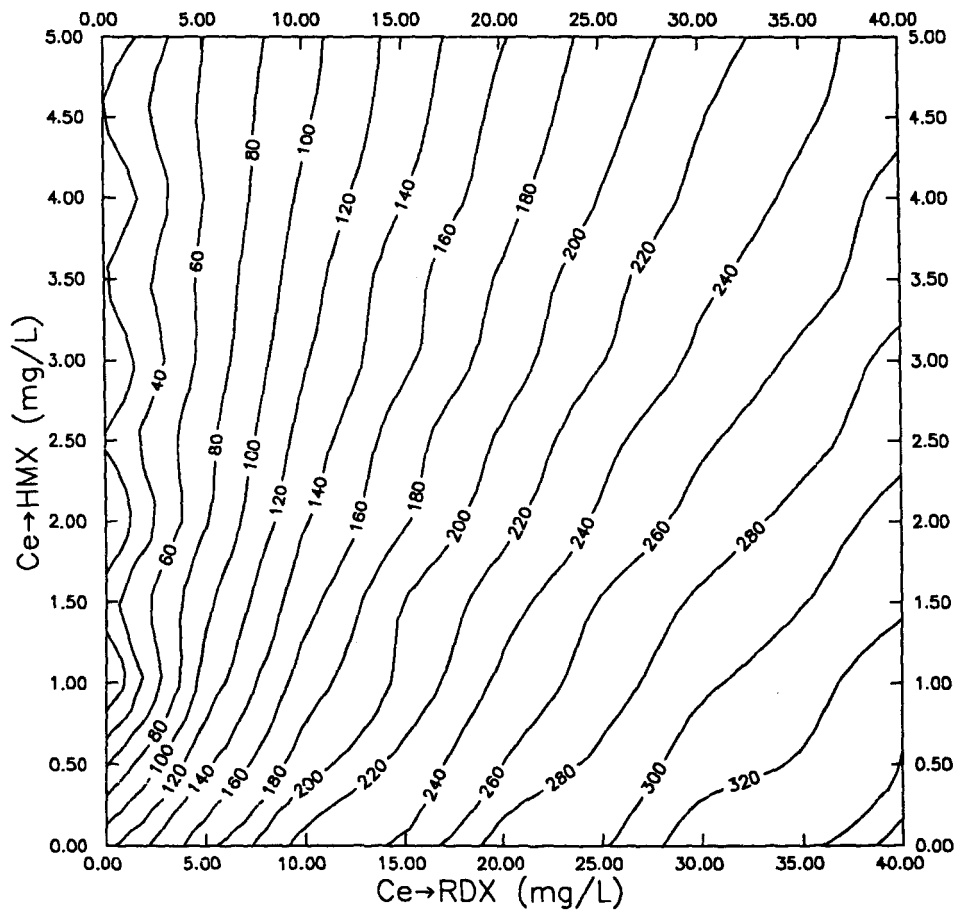
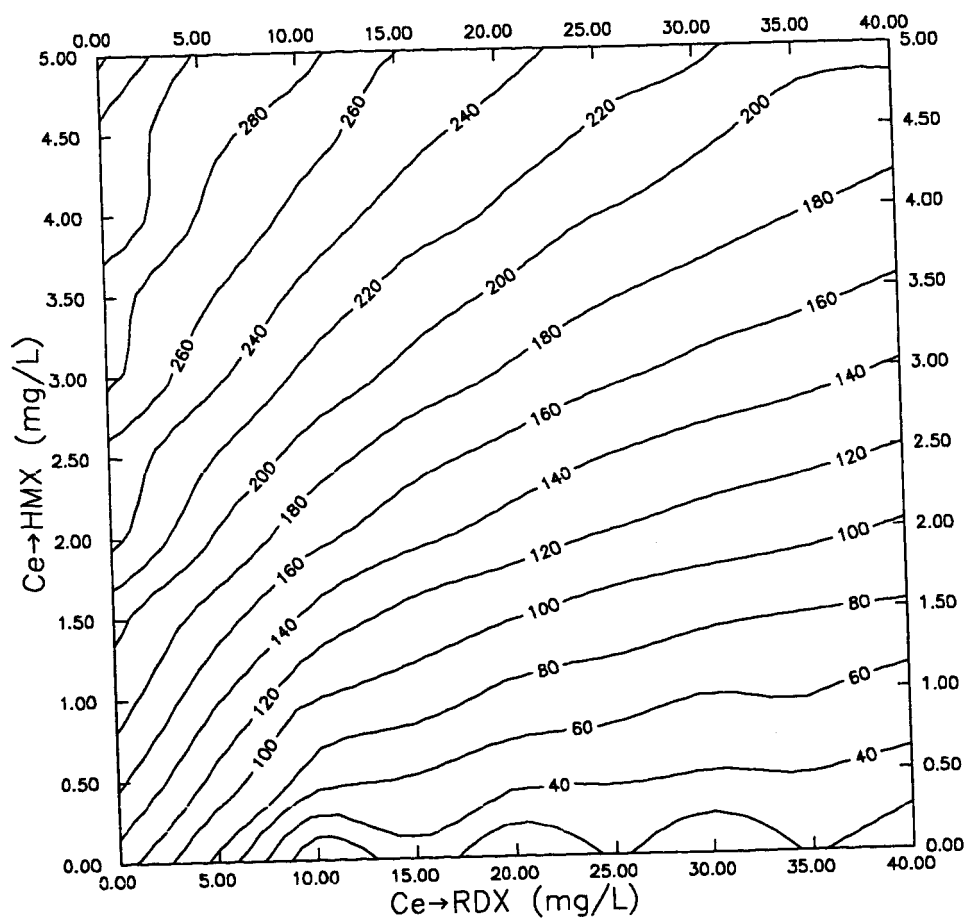


Figure 29 ISIAS Isotherm Contour for HMX



Other than the Freundlich Multicomponent Isotherm, this is the only one, among the five isotherms, which requires multisolute data to determine the isotherm's parameters. Yonge et al. (1986) suggested η_1 to be 1, and η_2 can be derived from the competitive adsorption data. From substituting several numeric guesses of η_2 into equation (2.23), the corresponding error is calculated for each η_2 guessing value. Figure 27 illustrates the dependency of sum of least squares (SSQ) subject to different η_2 's values. The author did not use the RDX's and the HMX's RMS errors in Figure 27 because both explosives' data must be considered together in order to select an appropriate η_2 . The best η_2 value is the one with the lowest SSQ and it is 0.975.

The ISIAS Isotherm represents the RDX sorption the best among the five isotherms, but its representation of the HMX sorption is slightly worse than the SIAS Isotherm. The RMS error for the RDX data is 35.34 mg/g, and it is 21.96 mg/g for the HMX data. The RMS errors between the last two isotherms are within at most 2.1% difference; therefore, both the SIAS Isotherm and the ISIAS Isotherm are very close in terms of modeling real adsorption data. Figure 28 and 29 are the two-dimensional contours generated by the ISIAS Isotherm, and they appear identical to Figure 25 and 26. It seems that the consideration of nonideal competition does not greatly enhance the

ISIAS Isotherm's modeling ability quantitatively, but the assumption has made the isotherm more realistic and acceptable than the SIAS Isotherm.

The 74 isotherm data points covered equilibrium concentration ranging from 0.00133 mg/L RDX to 36.6 mg/L RDX, 0.00086 mg/L HMX to 4.4 mg/L HMX. The RDX sorbed concentration varied from 2 mg/g to 409 mg/g, and it was 1.59 mg/g to 249 mg/g for the HMX sorbed concentration. Each isotherm's ability in describing the experimental data is determined by the RMS errors between the modeled values and the experimental data. The Langmuir Multicomponent Isotherm had the largest error, followed by the Langmuir Partially Competitive Isotherm, the Freundlich Multicomponent Isotherm, and the SIAS Isotherm; the ISIAS Isotherm was the most accurate. There was a large improvement from using the Langmuir Multicomponent Isotherm in modeling the HMX data to using the Langmuir Partially Competitive Isotherm. This suggested that HMX was at least partially competing with RDX for adsorption sites. The last three isotherms were quite comparable in modeling the RDX and the HMX data, but the Freundlich Multicomponent Isotherm had the largest error among the three. While the ISIAS Isotherm was better at modeling the RDX data than the SIAS Isotherm, the SIAS Isotherm was slightly better at modeling the HMX data. Since the ISIAS Isotherm incorporates the nonideal competition behavior, the ISIAS Isotherm is the best in representing the RDX-HMX adsorption system both quantitatively and qualitatively. A list of the RMS errors for various isotherms are shown in Table 5.

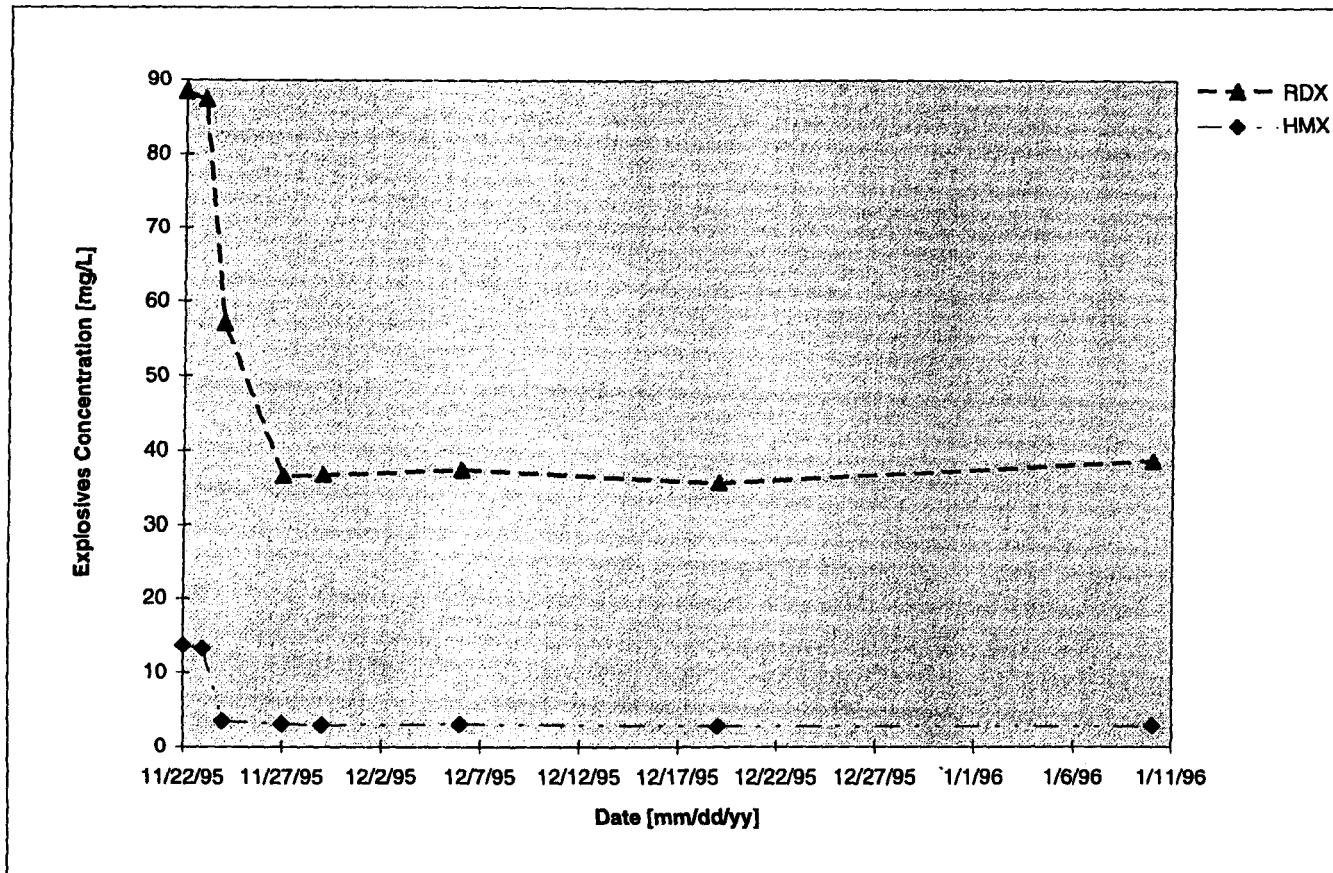
Table 5 Root Mean Squares Error for Various Multicomponent Isotherms

Isotherms	RMS Error for RDX Data (mg/g)	RMS Error for HMX Data (mg/g)
Langmuir Multicomponent Isotherm	54.37	61.70
Langmuir Partially Competitive Isotherm	54.37	29.56
Freundlich Multicomponent Isotherm	40.13	25.11
SIAS Model	36.07	21.85
ISIAS Model	35.34	21.96

4.3 RDX and HMX Aqueous Solubility Limits

Upon shaking the RDX and HMX solution for about a month and a half inside an incubator set at 20°C, the RDX and HMX concentration stabilized at 35 mg/L and 2.8 mg/L respectively. Some researchers reported the RDX aqueous solubility to be 7.6 mg/L to 42.3 mg/L at 20°C. Although no one has stated the HMX aqueous solubility at 20°C, studies indicated that it was 4 to 5 mg/L for HMX at 25°C. Most researchers failed to describe their testing procedures, therefore, it was difficult to determine the reliability of those tests. The author's results should be reliable because the solutions were kept at constant temperature, and the experiment was run for a long time. Figure 30 illustrates the change of the RDX and HMX concentration over the duration of a month and a half.

Figure 30 RDX & HMX Aqueous Solubility Tests



5. CONCLUSION

The RDX-HMX adsorption experimental results consist of 74 data points. These data's equilibrium concentrations range from 0.00133 mg/L to 36.6 mg/L RDX, and 0.00086 mg/L to 4.4 mg/L HMX. Five different isotherms were used for fitting the experimental data, and the more specific conclusions are as follows:

- The Improved Simplified Ideal Adsorbed Solution (ISIAS) Isotherm was the best in modeling the RDX-HMX adsorption data.
- The ISIAS isotherm accounts for nonideal competition by including the competition factor η_i ; for the RDX-HMX adsorption system, $\eta_1=1$, and $\eta_2=0.975$.
- Overall the ISIAS Isotherm was the most reliable in representing the RDX-HMX adsorption behavior; the Simplified Ideal Adsorbed Solution (SIAS) Isotherm was the second, the Freundlich Multicomponent Isotherm was the third, the Langmuir Partially Competitive Isotherm was the fourth, and the Langmuir Multicomponent Isotherm was the worst.
- The Langmuir Partially Competitive Isotherm, the Freundlich Multicomponent Isotherm, the SIAS Isotherm, and the ISIAS Isotherm were all able to describe the HMX adsorption better than the RDX adsorption.
- There was about 50 percent improvement when using the Langmuir Partially Competitive Isotherm compared to using the Langmuir Multicomponent Isotherm. This suggests that RDX and HMX at least partially compete for adsorption sites.

- Since RDX-HMX bisolute adsorption is a competitive process, the two explosives inhibit each other's adsorption.
- HMX is more efficiently adsorbed than RDX for two reasons: first, HMX has higher molecular weight and lower aqueous solubility than RDX (Lindelius' Rule); second, the extra nitro group or electron-withdrawal group on HMX allows it to form a stronger sorbate-carbon complex than RDX.
- Ion-exchange, physical, and chemical adsorption all contributed to the RDX-HMX adsorption system.
- The Freundlich isotherm gave a better fit for the RDX and HMX single-solute data than the Langmuir and the BET isotherms over the equilibrium concentration range of 0.293 mg/L to 31.9 mg/L RDX, and 0.152 mg/L to 2.95 mg/L HMX.
- The Freundlich parameters K and n for the pure RDX adsorption data were $101.9 \text{ (mg/g)(L/mg)}^{1/n}$ and 2.91 respectively.
- The author used Heilmann's (1995) pure HMX data for isotherm modeling. Heilmann's Freundlich parameters for the pure HMX adsorption data were $190.1 \text{ (mg/g)(L/mg)}^{1/n}$ for K and 2.71 for n .
- At 20°C RDX aqueous solubility limit was 35 mg/L, and HMX solubility limit was 2.8 mg/L.
- For solid phase extraction (SPE), styrene divinylbenzene (SDVB) sorbent gave the most satisfactory recovery for RDX and HMX among C8, C18, Porapak R, Hayesep R, salting out, and pesticide cartridges.

- The SPE procedures using the SDVB cartridges was able to improve the detection limit of the HPLC from 0.1 mg/L to about 0.0001 mg/L

APPENDIX A

- A-1 HPLC STANDARD CALIBRATION FOR RDX IN WATER
- A-2 HPLC STANDARD CALIBRATION FOR HMX IN WATER
- A-3 HPLC STANDARD CALIBRATION FOR RDX IN
ACETONITRILE
- A-4 HPLC STANDARD CALIBRATION FOR HMX IN
ACETONITRILE

HPLC Standard Calibration for RDX in D.I. Water

9/28/95 (for new column received 9/19/95)

For Setting: 50% methanol, 50% water

1.5ml per min.

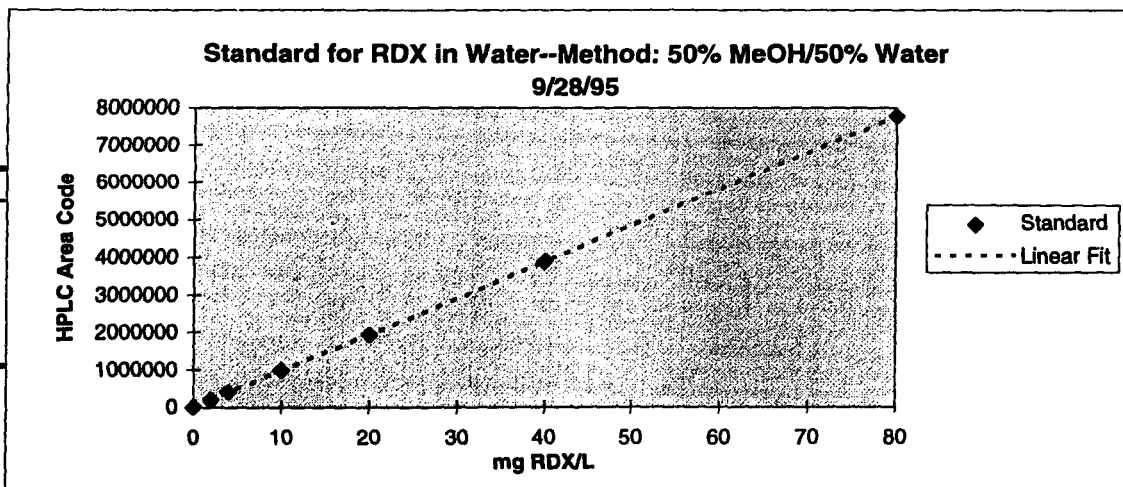
20 µL injections

Standard Solution: 40mg RDX/L

Injection volume	mg RDX/L	Area Codes				Linear
		x1	x2	x3	average x	
0µL	0	0	0	0	0	7822.036
1µL	2	196876	196407	195776	196353	201535.3
2µL	4	390105	440635	392413	407717.7	395248.5
5µL	10	977890	979298	976874	978020.7	976388.2
10µL	20	1938564	1946457	1941175	1942065	1944954
20µL	40	3884334	3891110	3881421	3885622	3882087
40µL	80	7757693	7754586	7751546	7754608	7756351

SUMMARY OUTPUT

<i>Regression Statistics</i>	
Multiple R	0.999997
R Square	0.999994
Adjusted R	0.999993
Standard E	7349.365
Observatio	7



	Coefficient	standard Err	t Stat	P-value	Lower 95%	Upper 95%	Lower 95.00%	Upper 95.00%
Intercept	7822.036	3610.419	2.166517	0.082505	-1458.83	17102.9	-1458.83	17102.9
X Variable	96856.62	103.4873	935.928	2.64E-14	96590.6	97122.64	96590.6	97122.64
Total	6	4.73E+13						

HPLC Standard Calibration for HMX in D.I. Water

9/28/95 (for new column received 9/19/95)

For Setting: 50% methanol, 50% water

1.5ml per min.

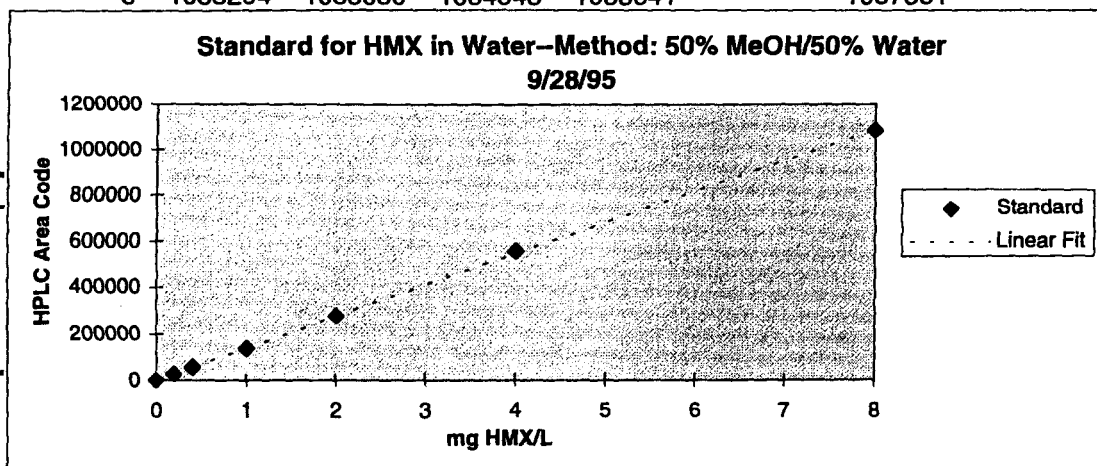
20 µL injections

Standard Solution: 4mg HMX/L

Injection volume	mg HMX/L	Area Codes				average x	Linear
		x1	x2	x3			
0µL	0	0	0	0	0	1543.877	
1µL	0.2	26888	26958	27300	27048.67	28694.81	
2µL	0.4	54272	54267	54920	54486.33	55845.74	
5µL	1	141410	134483	135526	137139.7	137298.5	
10µL	2	275281	269149	277789	274073	273053.2	
20µL	4	552285	553429	550860	552191.3	544562.5	
40µL	8	1083294	1083080	1084548	1083641	1087581	

SUMMARY OUTPUT

Regression Statistics	
Multiple R	0.999956
R Square	0.999912
Adjusted R	0.999894
Standard E	4043.09
Observatio	7



	Coefficient	standard Err.	t Stat	P-value	Lower 95%	Upper 95%	Lower 95.00%	Upper 95.00%
Intercept	1543.877	1986.192	0.777305	0.472135	-3561.78	6649.537	-3561.78	6649.537
X Variable	135754.6	569.3121	238.4538	2.46E-11	134291.2	137218.1	134291.2	137218.1
Total	6	9.3E+11						

HPLC Standard Calibration for RDX in ACN

9/28/95 (for new column received 9/19/95)

For Setting: 50% methanol, 50% water

1.5ml per min.

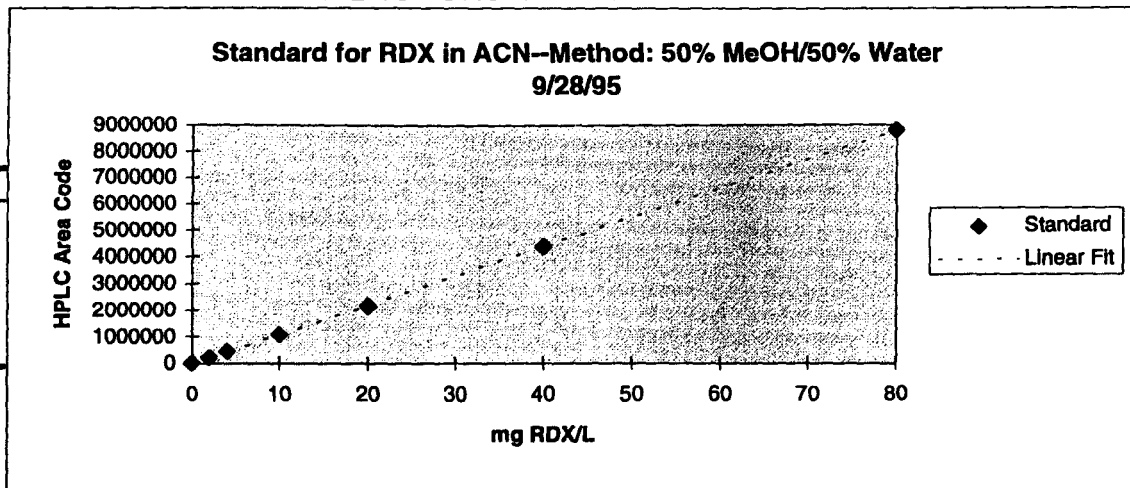
20 µL injections

Standard Solution: 40mg RDX/L

Injection volume	mg RDX/L	Area Codes				average x	Linear
		x1	x2	x3			
0µL	0	0	0	0	0	-6419.43	
1µL	2	217642	222097	220838	220192.3	213536.1	
2µL	4	482909	443537	438929	455125	433491.7	
5µL	10	1088712	1087082	1088588	1088127	1093358	
10µL	20	2168333	2168829	2165658	2167607	2193136	
20µL	40	4375619	4369859	4374179	4373219	4392692	
40µL	80	8818963	8792275	8810746	8807328	8791803	

SUMMARY OUTPUT

Regression Statistics	
Multiple R	0.999985
R Square	0.99997
Adjusted R	0.999964
Standard E	19250.19
Observatio	7



	Coefficient	standard Err	t Stat	P-value	Lower 95%	Upper 95%	Lower 95.00%	Upper 95.00%
Intercept	-6419.43	9456.77	-0.67882	0.527395	-30728.8	17889.93	-30728.8	17889.93
X Variable	109977.8	271.0641	405.7261	1.73E-12	109281	110674.6	109281	110674.6

HPLC Standard Calibration for HMX in ACN 9/28/95 (for new column received 9/19/95)

For Setting: 50% methanol, 50% water

1.5ml per min.

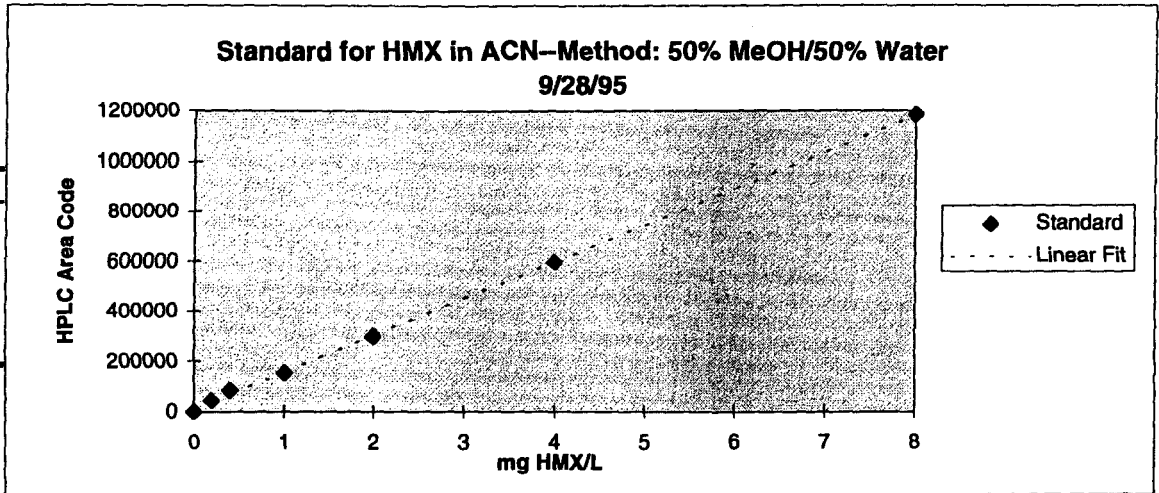
20 µL injections

Standard Solution: 4mg HMX/L

Injection volume	mg HMX/L	Area Codes				average x	Linear
		x1	x2	x3			
0µL	0	0	0	0	0	0	10201.44
1µL	0.2	42935	43963	42747	43215		39535.88
2µL	0.4	85952	84864	80460	83758.67		68870.32
5µL	1	154628	154419	153248	154098.3		156873.7
10µL	2	297472	297794	296832	297366		303545.9
20µL	4	591178	598338	598357	595957.7		596890.3
40µL	8	1195430	1190635	1181146	1185101		1183579

SUMMARY OUTPUT

<i>Regression Statistics</i>	
Multiple R	0.999821
R Square	0.999642
Adjusted R	0.999571
Standard E	8813.024
Observatio	7



	Coefficient	standard Err	t Stat	P-value	Lower 95%	Upper 95%	Lower 95.00%	Upper 95.00%
Intercept	10201.44	4329.451	2.356289	0.06505	-927.754	21330.62	-927.754	21330.62
X Variable	146672.2	1240.972	118.1914	8.22E-10	143482.2	149862.2	143482.2	149862.2
Total	6	1.09E+12						

SOLID PHASE EXTRACTION RECOVERY STUDIES

APPENDIX B

APPENDIX B SOLID PHASE EXTRACTION

I. SPE Recovery Factors for RDX—SDVB Sorbent

Sample Vol. [mL]	Percent Recovery					Recovery Factor
	x1	x2	x3	x4	average	
10		100.18	92.60	107.64	100.14	0.999
20	103.31		92.53	108.95	101.60	0.984
40	102.37		94.41	110.25	102.34	0.977
60	112.29	110.84	91.57	107.50	105.55	0.947
80	107.54		94.21	113.06	104.94	0.953
100	104.19	103.83	100.69	108.80	104.38	0.958
200	122.33		86.80	112.47	107.20	0.933
500	102.27		81.25	94.69	92.74	1.078

II. SPE Recovery Factors for HMX—SDVB Sorbent

Sample Vol. [mL]	Percent Recovery					Recovery Factor
	x1	x2	x3	x4	average	
10		69.33	60.60	107.12	79.02	1.266
20	79.23		61.39	113.24	84.62	1.182
40	80.23		63.14	113.69	85.69	1.167
60	76.60	74.21	65.02	108.78	81.15	1.232
80	81.38		60.70	94.49	78.85	1.268
100	72.89	69.90	74.21	99.99	79.25	1.262
200	109.77		50.84	106.09	88.90	1.125
500	64.82		51.56	86.97	67.78	1.475

APPENDIX C

C-1 PASCAL PROGRAM FOR PREDICTION

C-2 SAMPLE INPUT FILE

C-3 SAMPLE OUTPUT FILE

APPENDIX C-1 PASCAL PROGRAM FOR PREDICTION

program FindqCe (InData, OutData, Output);

{Based on Langmuir Multicomponent Adsorption Model, this program computes the sorbed concentration & the equilibrium concentration of the RDX-HMX-Carbon Adsorption System. Given various initial conditions which include carbon mass, solution volume, initial RDX & HMX concentration, the program will read each set of initial conditions and the four guesses on the equilibrium RDX & HMX concentration, refine guesses using the Complex Method of Box, and finally determine the true sorbed concentration of RDX & HMX that match the equilibrium concentration of RDX & HMX. In this program RDX is denoted as A; HMX is denoted as B}

const

QA=212.2037; *{Max. Sorbing Capacity of carbon for RDX or A [mg/g]}*
QB=305.8991; *{Max. Sorbing Capacity of carbon for HMX or B [mg/g]}*
bA=1.312403; *{Langmuir Parameters for RDX & HMX respectively[L/g]}*
bB=2.576349;

epsilon=0.000001; *{epsilon is the threshold value for minimizing error}*

type

ConcArray=array [1..2, 1..4] of Real; *{for storing the 4 guesses on the equilibrium liquid concentration of RDX and HMX}*
SorbArray=array [1..2, 1..4] of Real *{for storing the four possible sorbed concentration of RDX and HMX subject to initial experimental conditions and input guesses on the equilibrium concentration}*
ErrorArray=array [1..4] of Real; *{for storing the error between calculated and experimental sorbed concentration}*

var

TheoSorb, ExptSorb: SorbArray;
GuessConc: ConcArray;
Error: ErrorArray;
i, j, Counter, IndexWorst, MinIndex: Integer; *{indexes for loops and array}*
CentroidqA, CentroidqB, Alpha: Real;
InData, OutData: Text;
Mass, Volume, CoA, CoB: Real;

procedure PrintResult (Mass, Volume, CoA, CoB {input}: Real; GuessConc{input}: ConcArray; ExptSorb, TheoSorb{input}: SorbArray; MinIndex: Integer);

{This procedure prints the initial experimental conditions and the calculated results to the an output file called OutData}

```
begin {PrintResult}
  writeln ('Printing Result...');
  writeln (OutData, 'Mass [g]: ', Mass:8:6);
  writeln (OutData, 'Volume [L]: ', Volume:2);
  writeln (OutData, 'CoA [mg/L]: ', CoA:10:7);
  writeln (OutData, 'CoB[mg/L]: ', CoB:10:7);
  writeln (OutData, 'CeA[mg/L]   CeB[mg/L]   qA[mg/g]   qB[mg/g]');
  writeln (OutData, '-----');
  writeln (OutData, GuessConc[1,MinIndex]:10:7, ' ', GuessConc[2,MinIndex]:10:7,
    ' ', ExptSorb[1,MinIndex]:10:6, ' ', ExptSorb[2,MinIndex]:10:6);
  writeln (OutData, 'Theoretical Sorbed Conc. A: ', TheoSorb[1,MinIndex]:10:6);
  writeln (OutData, 'Theoretical Sorbed Conc. B: ', TheoSorb[2,MinIndex]:10:6);
  writeln (OutData);
end; {PrintResult}
```

```
procedure NewPoint (Mass, Volume, CoA, CoB, CentroidqA, CentroidqB {input}:
  Real; IndexWorst {input}: Integer; var Error {input/output}:
  ErrorArray; var TheoSorb, ExptSorb {input/output}: SorbArray;
  var GuessConc {input/output}: ConcArray);
```

{This procedure demonstrates the Complex Method of Box. After centroid of the 3 good points is found, a new point (NewExptqA, NewExptqB) will be found using the special formula that involves alpha(α). Alpha will be halved each time a new point is generated, and a new point will be found using the new alpha.. When the program returns a satisfactory newpoint, it will go through the process of searching for the new worst point, finding centroid of the 3 good points, and finding another new point until the new point has a very small error or until the process has repeated for another 100 times. The counter (InnerCounter) is used for a termination condition and for avoiding infinite loops.}

```
var
  NewExptqA, NewExptqB, NewCeA, NewCeB: Real;
  NewTheoqA, NewTheoqB, TempError: Real;
  InnerCounter: Integer;
begin
  Alpha := 1.3;
  InnerCounter:=0;

  Repeat
    NewExptqA:=Alpha*(CentroidqA-ExptSorb[1,IndexWorst])+CentroidqA;
    NewExptqB:=Alpha*(CentroidqB-ExptSorb[2,IndexWorst])+CentroidqB;
```

```

NewCeA:=CoA-(NewExptqA*Mass)/Volume;
NewCeB:=CoB-(NewExptqB*Mass)/Volume;
NewTheoqA:=QA*bA*NewCeA/(1+bA*NewCeA+bB*NewCeB);
NewTheoqB:=QB*bB*NewCeB/(1+bB*NewCeB+bA*NewCeA);
TempError:=SQR(NewTheoqA-NewExptqA)+SQR(NewTheoqB-NewExptqB);
Alpha := Alpha/2;
InnerCounter:=InnerCounter+1;
Until (InnerCounter > 100) or ((TempError < Error[IndexWorst])
and (NewExptqA > 0) and (NewExptqB >0) and
(NewCeA > 0) and (NewCeB > 0));

```

```

ExptSorb[1,IndexWorst]:=NewExptqA;
ExptSorb[2,IndexWorst]:=NewExptqB;
TheoSorb[1,IndexWorst]:=NewTheoqA;
TheoSorb[2,IndexWorst]:=NewTheoqB;
GuessConc[1,IndexWorst]:=NewCeA;
GuessConc[2,IndexWorst]:=NewCeB;
Error[IndexWorst] := TempError;

```

end; *{NewPoint}*

procedure Centroid (ExptSorb *{input}*: SorbArray; Error *{input}*: ErrorArray);
{Procedure Centroid first finds the point (among the 4 existing points) with the biggest error or the worst point; then it calculates the centroid of the 3 good points. CentroidqA and CentroidqB can be perceived as the x and y coordinate in a 2D domain}

var

Worst: Real;

begin

Worst:=Error[1]; *{assumption}*

IndexWorst:=1;

for j:=2 to 4 do

if Worst < Error [j]

then begin

Worst:=Error[j];

IndexWorst:=j

end; *{if}*

CentroidqA:=(ExptSorb[1,1]+ExptSorb[1,2]+ExptSorb[1,3]+ExptSorb[1,4]-
ExptSorb[1,IndexWorst])/3;

CentroidqB:=(ExptSorb[2,1]+ExptSorb[2,2]+ExptSorb[2,3]+ExptSorb[2,4]-
ExptSorb[2,IndexWorst])/3;

end; {Centroid}

procedure ErrorAssign (TheoSorb, ExptSorb {input}: SorbArray; var Error{output}: ErrorArray);

{This procedure calculates the error between the calculated theoretical sorbed concentration and experimental sorbed concentration (based on mass balance) by using sum of squares. Each error calculated represents each set parameters, and the error represent one point in the 2D domain. All together there are 4 points in space}

begin

for i:=1 to 4 do

Error[i]:=SQR(TheoSorb[1,i]-ExptSorb[1,i])+SQR(TheoSorb[2,i]-ExptSorb[2,i]);

end; {ErrorAssign}

procedure CalcSorption (GuessConc {input}: ConcArray; var TheoSorb, ExptSorb {output}: SorbArray; Mass, Volume, CoA, CoB {input}: Real);

{For each of the guesses for RDX and HMX equilibrium concentration entered as input, one theoretical sorbed concentration for RDX and HMX will be calculated by using Langmuir Bisolute Isotherm equations; for each set of experimental conditions and each set of guesses (M, V, Co_A, Co_B, Ce_A, Ce_B) input to the program, one set of experimental sorbed concentration will be calculated using the mass balance equation. The goal is to have experimental value matching the calculated values}

begin

for i:=1 to 2 do

for j:=1 to 4 do

begin {inner for loop}

if i=1 then

begin

TheoSorb[i,j]:=QA*bA*GuessConc[i,j]/(1+bA*
GuessConc[i,j]+bB*GuessConc[i+1,j]);

ExptSorb[i,j]:=(CoA-GuessConc[i,j])*Volume/Mass

end

else begin

TheoSorb[i,j]:=QB*bB*GuessConc[i,j]/(1+bB*
GuessConc[i,j]+bA*GuessConc[i-1,j]);

ExptSorb[i,j]:=(CoB-GuessConc[i,j])*Volume/Mass

end; {else}

end; {inner for loop}

end; {CalcSorption}

procedure ScanData (var GuessConc{output}: ConcArray);

{Procedure ScanData reads from input file InData the hypothetical initial experimental conditions and the four equilibrium concentration guesses for RDX and HMX; the guesses will then be stored in a 2x4 array}

```
begin
  read (InData, Mass, Volume, CoA, CoB);
  writeln (Mass, Volume, CoA, CoB);
  for i:=1 to 2 do
    for j:=1 to 4 do
      read (InData, GuessConc[i,j]);
    readln (InData);
  end; {ScanData}
```

procedure FindMinIndex (Error: ErrorArray; var MinIndex:Integer);
{This procedure searches for the point that has the minimum error so that it can find the corresponding equilibrium and sorbed concentration for RDX and HMX}

```
var
  MiniError: Real;
```

```
begin
  MiniError:=Error[1];
  MinIndex:=1;
  for i:=2 to 4 do
    if Error[i] < MiniError
    then begin
      MiniError:=Error[i];
      MinIndex:=i
    end; {if}
  end; {FindMinIndex}
```

function Min (Error: ErrorArray):Real;
{This function is for checking if the current minimum error, among the four errors, is less than epsilon.}

```
var
  TempMin: Real;
```

```
begin
  TempMin:= Error[1];           {assumption}
  for j:=2 to 4 do
    if Error [j] < TempMin
    then TempMin:=Error[j];
```

```
Min:=TempMin;  
end; {Min}
```

```
begin {main}  
  Assign (InData, 'b:\InData.txt');  
  Reset (InData);  
  Assign (OutData, 'b:\OutData.txt');  
  Rewrite (OutData);  
  while not EOF do begin  
    Counter:=0;  
    ScanData (GuessConc);  
    CalcSorption (GuessConc, TheoSorb, ExptSorb, Mass, Volume, CoA, CoB);  
    ErrorAssign (TheoSorb, ExptSorb, Error);  
    repeat  
      Centroid (ExptSorb, Error);  
      NewPoint (Mass, Volume, CoA, CoB, CentroidqA, CentroidqB,  
        IndexWorst, Error, TheoSorb, ExptSorb, GuessConc);  
      Counter:=Counter+1;  
    until (Min(Error) < Epsilon) or (Counter > 100);  
  end;
```

{The repeat-until loop above will keep searching for new points and reject the worst point until one of the following is true: i) the minimum error (Min(Error) is a function call) is less than 10^{-6} , this means that the points converge, or ii) the loop has been processed for over 100 times. The second condition is to avoid the loop being processed indefinitely}

```
    FindMinIndex (Error, MinIndex);  
    PrintResult (Mass, Volume, CoA, CoB, GuessConc, ExptSorb, TheoSorb,  
      MinIndex);  
  end; {while}  
  Close (InData);  
  Close (OutData);  
end. {main}
```

*{Further Improvement: 1. Counter can be increased to over 100 times
2. Input data file needs to be modified so that there won't be
a "division by zero" message at the end of the program.}*

APPENDIX C-2 SAMPLE INPUT FILE

0.5 1 1 1 0.5 0.4 0.3 0.2 0.8 0.7 0.6 0.1
0.23 1 1 1 0.5 0.4 0.3 0.2 0.8 0.7 0.6 0.1
0.1 1 1 1 0.5 0.4 0.3 0.2 0.8 0.7 0.6 0.1
0.05 1 1 1 0.5 0.4 0.3 0.2 0.8 0.7 0.6 0.1
0.023 1 1 1 0.5 0.4 0.3 0.2 0.8 0.7 0.6 0.1
0.5 1 40 5 30 10 15 5 4 3 2 1
0.23 1 40 5 30 10 15 5 4 3 2 1
0.1 1 40 5 30 10 15 5 4 3 2 1
0.05 1 40 5 30 10 15 5 4 3 2 1

Note: For each line in the input file, the numbers are defined as follow:

1st number: carbon dosage [g]

2nd number: volume of isotherm mixture [L]

3rd number: RDX initial concentration [mg/L]

4th number: HMX initial concentration [mg/L]

5th number: 1st guess on RDX equilibrium concentration [mg/L]

6th number: 2nd guess on RDX equilibrium concentration [mg/L]

7th number: 3rd guess on RDX equilibrium concentration [mg/L]

8th number: 4th guess on RDX equilibrium concentration [mg/L]

9th number: 1st guess on HMX equilibrium concentration [mg/L]

10th number: 2nd guess on HMX equilibrium concentration [mg/L]

11th number: 3rd guess on HMX equilibrium concentration [mg/L]

12th number: 4th guess on HMX equilibrium concentration [mg/L]

APPENDIX C-3 SAMPLE OUTPUT FILE

Mass [g]: 0.500000
Volume [L]: 1.0E+00
CoA [mg/L]: 1.0000000
CoB [mg/L]: 1.0000000
CeA [mg/L] CeB [mg/L] qA [mg/g] qB [mg/g]

0.0072484 0.0025723 1.985503 1.994855
Theoretical Sorbed Conc. A: 1.986597
Theoretical Sorbed Conc. B: 1.995065

Mass [g]: 0.230000
Volume [L]: 1.0E+00
CoA [mg/L]: 1.0000000
CoB [mg/L]: 1.0000000
CeA [mg/L] CeB [mg/L] qA [mg/g] qB [mg/g]

0.0159103 0.0056808 4.278651 4.323127
Theoretical Sorbed Conc. A: 4.279002
Theoretical Sorbed Conc. B: 4.323469

Mass [g]: 0.100000
Volume [L]: 1.0E+00
CoA [mg/L]: 1.0000000
CoB [mg/L]: 1.0000000
CeA [mg/L] CeB [mg/L] qA [mg/g] qB [mg/g]

0.0374659 0.0135696 9.625341 9.864304
Theoretical Sorbed Conc. A: 9.624419
Theoretical Sorbed Conc. B: 9.864317

Mass [g]: 0.050000
Volume [L]: 1.0E+00
CoA [mg/L]: 1.0000000
CoB [mg/L]: 1.0000000
CeA [mg/L] CeB [mg/L] qA [mg/g] qB [mg/g]

0.0779354 0.0290024 18.441292 19.419953
Theoretical Sorbed Conc. A: 18.440705
Theoretical Sorbed Conc. B: 19.419528

Mass [g]: 0.023000

Volume [L]: 1.0E+00
CoA [mg/L]: 1.0000000
CoB[mg/L]: 1.0000000
CeA[mg/L] CeB[mg/L] qA[mg/g] qB[mg/g]

0.1817431 0.0728047 35.576386 40.312838
Theoretical Sorbed Conc. A: 35.492048
Theoretical Sorbed Conc. B: 40.234194

Mass [g]: 0.500000
Volume [L]: 1.0E+00
CoA [mg/L]: 40.0000000
CoB[mg/L]: 5.0000000
CeA[mg/L] CeB[mg/L] qA[mg/g] qB[mg/g]

0.4770806 0.0212371 79.045839 9.957526
Theoretical Sorbed Conc. A: 79.047212
Theoretical Sorbed Conc. B: 9.957537

Mass [g]: 0.230000
Volume [L]: 1.0E+00
CoA [mg/L]: 40.0000000
CoB[mg/L]: 5.0000000
CeA[mg/L] CeB[mg/L] qA[mg/g] qB[mg/g]

3.2303411 0.1505476 159.868082 21.084576
Theoretical Sorbed Conc. A: 159.868492
Theoretical Sorbed Conc. B: 21.083909

Mass [g]: 0.100000
Volume [L]: 1.0E+00
CoA [mg/L]: 40.0000000
CoB[mg/L]: 5.0000000
CeA[mg/L] CeB[mg/L] qA[mg/g] qB[mg/g]

21.8487774 1.4915158 181.512226 35.084842
Theoretical Sorbed Conc. A: 181.543752
Theoretical Sorbed Conc. B: 35.070726

Mass [g]: 0.050000
Volume [L]: 1.0E+00
CoA [mg/L]: 40.0000000
CoB[mg/L]: 5.0000000

CeA[mg/L]	CeB[mg/L]	qA[mg/g]	qB[mg/g]
31.1517775	2.7719185	176.964451	44.561630
Theoretical Sorbed Conc. A: 176.963774			
Theoretical Sorbed Conc. B: 44.559953			

APPENDIX D

COMPETITIVE ISOTHERM EXPERIMENTAL DATA

APPENDIX D COMPETITIVE ISOTHERM EXPERIMENTAL DATA

<i>Sets</i>	<i>Expt. Codes</i>	<i>Ce_RDX</i>	<i>qe_RDX</i>	<i>Ce_HMX</i>	<i>qe_HMX</i>
AD40-05	AD40-05a	33.09710	269.61617	2.14027	135.30586
	AD40-05b	25.35134	268.94192	0.85369	85.39453
	AD40-05c	14.78459	241.65550	0.28832	49.40916
	AD40-05d	2.79710	158.98244	0.05965	22.86909
	AD40-05e	0.37110	77.20356	0.01441	10.50557
AD001-01	AD01-01a	0.23614	25.97019	0.06718	35.96679
	AD01-01b	0.03714	15.73809	0.00844	17.57618
	AD01-01c	0.00579	8.30575	0.00229	8.99042
	AD01-01d	0.00176	3.67044	0.00086	3.96023
AD05-05	AD05-05a	2.97775	80.30077	0.74784	119.96102
	AD05-05b	1.00822	75.12801	0.17978	65.78933
	AD05-05c	0.19196	45.59683	0.03183	34.37881
	AD05-05d	0.02349	20.86335	0.00680	15.28940
	AD05-05e	0.00824	9.65517	0.00348	7.05999
AD01-05	AD01-05a	0.36625	27.12124	1.06465	143.76801
	AD01-05b	0.15982	16.58141	0.62126	75.02357
	AD01-05c	0.01535	9.58384	0.02405	42.81228
	AD01-05d	0.00240	4.33152	0.00556	19.17824
	AD01-05e	0.00133	1.99517	0.00534	8.82476
AD40-0.5	AD40-0.5a*	34.94597	267.24319	0.33788	26.76461
	AD40-0.5b	22.24089	362.49892	0.12550	13.44302
	AD40-0.5c	11.50829	286.00901	0.03712	7.53811
	AD40-0.5d	2.42299	162.32395	0.00468	3.39268
	AD40-0.5e	0.31026	80.04476	0.00198	1.59015
AD20-02	AD20-02a	14.89193	219.71149	0.57524	65.39880
	AD20-02b	7.56187	247.26130	0.18474	38.07060
	AD20-02c	3.85501	157.04224	0.15165	18.95923
	AD20-02d	0.45635	83.95506	0.00618	8.99962
	AD20-02e	0.38764	39.15933	0.01174	4.17194
AD20-3.5	AD20-3.5a	15.40895	233.99933	1.13036	108.66409
	AD20-3.5b	9.98406	215.48151	0.54943	61.78203
	AD20-3.5c	3.33163	175.04498	0.08797	35.77672
	AD20-3.5d	0.50732	87.92622	0.01849	15.78092
	AD20-3.5e	0.06674	41.62018	0.00195	7.34498
Set II 1-4	AD40-05a	36.60963	409.27621	3.17981	200.83148
	AD29-4.3c	7.98360	224.00086	0.40896	41.49453
	AD39-2.8c	11.22300	279.03653	0.16015	29.03259
	AD37-2.5a	30.81197	308.67081	1.02611	68.75024
AD20-05	AD20-05a	15.89494	189.19805	1.66669	162.13099
	AD20-05b	10.45201	196.89321	0.69328	95.79819
	AD20-05c	4.14160	158.48838	0.29541	51.08788
AD30-05	AD30-05b	18.40474	240.44369	0.86780	89.32672
	AD30-05c	7.93738	221.63465	0.30091	49.51472
Set II 5-8	AD29-04a	25.40085	164.94063	1.65880	129.87443
	AD13-4.3a	12.54607	124.67215	1.65149	139.16410

	AD11-3.5a	8.28720	119.05202	1.09713	91.63419
	AD12-4.6b	5.19374	120.13023	0.53604	72.43918
AD10-05	AD10-05a	7.17238	128.96224	1.44550	154.99919
	AD10-05b	3.73981	126.09308	0.48742	89.35702
Set II 9-12	AD13-4.3a	11.64877	150.81220	2.27274	193.44106
	AD4.4-4.3a	4.27755	54.44770	3.12194	242.06861
	AD0.5-05a	0.21783	16.03633	0.69642	200.39432
	AD30-02a	25.18795	273.53540	1.04161	90.70492
AD30-3.5	AD30-3.5b	18.45081	261.24690	0.63906	67.74091
AD20-0.5	AD20-0.5b	6.63978	276.91146	0.04379	16.93443
	AD20-0.5a	12.60580	348.86683	0.24879	28.25163
Set II 13	AD25-4.7a	20.62984	247.93127	1.50630	119.57580
Set II 14	AD3.2-4.3a	2.30189	80.02987	1.49591	235.05561
Set II 16	AD8.3-4a	6.79485	127.98957	1.74375	161.71860
Set IV 21	AD13.5-4.95*	13.30112	133.99858	3.72390	197.06490
Set IV 23	AD22-4.2a	17.44110	238.92768	1.30377	109.10325
Set IV 24	AD37-1.9a	31.66005	294.36839	0.79412	50.29791
Set IV 25*	AD26-4.7a*	20.78148	141.71524	2.16573	121.00785
Set IV 26*	AD10.2-5.04*	9.86319	98.80212	4.24576	248.91794
	AD4.3-4.99	2.68840	31.31703	3.62915	203.85481
Set IV 28*	AD9.4-4.6*	7.87801	98.89948	3.52103	232.53327
Set IV 29-30	AD20-4.6	18.44395	161.34460	3.40457	167.76264
	AD22-4.9	20.79759	138.48904	4.40198	185.16470
Set IV 34	AD34.2-4.56	34.06478	227.10289	3.61951	166.67162
Set IV 35	AD31.2-4.1	29.20907	203.43786	2.53704	143.64176
Set IV 37-40	AD22.96-4.03	20.67391	177.25166	2.3944	149.6778
	AD18.6-4.72	16.32786	153.40371	2.6893	182.9424
	AD19.8-4.7	15.15614	152.11024	1.85268	127.63996
	AD6.28-4.96	5.30587	84.09575	2.44150	225.68452

Code	Carbon Mass (g)
a	0.023
b	0.05
c	0.1
d	0.23
e	0.5

Note: AD40-05a means adsorption experiment with the following initial experimental conditions:

40mg/L RDX

5mg/L HMX

a=0.023g F400 carbon

All codes are rough estimate of the initial concentrations.

* asterisk indicates a rerun of an experiment

The following is a list of experiments performed, but the data were not incorporated into modeling because they did not fit well with the rest of the contours:

<i>Sets</i>	<i>Expt. Codes</i>	<i>Ce_RDX</i>	<i>qe_RDX</i>	<i>Ce_HMX</i>	<i>qe_HMX</i>
	AD30-05a	24.80738	231.83600	1.87267	143.41658
	AD30-3.5a	26.25270	230.40902	1.54516	106.93180
Set IV 21	AD14-4.95a	12.84212	113.97031	3.09793	10.50897
Set IV 23	AD32-4.8a	27.39680	266.00726	1.78544	64.77883
Set IV 25	AD26-4.7a	21.86545	117.41373	1.61112	65.36180
Set IV 28	AD9.4-4.6a	8.40813	50.25413	3.07897	154.36885
Set IV 31	AD32-5.06	30.42163	116.16678	3.17060	152.16775
Set IV 32	AD24-4.9	20.83175	107.32326	3.97256	152.06116
Set IV 33	AD19-05	17.98588	147.65803	3.77919	221.53150
Set IV 36	AD27.38-4.64	23.84413	127.90103	4.06542	93.81603

REFERENCES

- Annesini, M.C., Gironi, F., Ruzzi, M., and Tomei C. (1987) "Adsorption of Organic Compounds onto Activated Carbon." *Water Resources*, Vol. 21, No. 5, pp. 567-571.
- Ansell, E. (1993). "Department of Defense/Department of Energy (DOD/DOE) Research and Development (R&D) of Techniques for Demilitarization." *Proceedings of the 1993 International Incineration Conference*, pp. 637-639.
- Aytekini, C. (1991) "Application of the Polanyi Adsorption Potential Theory to Adsorption Phenolic Compounds from Water Solution onto Activated Carbon." *Spectroscopy Letters*, Vol. 24, No. 5, pp. 653-664.
- Barr, A.J. (1976) *A Users' Guide to SAS-76*. SAS Institute Inc., Raleigh, NC.
- Berrueta, L.A., Gallo, B., and Vicente, F. (1995) "A Review of Solid Phase Extraction: Basic Principles and New Developments." *Chromatographia*, Vol. 40, No. 7/8, pp. 474-483.
- Bricka, R.M., and Sharp, W. (1992) "Treatment of Groundwater Contaminated with Low Levels of Military Munitions." *47th Prudue University Industrial Waste Conference Proceedings*, pp. 199-204.
- Box, M.J. (1965) "A New Method of Constrained Optimization and a Comparison with Other Methods." *Computer Journal*, Vol. 8, pp. 42-52.
- Burrows, W.D. (1982) "Tertiary Treatment of Effluent from Holston AAP Industrial Liquid Waste Treatment Facility I. Batch Carbon Adsorption Studies: TNT, RDX, HMX, TAX, and SEX." Technical Report 8207, U.S. Army Medical Research and Development Command, Frederick, MD.
- Burrows, W.D., Chyrek, R.H., Noss, C.I., Small, M.J., and Kobylinski, E.A. (1984) "Treatment for Removal of Munition Chemicals from Army Industrial Wastewaters." *Proceedings of the 16th Mid-Atlantic Industrial Waste Conference*, pp. 331-342.
- Crittenden, J.C., Luft, P., Hand, D.W., Oravitz, J.L., Loper, S.W., Arl, M. (1985) "Prediction of Multicomponent Adsorption Equilibria Using Ideal Adsorbed Solution Theory." *Environmental Science and Technology*, Vol. 19, No. 11, pp. 1037-1043.

- Dennis, R.M., Wujcik, W.J., Lowe, W.L., and Mark, P.J. (1990) "Task Order 7: Use of Activated Carbon for Treatment of Explosives--Contaminated Groundwater at the Milan Army Ammunition Plant (MAAP)." Report No. CETHA-TE-CR-90041, U.S. Army Toxic and Hazardous Materials Agency, Aberdeen Proving Ground, MD.
- DiGiano, F.A., Baldauf, G., Frick, B., and Sontheimer, H. (1978) "A Simplified Competitive Equilibrium Adsorption Model." *Chemical Engineering Science*, Vol. 33, No. 12, pp. 1667-1673.
- Farber, M. (1992) "Mass spectrometric investigations of the thermal decomposition of HMX and RDX." *Mass Spectrometry Reviews*, Vol. 11 No. 2, pp. 137-152.
- Fritz, W., and Schlunder, E.U. (1981) "Competitive Adsorption of Two Dissolved Organics onto Activated Carbon--I. Adsorption Equilibria." *Chemical Engineering Science*, Vol. 36, pp. 721-730.
- Gibbs, T.R., Popolato, A. (1980) *LASL Explosive Property Data*. University of California Press, Berkeley, CA.
- Green, D.R., and Le Pape, D. (1987) "Stability of Hydrocarbon Samples on Solid-Phase Extraction Columns." *Analytical Chemistry* Vol. 59, No. 5, pp.699-703.
- Haberman, J., and Castorina, T.C. (1982) "Charcoal Regeneration--Part III. Mechanism of RDX Adsorption." Technical Report ARLCD-TR-82002, U.S. Army Toxic and Hazardous Materials Agency, Aberdeen Proving Ground, MD.
- Haberman, J. (1983) "Charcoal Regeneration--Part IV. Competitive Adsorption of TNT and RDX." Technical Report ARLCD-TR-83031, U.S. Army Toxic and Hazardous Materials Agency, Aberdeen Proving Ground, MD.
- Heilmann, H.M., Wiesmann, U., and Stenstrom, M.K. (1995) "Kinetics of the Alkaline Hydrolysis of High Explosives RDX and HMX in Aqueous Solution and Adsorbed to Activated Carbon." Accepted for publication in *Environmental Science and Technology*.
- Heilmann, H. (1994) "Physico-chemical Treatment of Water Contaminated with the High Explosives RDX and HMX Using Activated Carbon Adsorption and Alkaline Hydrolysis." Doctoral Dissertation, Civil & Environmental Engineering Department, University of California, Los Angeles, CA.

- Hesselmann, R. (1992) "Treatment Concept for RDX-Contaminating Wastewater Using Activated Carbon with Offline Solvent Biological Regeneration." UCLA Engr. Report No. ENGR 94-23.
- Hinshaw, G.D., Fanska, C.B., Fiscus, D.E., and Sorensen, S.A. (1987) "Granular Activated Carbon (GAC) System Performance Capabilities and Optimization." Report No. AMXTH-TE-CR87111, U.S. Army Toxic and Hazardous Materials Agency, Aberdeen Proving Ground, MD.
- Hoffsommer, J.C., Kubose, D.A., and Glover, D.J. (1977) "Kinetic Isotope Effects and Intermediate Formation for the Aqueous Alkaline Homogeneous Hydrolysis of 1,3,5-triaza-1,3,5-trinitrocyclohexane (RDX)." *Journal of Physical Chemistry*, Vol. 81. pp.380-385.
- Jain, J.S., and Snoeyink, V.L. (1973) "Adsorption from Bislute Systems on Active Carbon." *Journal of Water Pollution Control Federation*, Vol. 45, No. 12, pp. 2463-2479.
- Jenkins, T.F., Miyares, P.H., Myers, K.F., McCormick, E.F., and Strong, A.B. (1994) "Comparison of Solid Phase Extraction with Salting-out Solvent Extraction for Preconcentration of Nitroaromatic and Nitramine Explosives from Water." *Analytica Chimica Acta*, Vol. 289, No. , pp. 69-78.
- Jenkins, T.F., Leggett, D.C., Grant, C.L., and Bauer, C.F. (1986) "Reversed-phase high-performance liquid chromatographic determination of nitroorganics in munitions wastewater." *Analytical Chemistry*, Vol. 58, No. 1, pp.170-175.
- Jossens, L., Prausnitz, J.M., Fritz, W., Schlunder, E.U., and Myers, A.L. (1978) "Thermodynamics of Multi-Solute Adsorption from Dilute Aqueous Solutions." *Chemical Engineering Science*, Vol. 33, No. 8, pp. 1097-1106.
- Keinath, T. M. (1971) Unpublished Class Notes, Chapter 8, Clemson University, Clemson, SC.
- Layton, D., Mallon, B., Mitchell, W., Hall, L., Fish, R., Perry, L., Snyder, G., Bogen, K., Malloch, W., Ham, C., and Dowd, P. (1987) "Conventional Weapons Demilitarization: A Health and Environmental Effects Database Assessment." NTIS No. AD-A220588, U.S. Army Biomedical Research and Development Laboratory, Frederick, MD.
- Lehr, J. H. (1991) "Granular Activated Carbon-Everyone knows of it, few understand it." *Groundwater Monitoring Review*, Vol.11, No.4, pp. 5-8.

- LeVan, M.D., and Vermeulen, T. (1981) "Binary Langmuir and Freundlich Isotherms for Ideal Adsorbed Solutions." *Journal of Physical Chemistry*, Vol. 85, No. 22, pp. 3247-3250.
- Lin, B., Ma, Z., Golshan-Shirazi, S., Guiochon, G. (1989) "Study of the Representation of Competitive Isotherms and of the Intersection between Adsorption Isotherms." *Journal of Chromatography*, Vol. 475, pp. 1-11.
- Liska, I., Kuthan, A., and Krupcik, J. (1990) "Comparison of Sorbents for Solid-Phase Extraction of Polar Compounds from Water." *Journal of Chromatography*, Vol. 509, pp. 123-134.
- Liska, I., Krupcik, J., and Leclercq, P.A. (1989) "The Use of Solid Sorbents for Direct Accumulation of Organic Compounds from Water Matrices--A Review of Solid-Phase Extraction Techniques." *Journal of High Resolution Chromatography*, Vol. 12, September, pp. 577-590.
- Maleki, N. (1994) "Treatment and Biodegradation of High Explosives: A Literature Review." Master's Thesis, Civil & Environmental Engineering Department, University of California, Los Angeles, CA.
- Major, M.A., Checkai, R.T., Phillips, C.T., Wentzel, R.S., and Nwanguma, R.O. (1992) *International Journal of Environmental Analytical Chemistry*, Vol. 48, PP. 217-227.
- Martin, R.J., and Al-Bahrani, K.S. (1979) "Adsorption Studies Using Gas-Liquid Chromatography--IV. Adsorption from Bisolute Systems." *Water Research*, Vol. 13, pp. 1301-1304.
- McCormick, N.G., Cornell, J.H., and Kaplan, A.M. (1981) "Biodegradation of Hexahydro-1,3,5-Trinitro-1,3,5-Triazine." *Applied and Environmental Microbiology*, Vol. 42, No. 5, pp. 817-823.
- McCormick, N.G., Cornell, J.H., and Kaplan, A.M. (1984) "The Fate of Hexahydro-1,3,5-Trinitro-1,3,5-Triazine (RDX) and Related Compounds in Anaerobic Denitrifying Continuous Culture Systems Using Simulated Waste Water." Report No. NATICK/TR-85/008. U.S. Army Toxic and Hazardous Materials Agency, Aberdeen Proving Ground, MD.
- McKay, G. and Duri, B.A. (1989) "Prediction of Multicomponent Adsorption Equilibrium Data Using Empirical Correlations." *The Chemical Engineering Journal*, Vol. 41, pp. 9-23.

- McLellan, W.L., Hartley, W.R., Brower, M.E. (1988a) *Health Advisory for Hexahydro-1,3,5-trinitro-1,3,5-triazine (RDX)*. Technical Report No. PB90-273533. Office of Drinking Water, U.S. Environmental Protection Agency, Washington, D.C.
- McLellan, W.L., Hartley, W.R., Brower, M.E. (1988b) *Health Advisory for Octahydro-1,3,5,7-tetranitro-1,3,5,7-tetrazocine (HMX)*. Technical Report No. PB90-273525. Office of Drinking Water, U.S. Environmental Protection Agency, Washington, D.C.
- McLellan, W.L., Hartley, W.R., and Brower, M.E. (1992) *Drinking Water Health Advisory: Munitions*. Lewis Publishers, Boca Raton, Fl.
- Najim, I.N., Snoeyink, V. L., Lykins Jr., B.W. and Adams, J.Q. (1991) "Using Powdered Activated Carbon: A Critical Review." *Journal of American Water Works Association*, Vol. 83, No. 1, pp. 65-76.
- Patterson, J., Shapira, N.I, Brown, J., Duckert, W., and Polson, J. (1976a) "State of the Art: Military Explosives and Propellants Production Industry--Volume I The Military Explosives and Propellants Industry" Technical Report No. PB 265 385. U.S.Environmental Protection Agency, Cincinnati, Ohio.
- Patterson, J., Shapira, N.I., Brown, J., Duckert, W., and Polson, J. (1976b) "State of the Art: Military Explosives and Propellants Production Industry--Volume II Wastewater Characterization." Technical Report No. PB-260 918. U.S. Environmental Protection Agency, Cincinnati, Ohio.
- Patterson, J., Shapira, N.I., Brown, J., Duckert, W., and Polson, J. (1976c) "State of the Art: Military Explosives and Propellants Production Industry--Volume III Wastewater Treatment." Technical Report No. PB-265 042. U.S. Environmental Protection Agency, Cincinnati, Ohio.
- Patterson, J.W., Shapira, N.I., Brown, J. (1976) "Pollution Abatement in the Military Explosives Industry." *Proceedings of the 31st Industrial Waste Conference*, Purdue University, pp. 385-394.
- Pruneda, C.O., Mitchell, A.R., Humphrey, J.R. (1993) "Reusing the High Explosives from Dismantled Nuclear Weapons." *Energy and Technology Review*, Nov/Dec., pp.19-27.
- Radke, C.J., and Prausnitz, J.M. (1972a) "Adsorption of Organic Solutes from Dilute Aqueous Solution on Activated Carbon." *Industrial Engineering Chemistry Fundamental*, Vol. 11, No. 4, pp. 445-451.

- Radke, C.J., and Prausnitz, J.M. (1972b) "Thermodynamics of Multi-Solute Adsorption from Dilute Liquid Solutions." *A.I.Ch.E. Journal*, Vol. 18, No. 4, pp. 761-768.
- Randtke, S.J., and Snoeyink, V.L. (1983) "Evaluating GAC adsorptive capacity." *Journal of American Water Works Association*, Vol. 75, No.8, pp.406-414.
- Richard, J.J., and Junk, G.A. (1986) "Determination of Munitions in Water Using Macroreticular Resins." *Analytical Chemistry*, Vol.58, No. 4, pp.723-725.
- Rosenblatt, D.H., Burrows, E.P., Mitchell, W.R., and Parmer, D.L. (1991) "Organic Explosives and Related Compounds." *The Handbook of Environmental Chemistry*, Part 3, Part G. Springer-Verlag, Berlin.
- Rosene, M.R., and Manes, M. (1976) "Application of the Polanyi Adsorption Potential Theory to Adsorption from Solution on Activated Carbon. VII. Competitive Adsorption of Solids from Water Solution." *The Journal of Physical Chemistry*, Vol. 80, No. 9, pp. 953-959.
- Ryon, M.G., Pal, B.C., Talmage, S.S., and Ross, R.H. (1984) "Database Assessment of Health and Environmental Effects of Munition Production Waste Products." NTIS No. A145 417. U.S. Army Medical Research and Development Command, Frederick, MD.
- Schneider, N.R., Bradley, S.L., and Andersen, M.E. (1976) "Toxicology of Cyclotrimethylene-trinitramine (RDX): Distribution and Metabolism in the Rat and the Miniature Swine." NTIS No. AD-A026 892. Defense Nuclear Agency, Washington, D.C.
- Sheindorf, CH., Rebhun, M., and Sheintuch, M. (1981) "A Freundlich-Type Multicomponent Isotherm." *Journal of Colloid and Interface Science*, Vol. 79, No. 1, pp. 136-142.
- Sheintuch, M., and Rebhun, M. (1988) "Adsorption Isotherms for Multisolute Systems with Known and Unknown Composition." *Water Resources*, Vol. 22, No. 4, pp. 421-430.
- Singer, P.C., and Yen, C.Y. (1980) "Adsorption of Alkyl Phenols by Activated Carbon." *Activated Carbon Adsorption of Organics from the Aqueous Phase, Volume I*, edited by I.H. Suffet and M.J. McGuire, Ann Arbor Science Publishers, Inc., Ann Arbor, MI.
- Spanggord, R.J., Mill, T., Chou, T.W., Mabey, W.R., and Smith, J.H. (1980) "Environmental Fate Studies on Certain Munition Wastewater Constituents-

-Laboratory Studies." NTIS No. AD-A099256. U.S. Army Medical Bioengineering Research and Development Laboratory, Frederick, Maryland.

- Sublette, K.L., Ganapathy, E.V., and Schwartz, S. (1992) "Degradation of Munition Wastes by *Phanerochaete chrysosporium*." *Applied Biochemistry and Biotechnology*, Vol. 34/35, pp. 709-723.
- Szachta, J.M. (1978) "Analysis of Carbon Versus Resin." Technical Report ARCSL-TR-78013, U.S. Army Toxic and Hazardous Materials Agency, Aberdeen Proving Ground, MD.
- Tchobanoglous, G. and Burton, F. (1991) *Wastewater Engineering Treatment, Disposal, and Reuse*, 3rd Edition. McGraw-Hill, Inc. New York, NY.
- Thurman, E.M., Malcolm, R.L., and Aiken, G.R. (1978) "Prediction of Capacity Factors for Aqueous Organic Solutes Adsorbed on a Porous Acrylic Resin." *Analytical Chemistry* Vol. 50, No. 6, pp. 775-779.
- Urbanski, T. (1964) *Chemistry and Technology of Explosives Vol. 3*. Pergamon Press, New York, NY.
- Vlahakis, J.G. (1974) "A Laboratory Study of RDX Adsorption by Carbon." NTIS No. AD/A- 002 049, Naval Facilities Engineering Command, Alexandria, VA.
- Weber, W.J. (1972) *Physicochemical Processes for Water Quality Control*. John Wiley & Sons, Inc., New York, NY.
- Wilkie, J.A. (1994) "Biological Degradation of RDX." Master's Thesis, Chemical Engineering Department, University of California, Los Angeles, CA.
- Winslow, M.G., Weichert, B.A., and Baker, R.D. (1991) "Determination of Low-Level Explosive Residues in Water by HPLC: Solid-Phase Extraction vs. Salting-out Solvent Extraction." Proceedings of the EPA 7th Annual Waste Testing and Quality Assurance Symposium, July 8-12, Washington, D.C.
- Wujcik, W.J., Lowe, W.L., Marks, P.J., and Sisk, W.E. (1992) "Granular Activated Carbon Pilot Treatment Studies for Explosives Removal from Contaminated Groundwater." *Environmental Progress*, Vol. 11, No.3, pp. 178-189.
- Yen, C.Y., and Singer, P.C. (1984) "Competitive Adsorption of Phenols on Activated Carbon." *Journal of Environmental Engineering*, Vol. 110, No. 5, pp. 976-989.

- Yinon, J. (1990) *Toxicity and Metabolism of Explosives*. CRC Press, Inc., Boca Raton, FL.
- Yonge, D.R., Keinath, T.M., Poznanska, K., and Jiang, Z.P. (1985) "Single-Solute Irreversible Adsorption on Granular Activated Carbon." *Environmental Science Technology*, Vol. 19, No. 8, 690-694.
- Yonge, D.R., and Keinath, T.M. (1986) "The Effects of Non-ideal Competition on Multi-component Adsorption Equilibria." *Journal of Water Pollution Control Federation*, Vol. 58, No. 1, pp. 77-81.
- Zhu, J., Katti, A.M., and Guiochon, G. (1991) "Comparison of Various Isotherm Models for Predicting Competitive Adsorption Data." *Journal of Chromatography*, Vol. 552, pp. 71-89.